CONSTRUCTION WITH HOLLOW STEEL SECTIONS

8

DESIGN GUIDE

FOR CIRCULAR AND RECTANGULAR HOLLOW SECTION WELDED JOINTS UNDER FATIGUE LOADING

X.-L. Zhao, S. Herion, J. A. Packer, R. S. Puthli, G. Sedlacek,
J. Wardenier, K. Weynand, A. M. van Wingerde, N. F. Yeomans

TÜV-Verlag

DESIGN GUIDE

FOR CIRCULAR AND RECTANGULAR HOLLOW SECTION WELDED JOINTS UNDER FATIGUE LOADING

CONSTRUCTION WITH HOLLOW STEEL SECTIONS

Edited by: Comité International pour le Développement et l'Etude de la Construction Tubulaire

Authors: X.-L. Zhao, Monash University
S. Herion, University of Karlsruhe
J. A. Packer, University of Toronto
R. S. Puthli, University of Karlsruhe
G. Sedlacek, University of Aachen
J. Wardenier, Delft University of Technology
K. Weynand, University of Aachen
A. M. van Wingerde, Delft University of Technology
N. F. Yeomans, Chairman CIDECT Technical Commission

DESIGN GUIDE

FOR CIRCULAR AND RECTANGULAR HOLLOW SECTION WELDED JOINTS UNDER FATIGUE LOADING

X.-L. Zhao, S. Herion, J. A. Packer, R. S. Puhtli, G. Sedlacek,
J. Wardenier, K. Weynand, A. M. van Wingerde, N. F. Yeomans

TÜV-Verlag

Die Deutsche Bibliothek – CIP-Einheitsaufnahme

Design guide for circular and rectangular hollow section welded joints under fatigue loading / [ed. by: Comité International pour le Développment et l'Etude de la Construction Tubulaire]. X.-L. Zhao ……– Köln:
TÜV-Verlag, 2000
(Construction with hollow steel sections ; 8)
ISBN 3-8249-0565-5

ISBN 3-8249-0565-5

Entirely printed by: TÜV-Verlag GmbH, Köln
Printed in Germany 2001

Preface

Structural hollow sections are widely used in many applications in the field of construction and mechanical engineering, where fatigue is an essential aspect in design and fabrication. Basically, the same fatigue design aspects and design principles apply for hollow sections as they do for open profiles. However, the welded connections between hollow sections (for example K-joints) need to be considered in a different way, based on the non-uniform stress distribution around the welded intersection and the secondary bending stresses in the joint.

The objective of this design guide is to give design recommendations for structural hollow sections under fatigue loading. Principally the theory applied in this book is based on the hot spot stress approach. The latest results of research work carried out by CIDECT and other research organisations, particularly dealing with the stress concentration factors, have been utilised in this design guide.

This design guide is the eighth in the series “Construction with Hollow Steel Sections”, which CIDECT has published:

1. Design guide for circular hollow section (CHS) joints under predominantly static loading
2. Structural stability of hollow sections
3. Design guide for rectangular hollow section (RHS) joints under predominantly static loading
4. Design guide for structural hollow section columns exposed to fire
5. Design guide for concrete filled hollow section columns under static and seismic loading
6. Design guide for structural hollow sections in mechanical applications
7. Design guide for fabrication, assembly and erection of hollow section structures
8. Design guide for circular and rectangular hollow section welded joints under fatigue loading

We express our sincere thanks to Dipl.-Ing. D. Dutta, Germany, Dr.-Ing. D. Grotmann of RWTH Aachen, Germany, Dr.-Ing. S. Herion of University of Karlsruhe, Germany, Prof. Dr.-Ing. F. Mang of University of Karlsruhe, Germany, Prof. Dr. J.A. Packer of University of Toronto, Canada, Dr.Ir. E. Panjeh Shahi of Vekoma, The Netherlands, Prof. Dr.-Ing. R. S. Puthli of University of Karlsruhe, Germany, Dr.Ir. A. Romeijn of Delft University of Technology, The Netherlands, Prof. Dr.-Ing. G. Sedlacek of RWTH Aachen, Germany, Dr.-Ing. N. Stranghöner of RWTH Aachen, Germany, Prof.Dr.Ir. J. Wardenier of Delft University of Technology, The Netherlands, Dr.-Ing. K. Weynand of RWTH Aachen, Germany, Dr.Ir. A. M. van Wingerde of Delft University of Technology, The Netherlands, Mr. N.F. Yeomans of British Steel Tubes and Pipes, United Kingdom, and Dr. X.-L. Zhao of Monash University, Australia, for their valuable contributions and comments. Further, the support of the CIDECT member firms is gratefully acknowledged.

Reijo Ilvonen
Chairman of the Technical Commission
CIDECT

CONTENTS

Notation

Definition of geometrical parameters

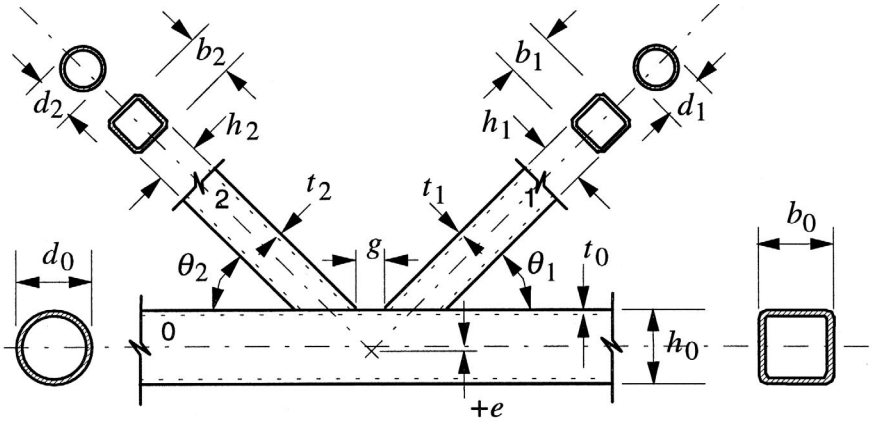

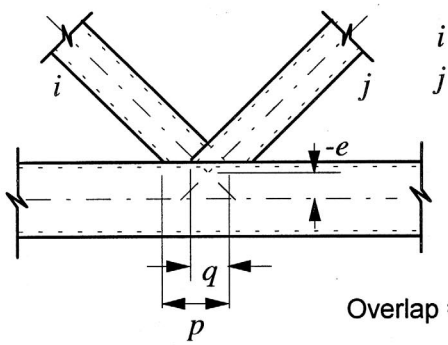

i = 1 or 2 (overlapping member)

j = overlapped member

$$\text{Overlap} = \frac{q}{p} \times 100\%$$

Abbreviations

CHS	Circular Hollow Section
RHS	Rectangular Hollow Section including square hollow section
SHS	Structural Hollow Section
FE	Finite Element
MCF	Multiplaner Correction Factor
MF	Magnification Factor
SCF	Stress Concentration Factor
SNCF	Strain Concentration Factor

Notation

A	area
D	damage accumulation index
L	chord length between effective support points
L_r	distance from weld toe
M_{ipb}	in-plane bending moment
M_{opb}	out-of-plane bending moment
N	number of cycles
N_f	number of cycles to failure
R	ratio of minimum to maximum stress in a cycle
P_{ax}	axial force
S_n	nominal stress range
S_{rhs}	hot spot stress range
W_o,W_i	elastic section modulus of chord, brace
b_o	chord width of RHS
d_o	chord diameter of CHS
b_i	width of brace i (RHS)
d_i	diameter of brace i (CHS)
e	joint eccentricity
g	gap length
g'	g/t_o
h_o	chord depth of RHS
h_i	brace depth of RHS
m	slope in S-N curves or ratio of brace axial load
p	projected connecting length to chord of overlapping brace in overlapped joint
q	overlap length
r_o	external radius of chord member
r_i	internal radius of brace member
t_o	chord wall thickness
t_i	brace wall thickness
α	relative chord length ($2L/d_o$ or $2L/b_o$)
β	diameter or width ratio (d_i/d_o or b_i/b_o)
γ	half chord diameter or width to thickness ratio ($d_o/(2t_o)$ or $b_o/(2t_o)$)
γ_{Ff}	partial safety factor for fatigue loading
γ_{Mf}	partial safety factor for fatigue strength
O_v	overlapping percentage of braces (q/p in %)
ζ	relative gap (g/d_o or g/b_o)
ϕ	angle between planes with braces in multiplanar joints
θ	acute angle between brace and chord axes (in Y-, X-, N-, K- and KT-joints)
σ_{ax}	normal stress due to axial force

σ_{ipb}	normal stress due to in-plane bending
σ_{opb}	normal stress due to out-of-plane bending
τ	wall thickness ratio (t_i/t_o)

Subscripts

0	chord
i	brace number (1, 2, 3, etc.)
ax	axial
ipb	in plane
opb	out of plane
ref	reference brace
cov	carry-over brace

Abbreviations of organisations, institutes etc.

API	American Petroleum Institute
AWS	American Welding Society
CEN	European Standards Commission
DEn	Department of Energy
EN	European Standards
EC3	Eurocode 3
ECCS	European Convention for Constructional Steelwork
IIW	International Institute of Welding

1 Introduction

1.1 Applications

Structural hollow sections, both circular (CHS) and rectangular (RHS), are widely used in all kinds of structures under different types of loading, as shown in previous CIDECT Design Guides (Wardenier et al. [1991], Rondal et al. [1991], Packer et al. [1992], Twilt et al. [1996], Bergmann et al. [1995], Wardenier et al. [1995], Dutta et al. [1997]). The published CIDECT Design Guides for structural hollow section joints have mainly dealt with CHS and RHS joints under static loading (Wardenier et al. [1991], Packer et al. [1992]).

Many tubular structures are subjected to fatigue loading. Some typical examples are shown in Figure 1.1 to Figure 1.11. The aim of this guide is to provide design recommendations for welded CHS and RHS joints under fatigue loading.

Figure 1.1 – Full revolving plough machine

Figure 1.2 – Air seeder farming equipment

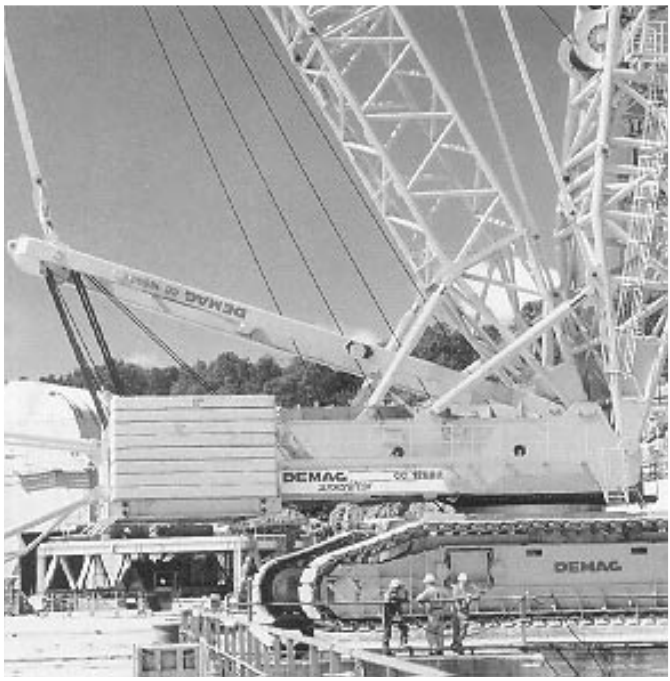

Figure 1.3 – Mobile crane

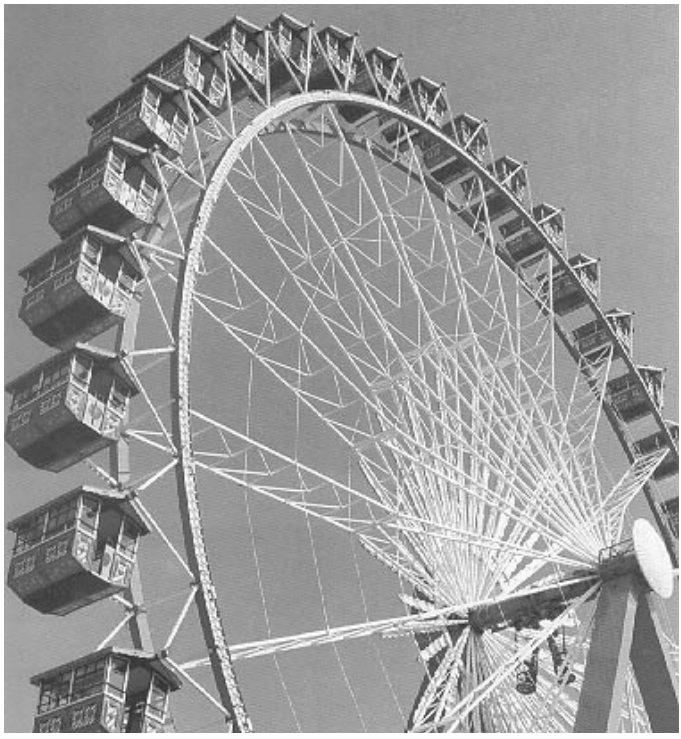

Figure 1.4 – Giant wheel in an amusement park

Figure 1.5 – Offshore platforms

Figure 1.6 – Grab bucket

Figure 1.7 – Ski installation

Figure 1.8 – Bridge

Figure 1.9 – Bridge

Figure 1.10 – Bridge

Figure 1.11 – Communication tower

1.2 Types of Joints and Loading

The types of joints and loading covered in this design guide are summarised in Table 1.1. A "yes" in the table means that design rules for these joint types are given in the guide whereas a "no" indicates that no design rules are available or necessary. The types of joints are shown schematically in Figure 1.12 and Figure 1.13, and the types of loading in Figure 1.14. For K-joints both bracings are identical and at the same angle.

Table 1.1 – Types of joints and loading covered in this design guide

Joint type: u = uniplanar m = multiplanar Section type: CHS = circular hollow sections RHS = rectangular hollow sections			Brace load			Chord load	
			Axial force	In-plane bending	Out-of-plane bending	Axial force	In-plane bending
CHS	T/Y	u	yes	yes	yes	no	no
	X	u	yes	yes	yes	no	no
	K(gap)	u	yes	no	no	yes	yes
	XX	m	yes	yes	yes	yes	no
	KK(gap)	m	yes	no	no	yes	yes
RHS	T/X	u	yes	yes	no	yes	yes
	K(gap)	u	yes	no	no	yes	yes
	K(overlap)	u	yes	no	no	yes	yes
	KK(gap)	m	yes	no	no	yes	yes

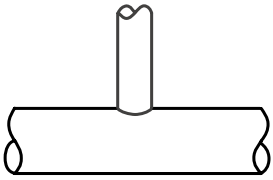

(a) CHS T-Joints

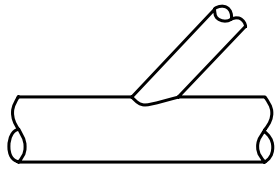

(b) CHS Y-Joints

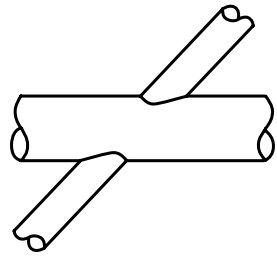

(c) CHS X-joints

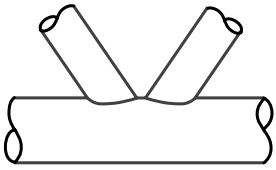

(d) CHS K-joints with gap

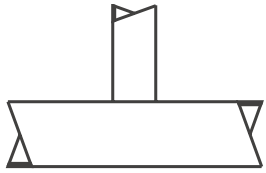

(e) RHS T-joints

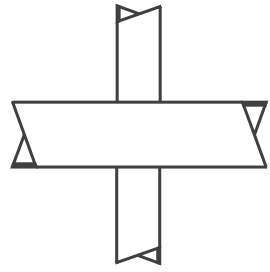

(f) RHS X-joints

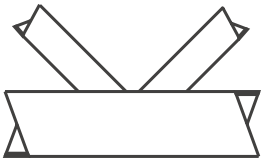

(g) RHS K-joints with gap

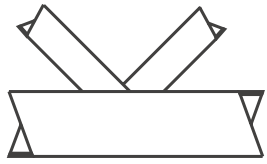

(h) RHS K-joints with overlap

Figure 1.12 – Types of uniplanar joints considered in this guide

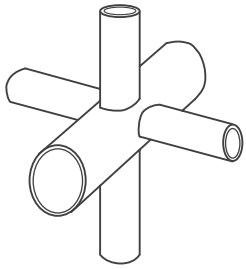

(a) CHS XX-joints

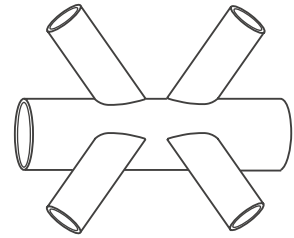

(b) CHS KK-joints with gap

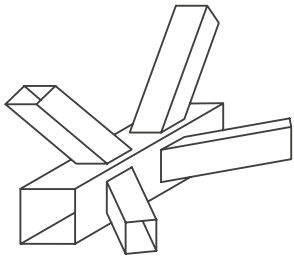

(c) RHS KK-joints with gap

Figure 1.13 – Types of multiplanar joints considered in this guide

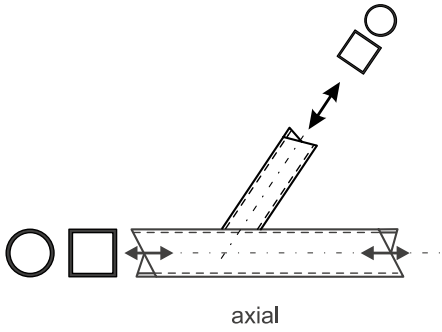

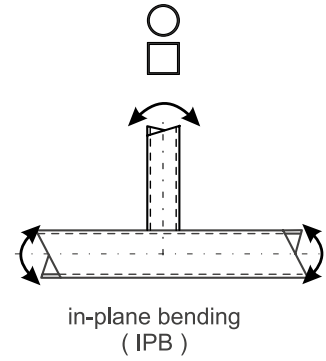

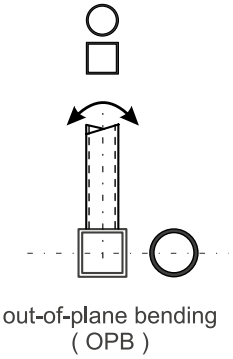

Figure 1.14 – Types of Loading

1.3 Fatigue Life Estimation

The fatigue phenomenon is characterised by a progressive degradation of strength under time variant stresses that result in the appearance of visible cracks and subsequent crack growth, which eventually may include fracture of a member or even the collapse of a structure. The fatigue life of a structure may be divided into two parts: a crack initiation phase, during which micro-cracks may form, and a crack propagation phase, which may lead to visible cracks or even critical crack sizes that result in failure.

The fatigue life of welded joints depends upon the joint type, joint loading and structural detailing of the joint. The loading (axial force or bending moment) in the joint depends on the type of structure and the fatigue actions, as described in Appendix A. The effect of structural detailing of joints on fatigue life is discussed in Chapter 6. This guide mainly concentrates on determining the fatigue resistance of CHS and RHS joints, i.e. the number of cycles to fatigue failure under a given loading condition for different joint types.

1.4 Fatigue Resistance

Several methods have been developed to determine the fatigue resistance of welded structural hollow section joints. They include:

a) Classification method
b) Punching shear method
c) Failure criterion method
d) Static strength method
e) Hot spot stress method (also called geometric stress method)
f) Fracture mechanics method

Each method is described briefly below.

a) The classification method is based on structural details for different types of joints which are classified into various detail categories with about the same fatigue life. Each detail category corresponds to a nominal stress range under which a joint will fail after 2 million cycles. This method will be described in detail in Chapter 2. The classification method has been adopted by many standards (EC3 [1992], SAA [1990], JSSC [1995], AISC [1993], CSA [1994]).

b) The punching shear method is nearly similar to the classification method except that the punching shear stress range is used instead of the nominal stress range. It has been adopted by the American Petroleum Institute (API [1991]) and the American Welding Society (AWS [1998]). This method is described in detail by Marshall [1992].

c) The failure criterion method provides diagrams showing the nominal stress ranges or maximum stresses at 2 million cycles in relation to joint geometry and loading parameters. The critical member in a joint can be determined using these diagrams. This method is only applicable to certain types of joints with a limited validity range. More details can be found in Mang and Bucak (1982).

d) The static strength method relates the fatigue behaviour to the static behaviour of a joint. Within certain parameter ranges, a reasonable relationship can be obtained. There are a few theoretical objections against using this approach. For example, fatigue behaviour is a weakest link driven mechanism (i.e. a strong joint will still have a low

fatigue life if there is one point of weakness), whereas the static behaviour is more dependent on the total strength and allows stress redistribution (van Wingerde et al. [1997a]). The static strength approach has been described in detail in Kurobane (1989) and Niemi (1995). It may be applied as a preliminary design tool, before a better selection of stress concentration factors based on finite element analysis is available.

e) The hot spot stress (also called geometric stress) method relates the fatigue life of a joint to the so-called hot spot stress at the joint. It takes the uneven stress distribution around the perimeter of the joint into account directly. This method will be described in detail in Chapter 3. The hot spot stress method has been recommended by the International Institute of Welding Subcommission XV-E (IIW [1985]) for design of welded tubular joints under fatigue loading.

f) The fracture mechanics method can be used to estimate the fatigue crack propagation life of a structural component with crack-like defects. It has been mainly applied to welded simple joints (Fisher et al. [1970], Gurney [1979], Bell et al. [1989], Swanmidas et al. [1989], Maddox [1991], Sedlacek et al. [1992], Nguyen and Wahab [1995], Mori et al. [1997], Mashiri et al [1998]). This method demands much higher computing capacity and more sophisticated software in order to predict the fatigue life of welded tubular joints (Sedlacek et al. [1998]).

In this guide only the classification method (see Chapter 2) and the hot spot stress method (see chapter 3) are discussed in detail.

1.5 Fatigue Damage Accumulation

As shown in Appendix A, the stress range ($S = S_{max} - S_{min}$) is a governing parameter for fatigue design. Due to the presence of residual stresses, the stress ratio R ($= S_{min}/S_{max}$) is not taken into account in modern fatigue design. Only if the structure is fully stress relieved, might it be advantageous to take the stress ratios into account.

For constant amplitude loading, it is assumed that there is no fatigue damage when the stress ranges are below the Constant Amplitude Fatigue Limit, which is typically defined as the stress range for a specific S-N curve (Figures 2.1 and 3.3) when the number of cycles is $N = 5 \cdot 10^6$.

For variable amplitude loading, the stress ranges below the Cut-Off Limit at $N = 10^8$ (Figures 2.1, 2.2 and 3.3) do not contribute to fatigue damage.

When the stress range for a constant amplitude loaded structure or when the maximum stress range for a variable amplitude loaded structure is above the Constant Amplitude Fatigue Limit, the fatigue damage accumulation (D) can be assessed using the Palmgren-Miner linear rule, i.e.

$$D = \Sigma\, n_i/N_i$$

in which n_i is the number of cycles of a particular stress range S_i and N_i is the number of cycles to failure for that particular stress range.

The allowable fatigue damage (D) for structures in a non-aggressive environment is generally taken as 1.0, if the effect of fatigue cracks and the possibility for inspection are taken into account by partial safety factors.

1.6 Partial Safety Factors

In limit states design codes, partial safety factors for fatigue loading (γ_{Ff}) and for fatigue strength (γ_{Mf}) need to be taken into consideration during design. For example Eurocode3: Section 9.3 (EC3 [1992]) recommends that γ_{Ff} = 1.0 and γ_{Mf}, which is dependant upon both the consequences of failure and the inspection routine, takes the values shown in Table 1.2. For a fail-safe structural component, the failure of a joint has reduced consequences of failure, such that the local failure of one component does not result in failure of the structure.

Table 1.2 – Partial safety factor for fatigue strength γ_{Mf} according to Eurocode 3

Inspection and access	Fail-safe component	Non fail-safe component
Periodic inspection and maintenance. Accessible joint detail.	1	1.25
Periodic inspection and maintenance. Poor accessibility.	1.15	1.35

2 Classification Method

2.1 General

The classification method is based on structural details for different types of joints which are classified into various detail categories. Each detail category corresponds to a nominal stress range under which a joint will fail after 2 million cycles. The classification is derived on the basis of an analysis of relevant test results, taking account of the chord to brace thickness ratio (t_o/t_1) and using a lower bound. In this method, the effects of other parameters and the thickness effects are combined to some extent (Noordhoek et al. [1980], Wardenier [1982]).

This method is simple to use. The design procedures can be summarised as follows:

- Determine the detail category from the types of joints and the detail geometry, as described in Section 2.2
- Determine the nominal stress ranges using an elastic analysis as described in Section 2.3
- Determine the permissible load cycles at this stress range, using the fatigue strength curve shown in Section 2.4 relating to the corresponding detail category

The application of this method is limited to the tubular joint types (attachments and lattice girders) and parameter ranges given in Appendix B. For lattice girders, detail categories are only available for uniplanar K- and N-joints, but parameters are very limited. A large variation in fatigue behaviour may occur for joints within the same category, which may result in a considerable variation in fatigue life (van Wingerde et al. [1997b]).

2.2 Detail Categories

The detail categories for the classification method are listed in Appendix B for both attachments and lattice girder joints. They are also given in Eurocode 3 (EC3 [1992]).

The construction details with descriptions and the corresponding detail categories are given in the tables in Appendix B. It should be noted that the arrow in the construction detail indicates the direction of the applied stress range while the thick curved line perpendicular to the arrow indicates the fatigue crack. For lattice girder joints, thickness ratio (t_o/t_1) has a great effect on the detail category.

2.3 Nominal Stress Ranges

For fatigue design, the nominal stress ranges in the members have to be determined. This can be done easily for attachments. For lattice girders and all triangulated truss systems (both 2D and 3D) axial forces and bending moments in the members can be determined using a structural analysis method as described in Section 3.2. The nominal stress ranges can be determined in accordance with Section 3.3, where MF is the magnification factor to account for secondary bending moments in lattice girders. Recommended MF factors are given in Eurocode 3 (EC3 [1992]). They are summarised in Table 2.1 for CHS joints and Table 2.2 for RHS joints.

Table 2.1 – Magnification factors to account for secondary bending moments in CHS joints of lattice girders

Type of joint		Chords	Braces (vertical members)	Braces (diagonal members)
Gap joints	K	1.5	–	1.3
	N		1.8	1.4
Overlap joints	K		–	1.2
	N		1.65	1.25

Table 2.2 – Magnification factors to account for secondary bending moments in RHS joints of lattice girders

Type of joint		Chords	Braces (vertical members)	Braces (diagonal members)
Gap joints	K	1.5	–	1.5
	N		2.2	1.6
Overlap joints	K		–	1.3
	N		2.0	1.4

2.4 Fatigue Strength Curves

The fatigue strength curves are usually called S_n-N_f curves where S_n is the nominal stress range and N_f is the corresponding number of cycles to failure. They are plotted on a log-log scale. The S_n-N_f curves in Eurocode 3 are plotted in Figure 2.1 for attachments under normal stress ranges and in Figure 2.2 for tubular joints in lattice girders. The S_n-N_f curves given in other national codes are similar to those in Eurocode 3. Figure 2.1 should be used in conjunction with Table B.1 in Appendix B, while Figure 2.2 should be used in conjunction with Table B.2 in Appendix B.

In Figure 2.1, attention should be paid to three important values, i.e. Detail Category, Constant Amplitude Fatigue Limit and Cut-Off Limit, as explained in Section 1.5. A summary of these values is given in Table 2.3. In Figure 2.1, all the S_n-N_f curves have a slope of m = 3 when N_f is less than $5 \cdot 10^6$ and a slope of m = 5 when N_f is between $5 \cdot 10^6$ and 10^8. In Figure 2.2, only a single slope of m = 5 is used. The Cut-Off Limits in Figure 2.2 are given in Table 2.4.

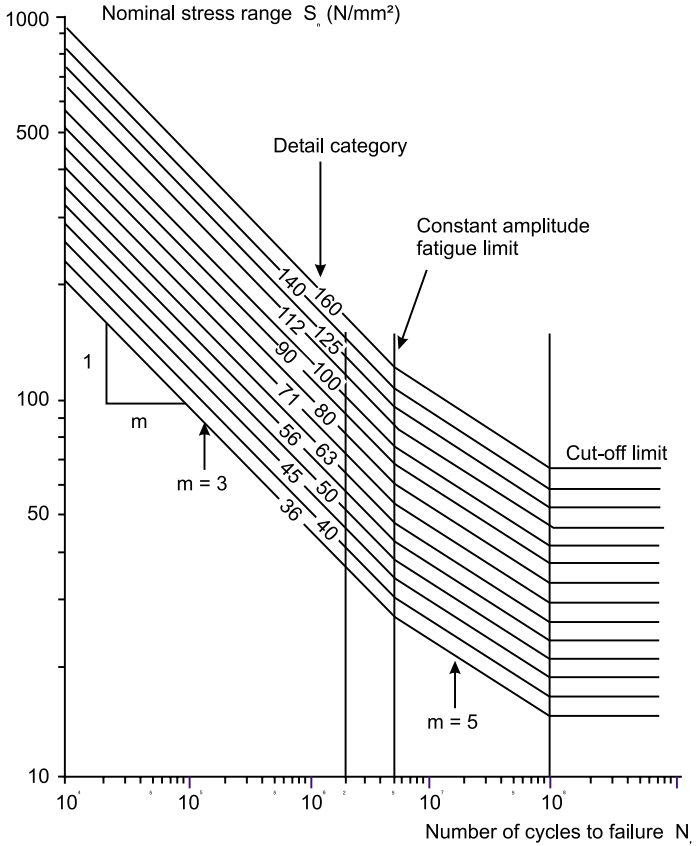

Figure 2.1 – Fatigue strength curves for attachments under normal stress ranges

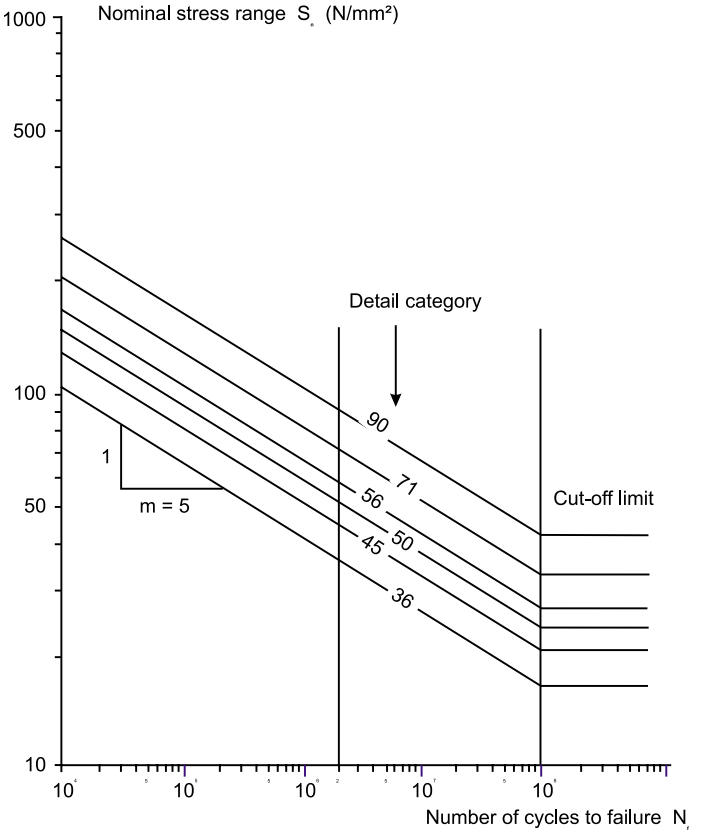

Figure 2.2 – Fatigue strength curves for tubular joints in lattice girders according to the classification method

Table 2.3 – Constant Amplitude Fatigue Limit and Cut-Off Limit for Attachments

Detail Category (N/mm^2)	Constant Amplitude Fatigue Limit (N/mm^2)	Cut-Off Limit (N/mm^2)
160	117	64
140	104	57
125	93	51
112	83	45
100	74	40
90	66	36
80	59	32
71	52	29
63	46	26
56	41	23
50	37	20
45	33	18
40	29	16
36	26	14

Table 2.4 – Cut-Off Limit for Lattice Girder Joints

Detail Category (N/mm^2)	Cut-Off Limit (N/mm^2)
90	41
71	32
56	26
50	23
45	20
36	16

3 Hot Spot Stress Method

3.1 General

In welded tubular joints the stiffness around the intersection is not uniform, resulting in a geometrical non-uniform stress distribution. An example is shown in Figure 3.1.

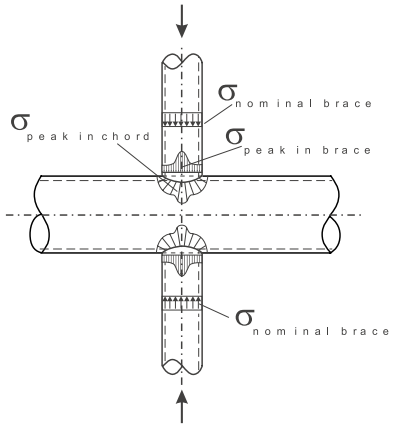

Figure 3.1 – Geometrical stress distribution in an axially loaded CHS X-joint

The hot spot stress (also called geometric stress) method relates the fatigue life of a joint to the so-called hot spot stress at the joint rather than the nominal stress. It takes the uneven stress distribution around the perimeter of the joint into account directly. The hot spot stress range includes the influences of the geometry and type of load but excludes the effects related to fabrication such as the configuration of the weld (flat, convex, concave) and the local condition of the weld toe (radius of weld toe, undercut, etc.). The hot spot stress is the maximum geometrical stress occurring in the joint where the cracks are usually initiated. In the case of welded joints, this generally occurs at the weld toe. More information about hot-spot stresses can be found in Appendix C.

The design procedures can be summarised as follows:

1. Determine axial forces and bending moments in chord and braces using a structural analysis as described in Section 3.2.
2. Determine nominal stress ranges (S_n or σ_n) as described in detail in Section 3.3
3. Determine the Stress Concentration Factors (SCFs) as described in Section 3.4
4. Determine the hot spot stress ranges (S_{rhs}) as described in Section 3.5
5. Determine the permissible number of load cycles for a given hot spot stress range at a specific joint location from a fatigue strength curve given in Section 3.6

This method can be applied to the types of joints and loading summarised in Table 1.1.

3.2 Member Forces

For welded hollow section structures, member forces must be obtained by analysis of the complete structure, in which noding eccentricity of the member centrelines at the joint (connection) as well as local joint flexibility is taken into account (Romeijn et al [1997] and Herion and Puthli [1998]). This can be achieved by the methods described in 3.2.1 to 3.2.3.

3.2.1 Sophisticated three dimensional finite element modelling where plate, shell and solid elements are used at the joints (appropriate for experienced analysts), or
3.2.2 Simplified structural analysis using frame analysis for triangulated trusses or lattice girders. Axial forces and bending moments in the members can be determined using a structural analysis assuming a continuous chord and pin-ended braces (see Figure 3.2). This produces axial forces in the braces, and both axial forces and bending moments in the chord. This modelling assumption is particularly appropriate for moving loads along the chord members in structures such as cranes and bridges.

3.2.3 Rigid frame analysis for two- or three-dimensional Vierendeel type girders

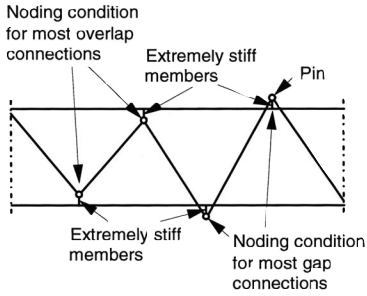

Figure 3.2 – Plane frame joint modelling assumptions

3.3 Nominal Stress Ranges

The determination of nominal stress ranges depends on the method used to determine member forces.

3.3.1 For analysis undertaken using the approach in Section 3.2.1, the nominal stress range in any member can be determined by

$$S_{r,\,ax} = \frac{P_{ax}}{A} \qquad S_{r,\,ipb} = \frac{M_{ipb}}{W_{ipb}} \qquad S_{r,\,opb} = \frac{M_{opb}}{W_{opb}}$$

3.3.2 For analysis undertaken using the approach in Section 3.2.2, the nominal stress range in any member can be determined by

$$S_{r,\,ax} = MF \bullet \frac{P_{ax}}{A} \qquad S_{r,\,ipb} = \frac{M_{ipb}}{W_{ipb}}$$

where MF is the magnification factor given in Tables 2.1 and 2.2.

3.3.3 For analysis undertaken using the approach in Section 3.2.3, the nominal stress range in any member can be determined by the same formulae given in Section 3.3.1.

3.4 SCF Calculations

To determine the hot spot stress ranges along a large number of lines perpendicular to the weld toe by means of strain gauges on test specimens or Finite Element (FE) analysis is typically not feasible for designers. Therefore stress concentration factors (SCFs) are used as simple multiplication factors on the nominal stress range. The SCF is the ratio between the hot spot stress at the joint and the nominal stress in the member due to a basic member load which causes this hot spot stress. It may vary around the perimeter of the joint.

Several fixed lines (called locations of interest) are chosen for a joint, along which the SCFs are determined. The commonly used lines of measurement are given for CHS K-joints in Romeijn et al. (1992) and Karamanos et al. (1997), for RHS T and X-joints in van Wingerde (1992) and for RHS K-joints in Mang et al. (1989) and van Wingerde et al. (1997a). They are shown in detail in Chapters 4 and 5.

Three different levels of SCF calculations are available. They are

- Determine SCFs by experimental testing or FE simulation as described in Appendix C
- Determine SCFs using detailed parametric formulae
- Determine SCFs using simplified parametric formulae or graphs

This design guide will mainly utilise the simplified parametric formulae or graphs for SCF calculation as shown in Chapters 4 and 5. For the detailed parametric formulae, references will be made to the original publications.

If the analysis has been undertaken using the approach in Section 3.2.1, the SCFs can be determined from the analysis or using Chapter 4 (for CHS joints) or Chapter 5 (for RHS joints). If the analysis has been undertaken using the approach in Section 3.2.2 or Section 3.2.3, the SCFs can be calculated using Chapters 4 or 5.

3.5 Hot Spot Stress Ranges

For analysis undertaken using the approach in Section 3.2.1, the hot spot stress ranges can be obtained directly from the analysis for each load combination. In all other cases the following procedures should be used to determine the hot spot stress ranges.

The hot spot stress range at one location under one load case is the product of the nominal stress range and the corresponding stress concentration factor (SCF). Superposition of the hot spot stress ranges at the same location can be used for combined load cases. If the position of the maximum hot spot stress in a member, for the relevant loading condition, cannot be determined, then the maximum SCF values must be applied to all points around the periphery of the member at a joint. Hot spot stress ranges must be calculated for both the chord member and brace members.

Under general loading conditions, the hot spot stress range at any location, in the chord member, is given by:

- For all joints except CHS XX-joints

$$S_{rhs} = SCF_{\text{axial-force-in-brace}} \cdot S_{r,\ \text{axial-force-in-brace}} + SCF_{\text{ipb-in-brace}} \cdot S_{r,\ \text{ipb-in-brace}} + SCF_{\text{opb-in-brace}} \cdot S_{r,\ \text{opb-in-brace}} + SCF_{\text{axial-force-in-chord}} \cdot S_{r,\ \text{axial-force-in-chord}} + SCF_{\text{ipb-in-chord}} \cdot S_{r,\ \text{ipb-in-chord}}$$

For K-joints, $S_{r,\text{axial-force-in-chord}}$ refers to the additional stress range caused by P_{ch} shown in Tables D.3, E.2 and E.3.

- For CHS XX-joints where no MCFs (multiplanar correction factors) are as yet available

$$S_{rhs} = SCF_{\text{axial-force-in-REF-brace}} \cdot S_{r,\ \text{axial-force-in-REF-brace}} + SCF_{\text{ipb-in-REF-brace}} \cdot S_{r,\ \text{ipb-in-REF-brace}} + SCF_{\text{opb-in-REF-brace}} \cdot S_{r,\ \text{opb-in-REF-brace}} + SCF_{\text{axial-force-in-chord}} \cdot S_{r,\ \text{axial-force-in-chord}} + SCF_{\text{axial-force-in-COV-brace}} \cdot S_{r,\ \text{axial-force-in-COV-brace}} + SCF_{\text{opb-in-cov-brace}} \cdot S_{r,\ \text{opb-in-cov-brace}}$$

Under general loading conditions, the hot spot stress range at any location, in the brace member, is given by:

- For all joints except for CHS XX-joints

$$S_{rhs} = SCF_{axial\text{-}force\text{-}in\text{-}brace} \cdot S_{r,\ axial\text{-}force\text{-}in\text{-}brace} + SCF_{ipb\text{-}in\text{-}brace} \cdot S_{r,\ ipb\text{-}in\text{-}brace} + SCF_{opb\text{-}in\text{-}brace} \cdot S_{r,opb\text{-}in\text{-}brace}$$

- For CHS XX-joints where no MCFs (multiplanar correction factors) are as yet availabale

$$S_{rhs} = SCF_{axial\text{-}in\text{-}force\text{-}in\text{-}REF\text{-}brace} \cdot S_{r,\ axial\text{-}force\text{-}in\text{-}REF\text{-}brace} + SCF_{ipb\text{-}in\text{-}REF\text{-}brace} \cdot S_{r,\ ipb\text{-}in\text{-}REF\text{-}brace} + SCF_{opb\text{-}in\text{-}REF\text{-}brace} \cdot S_{r,\ opb\text{-}in\text{-}REF\text{-}brace} + SCF_{axial\text{-}force\text{-}in\text{-}COV\text{-}brace} \cdot S_{r,\ axial\text{-}force\text{-}in\text{-}COV\text{-}brace} + SCF_{opb\text{-}in\text{-}COV\text{-}brace} \cdot S_{r,\ opb\text{-}in\text{-}COV\text{-}brace}$$

For multiplanar joints the load in one brace plane may affect the hot spot stress range in another brace plane. This is called the carry-over effect and is discussed in Sections 4.4 and 4.5.

3.6 Fatigue Strength Curves with Thickness Correction

Similar to the classification method, fatigue strength curves (S_{rhs}-N_f curves) are used in the design, where S_{rhs} is the hot spot stress range. A basic S_{rhs}-N_f curve is used for hollow section joints with a wall thickness of 16 mm (Thorpe and Sharp [1989], DEn [1993], Dimitrakis et al. [1995], van Wingerde et al. [1996, 1997a, 1997b]). For joints with wall thicknesses other than 16 mm, thickness correction factors are introduced. The influence of the thickness effect on fatigue behaviour of hollow section joints has been widely investigated (Gurney [1979], van Delft [1981], Marshall [1984,1992], van Delft et al. [1985], Berge and Webster [1987], Haagensen [1989], Thorpe and Sharp [1989], van Wingerde [1992]). The thickness effect is also recognized in most design recommendations (IIW [1985], DEn [1990], EC3 [1992], AWS [1998]), usually resulting in higher S_{rhs}-N_f curves for smaller wall thicknesses. Two different sets of S_{rhs}-N_f curves were originally developed for RHS joints and CHS joints respectively (van Wingerde et al. [1997b] and Wardenier et al. [1995]).

Most recently, a common set of S_{rhs}-N_f curves and thickness correction formulae have been established (van Wingerde et al. [1997c, 1998a]). Based on the analysis in the data sets for square and circular hollow sections, the DEn T' line (equivalent to a class 114 in EC3, following the criteria of EC3) is recommended as a reference S_{rhs}-N_f line (for 16 mm wall thickness) for joints between both circular and square members. The S_{rhs}-N_f curves with thickness corrections are shown in Figure 3.3. The equations for the S_{rhs}-N_f curves are presented in Table 3.1.

Attention should be paid to the following notes when using Figure 3.3 and Table 3.1.

(1) Figure 3.3 and Table 3.1 only apply to CHS joints with thickness between 4 mm and 50 mm and RHS joints with thickness between 4 mm and 16 mm.
(2) For welded joints with a thickness below 4 mm possible weld defects may overrule the geometrical influence, and sometimes may result in considerably lower fatigue strengths (Wardenier [1982], Puthli et al. [1989], van Wingerde et al. [1996], Mashiri et al. [1998]).
(3) The Constant Amplitude Fatigue Limit and Cut-Off Limit in Figure 3.3 are summarised in Table 3.2.

Table 3.1 – Equations for the S_{rhs}-N_f curves for CHS joints (4 mm ≤ t ≤ 50 mm) and RHS joints (4 mm ≤ t ≤ 16 mm)

for $10^3 < N_f < 5 \cdot 10^6$	$\log(S_{rhs}) = \frac{1}{3} \cdot (12.476 - \log(N_f)) + 0.06 \cdot \log(N_f) \cdot \log\left(\frac{16}{t}\right)$ or $\log(N_f) = \frac{12.476 - 3 \cdot \log(S_{rhs})}{1 - 0.18 \cdot \log\left(\frac{16}{t}\right)}$
for $5 \cdot 10^6 < N_f < 10^8$ (variable amplitude only)	$\log(S_{rhs}) = \frac{1}{5} \cdot (16.327 - \log(N_f)) + 0.402 \cdot \log\left(\frac{16}{t}\right)$ or $\log(N_f) = 16.327 - 5 \cdot \log(S_{rhs}) + 2.01 \cdot \log\left(\frac{16}{t}\right)$

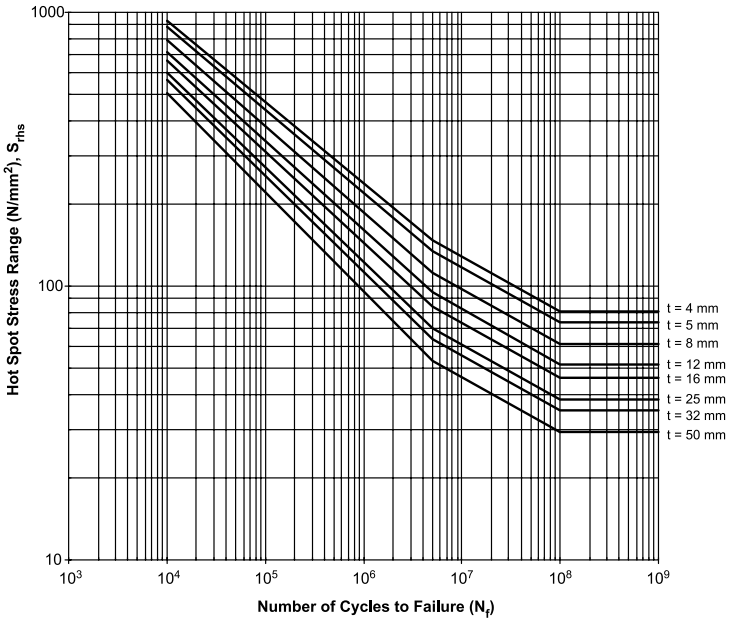

Figure 3.3 – Fatigue strength curves for CHS joints (4 mm ≤ t ≤ 50 mm) and RHS joints (4 mm ≤ t ≤ 16 mm) according to the hot spot stress method

Table 3.2 – The Constant Amplitude Fatigue Limit and Cut-Off Limit in Figure 3.3

Section Type	Thickness (mm)	Constant Amplitude Fatigue Limit (N/mm²)	Cut-Off Limit (N/mm²)
CHS & RHS	4	147	81
	5	134	74
	8	111	61
	12	95	52
	16	84	46
	25	71	39
CHS	32	64	35
	50	53	29

4 SCF Calculations for CHS Joints

The SCF calculations for CHS joints are described in this chapter. A summary is given in Table 4.1 where relevant Tables and Figures can be found. A minimum SCF = 2.0 is recommended as explained in Appendix C.1 unless otherwise specified such as “negligible“ or ”no minimum SCF value required“.

Table 4.1 – Summary of SCF calculations for CHS joints

Type of joints	Tables and Figures for SCF calculations
uniplanar CHS T and Y-joints	Table D.1 Figures 4.2 to 4.4
uniplanar CHS X-joints	Table D.2 Figures 4.6 to 4.8
uniplanar CHS K-joints with gap	Table D.3
multiplanar CHS XX-joints	Table D.4
multiplanar CHS KK-joints with gap	Table D.3 and Table 4.2

4.1 Uniplanar T and Y-Joints

Definition of the joint
A uniplanar CHS T or Y-joint is shown in Figure 4.1 where the geometric parameters (γ, τ, β, θ and α) and locations of interest (crown and saddle) are defined.

Typical SCF formulae
The SCF calculations for this type of joint are based on the work of Efthymiou and Durkin (1985) and Efthymiou (1988). A typical SCF equation for the chord crown location in a Y-joint under axial load is given below.

$$SCF = \gamma^{0.2}\tau(2.65 + 5(\beta - 0.65)^2) + \tau\beta(0.5\ C\ \alpha - 3)\sin\theta$$

It can be seen that the SCF is a function of γ, τ, β, θ, α and C. The factor C corresponds to the chord-end fixity. In the case of fully fixed chord-ends, C is taken as 0.5. If the chord-ends are pinned, C is taken as 1.0. A typical value for C is found to be 0.7 (Efthymiou [1988]). When α is less than 12, a short chord correction factor is used to take account of the reduced deformation and stresses in short chords.

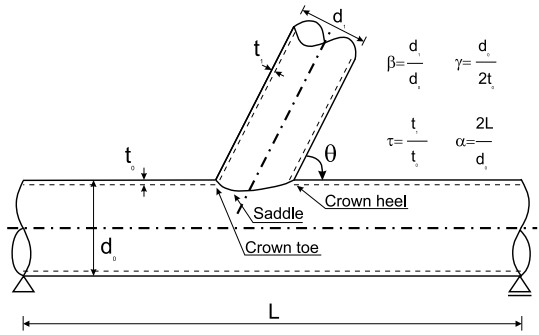

Figure 4.1 – A uniplanar CHS T or Y-joint

Insight into parameters

The SCFs for limited joint configurations are shown graphically in Figures 4.2 to 4.4 for CHS T-joints under axial load, in-plane bending and out-of-plane bending respectively. The following conclusions can be made for the chord and brace:

- Generally the highest SCF occurs at the saddle position
- Highest SCFs at the saddle are obtained for medium β ratios
- SCF decreases with decreasing τ value except for the brace crown position under axial loading
- SCF decreases with decreasing 2γ value except for the brace crown position under axial loading

It should be noted that in the case of $\beta \geq 0.95$, use SCFs for $\beta = 0.95$.

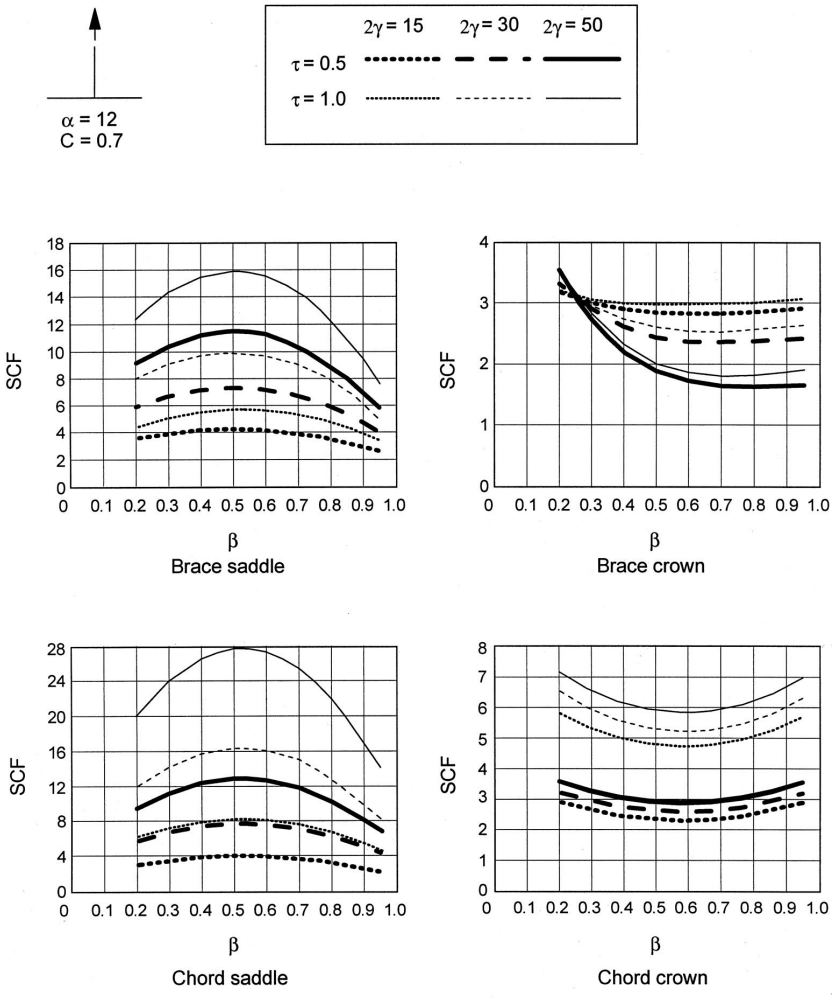

Figure 4.2 – SCFs for CHS T-joints under axial loading (α = 12 and C = 0.7)

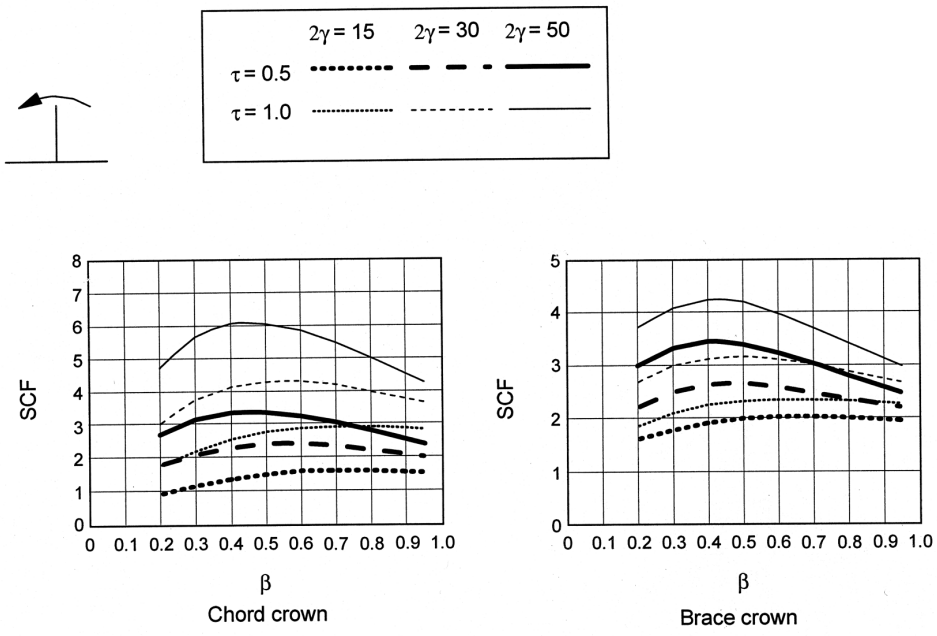

Figure 4.3 – SCFs for CHS T-joints under in-plane bending moment (α = 12)

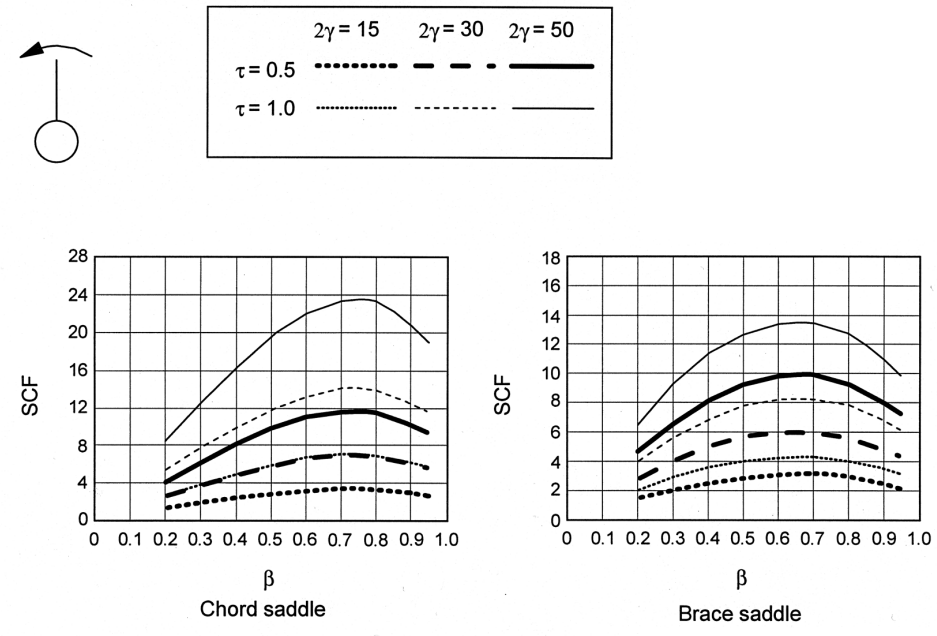

Figure 4.4 – SCFs for CHS T-joints under out-of-plane bending moment (α = 12)

Detailed formulae and graphs
The graphs in Figures 4.2 to 4.4 may be used to get a quick estimation of SCFs. The SCF equations for all the locations of interest (chord saddle, chord crown, brace saddle and brace crown) in T and Y-joints under axial load, in-plane bending and out-of-plane bending are given in Appendix D.1 with the range of validity as listed below.

$0.2 \le \beta \le 1.0$
$15 \le 2\gamma \le 64$
$0.2 \le \tau \le 1.0$
$4 \le \alpha \le 40$
$30^{o} \le \theta \le 90°$

4.2 Uniplanar X-Joints

Definition of the joint
A uniplanar CHS X-joint is shown in Figure 4.5 where the geometric parameters (γ, τ, β, θ and α) and locations of interest (crown and saddle) are defined.

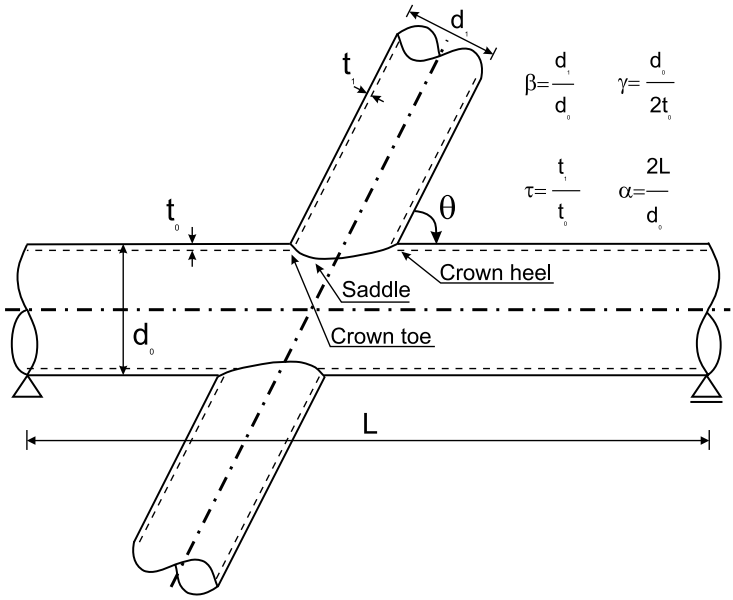

Figure 4.5 – A uniplanar CHS X-joint

Typical SCF formulae
The SCF calculations for this type of joint are based on the work of Efthymiou and Durkin (1985) and Efthymiou (1988). A typical SCF equation for the chord crown location in an X-joint under axial load is given below.

$$SCF = \gamma^{0.2}\,\tau(2.65 + 5(\beta - 0.65)^2) - 3\tau\beta\sin\theta$$

It can be seen that the SCF is a function of γ, τ, β and θ. When α is less than 12, a short chord correction factor is used to take account of the reduced deformation and stresses in short chords.

Insight into parameters

The SCFs for certain joint configurations are shown graphically in Figures 4.6 to 4.8 for CHS X-joints under axial load, in-plane bending and out-of-plane loading respectively. Similar conclusions can be made as for the T and Y-joints shown in Section 4.1. It should be noted that in the case of $\beta \geq 0.95$, use SCFs for $\beta = 0.95$.

Detailed formulae and graphs

The graphs in Figures 4.6 to 4.8 may be used to get a quick estimation of SCFs. The SCF equations for all the locations of interest (chord saddle, chord crown, brace saddle and brace crown) in X-joints under axial load, in-plane bending and out-of-plane bending are given in Appendix D.2 with the range of validity as listed below.

$0.2 \leq \beta \leq 1.0$
$15 \leq 2\gamma \leq 64$
$0.2 \leq \tau \leq 1.0$
$4 \leq \alpha \leq 40$
$30^{o} \leq \theta \leq 90°$

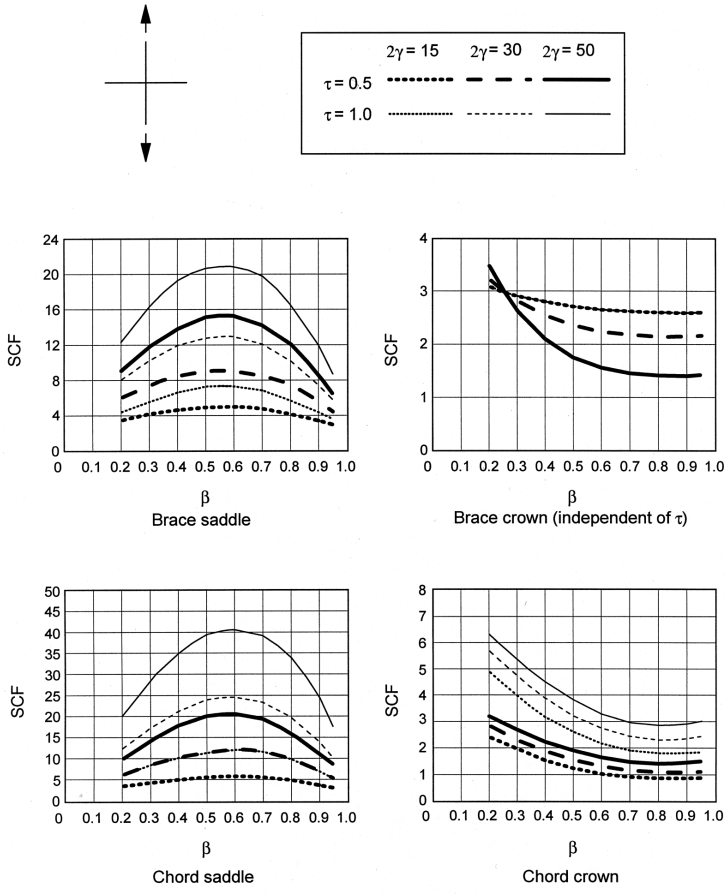

Figure 4.6 – SCFs for CHS X-joints under axial loading (α = 12 and C = 1)

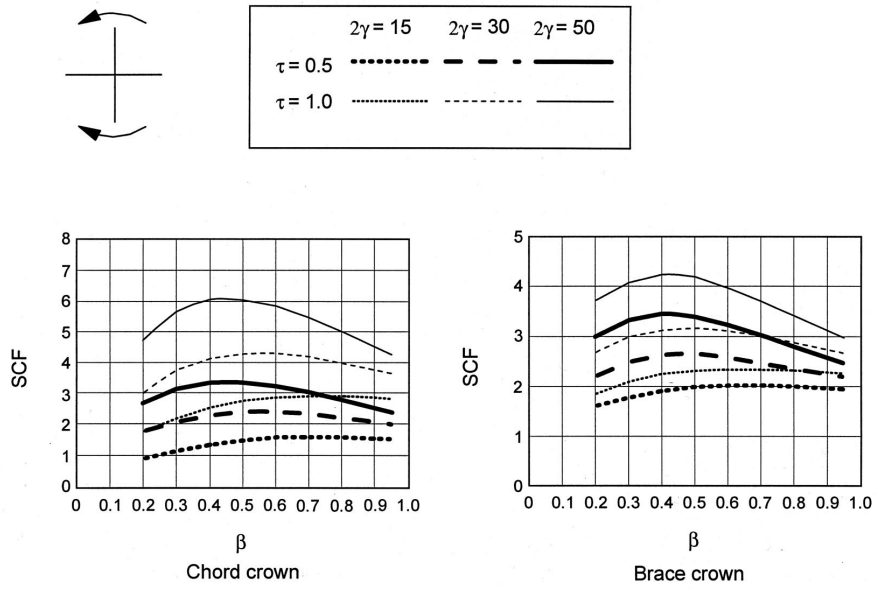

Figure 4.7 – SCFs for CHS X-joints under in-plane bending moment (α = 12)

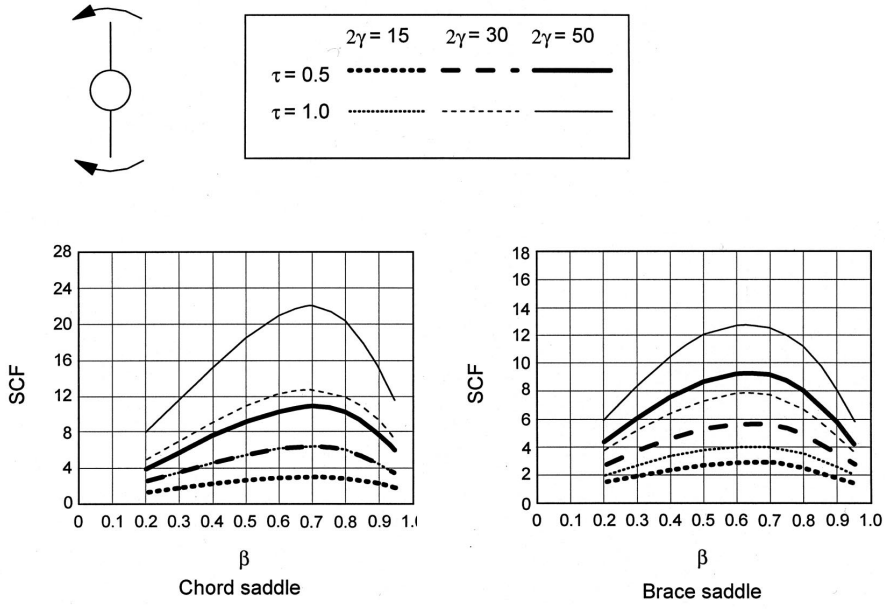

Figure 4.8 – SCFs for CHS X-joints under out-of-plane bending moment (α = 12)

4.3 Uniplanar K-Joints with Gap

Definition of the joint
A uniplanar CHS K-joint with gap is shown in Figure 4.9 where the geometric parameters and locations of interest (1 to 4) are defined. In general, for chord locations and for balanced load, the hot spot is located at either the crown toe (location 1) or the chord saddle (location 2). For braces, the hot spot locations vary depending on the joint parameters, but in general, the brace crown heel (location 3) and brace saddle (location 4) are the hot spot locations.

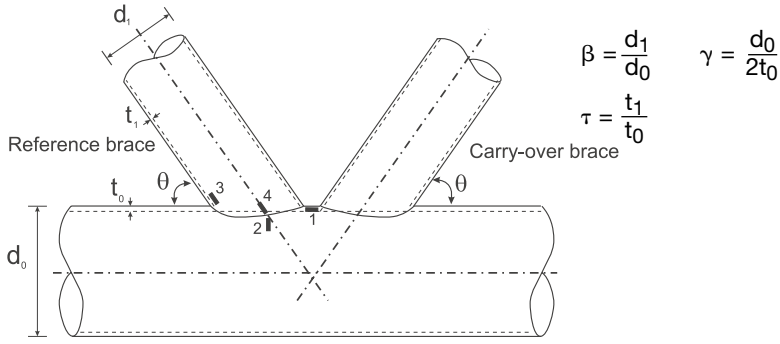

Figure 4.9 – A uniplanar CHS K-joint with gap

Typical SCF formulae
The SCF calculations for this type of joint are based on the work of Romeijn (1994), Dijkstra et al. (1996) and Karamanos et al. (1997) and subsequent simplifications by van Wingerde et al. (1998a). The general format is similar to that given in IIW (1985), i.e. presenting diagrams of SCFs for different values of β and θ and for some constant basic values of γ and τ (i.e. γ_o, τ_o). The values of 12 and 0.5 were chosen as a basis for γ_o and τ_o respectively, and the corresponding stress concentration factor will be denoted as the reference value SCF_o. A typical SCF formula can be expressed as

$$SCF = \left(\frac{\gamma}{\gamma_0}\right)^{\chi_1} \cdot \left(\frac{\tau}{\tau_o}\right)^{\chi_2} SCF_0 = \left(\frac{\gamma}{12}\right)^{\chi_1} \cdot \left(\frac{\tau}{0.5}\right)^{\chi_2} \cdot SCF_0$$

The exponents χ_1 and χ_2 depend on the loading type and the location of interest, which may vary from 0 to 1.1. The values of χ_1, χ_2 and SCF_o are given in Table D.3 in Appendix D.

Insight into parameters
From the general equation, the following conclusions can be made as for CHS T, Y and X-joints

- SCF decreases with decreasing τ value
- SCF decreases with decreasing 2γ value

From the graphs in Appendix D.3, the following conclusions can be made

- For basic balanced axial load, SCF decreases as θ decreases
- For basic balanced axial load, SCF decreases as β increases
- For chord load, SCF decreases as θ increases

Detailed formulae and graphs
The SCF equations for chord and braces in CHS K-joints with gap subjected to basic balanced axial load and chord load are given in Appendix D.3 with the range of validity as listed below.

No eccentricity
Equal braces
$0.3 \le \beta \le 0.6$
$24 \le 2\gamma \le 60$
$0.25 \le \tau \le 1.0$
$30^{o} \le \theta \le 60°$

4.4 Multiplanar XX-Joints

Definition of the joint
A multiplanar CHS XX-joint is shown in Figure 4.10 where the geometric parameters and locations of interest are defined. Four locations in this type of joint are considered as being critical, i.e.
location 1: chord crown
location 2: chord saddle
location 3: brace crown in reference brace
location 4: brace saddle in reference brace

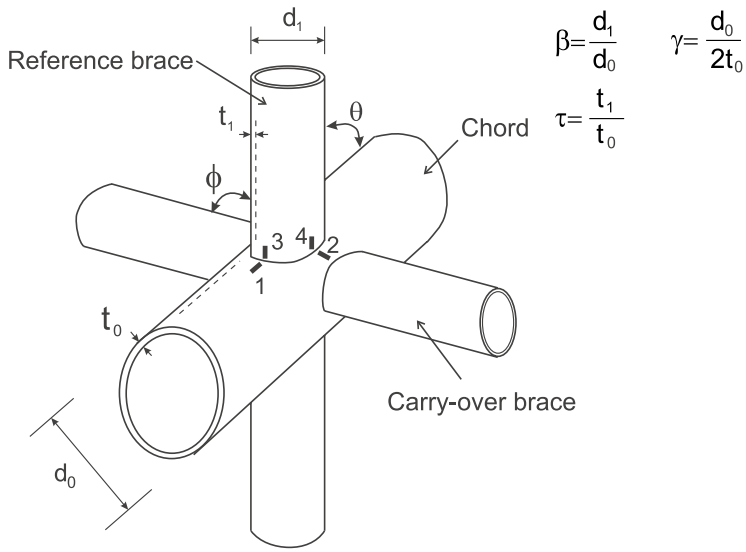

Figure 4.10 – A multiplanar CHS XX-joint

Typical SCF formulae
The SCF calculations for this type of joint are based on the work by Romeijn (1994), Dijkstra et al. (1996) and Karamanos et al. (1997). Four load cases are considered, namely

1. only axial balanced brace loading
2. only balanced in-plane bending on reference braces
3. only balanced out-of-plane bending on reference braces
4. only axial balanced chord loading

Similar to uniplanar K-joints, this Guide is aimed at proposing simplified equations and/or graphs for predicting SCFs in multiplanar XX-joints. The general format for SCFs for all types of loading can be expressed as

$$SCF = \left(\frac{\gamma}{\gamma_0}\right)^{\chi_1} \cdot \left(\frac{\tau}{\tau_o}\right)^{\chi_2} SCF_0 = \left(\frac{\gamma}{12}\right)^{\chi_1} \cdot \left(\frac{\tau}{0.5}\right)^{\chi_2} \cdot SCF_0$$

The values for the exponents (χ_1 and χ_2) and the SCF_o are given in Appendix D.4.

Insight into parameters
Similar conclusions can be made as for uniplanar CHS X-joints.

For multiplanar joints the load in one brace plane may effect the hot spot stress range in another brace plane. This is called the multiplanar effect or Carry-over effect.

This effect is considered only at the saddle locations for axial loading of the brace members or out-of-plane bending. In-plane bending does not introduce any multiplanar phenomena.

The chord axial loading effects are concentrated only on crown locations of the chord.

Detailed formulae and graphs
The detailed SCF formulae and graphs for multiplanar CHS XX-joints are summarised in Appendix D.4. The ranges of validity in calculating SCFs for multiplanar XX-joints are listed below.

No eccentricity
Equal braces
$0.3 \le \beta \le 0.60$
$15 \le 2\gamma \le 64$
$0.25 \le \tau \le 1.0$
$\theta = 90°$
$\phi = 90°$
$\psi = \phi - 2 \arcsin(\beta) \ge 16.2°$

4.5 Multiplanar KK-Joints with Gap

Definition of the joint
A multiplanar CHS KK-joint is shown in Figure 4.11 where the geometric parameters and locations of interest are defined. Six locations in this type of joint are considered as being critical, ie.

location 1: chord crown toe
location 2: chord near-saddle
location 3: chord far-saddle
location 4: brace crown heel in reference brace
location 5: brace near-saddle in reference brace
location 6: brace far-saddle in reference brace

Typical SCF formulae
The SCF calculations for this type of joint are based on the work by Romeijn et al. (1993), Romeijn (1994), Dijkstra et al. (1996) and Karamanos et al. (1997) and subsequent simplifications by van Wingerde et al. (1998b). Two load cases are considered, namely

1. only axial balanced brace loading
2. only chord loading (axial and bending)

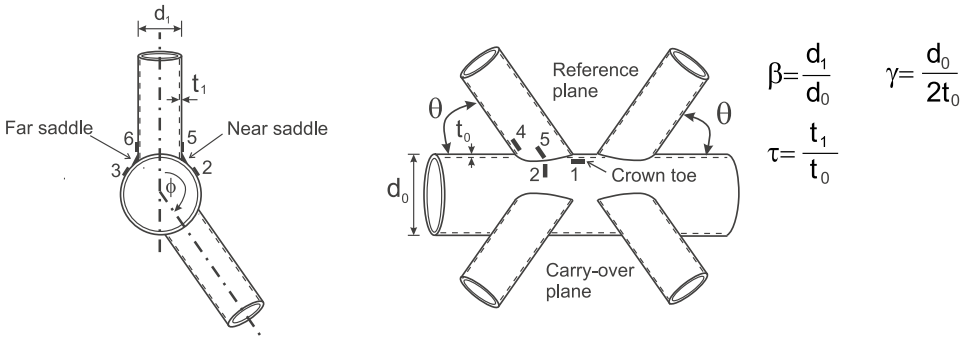

Figure 4.11 – A multiplanar CHS KK-joint

The axial balanced brace loading condition is defined in Figure 4.12. The braces of the joint can be considered as either braces in a reference plane or braces in a carry-over plane. The loads in both planes may be different and are related to each other by a factor m.

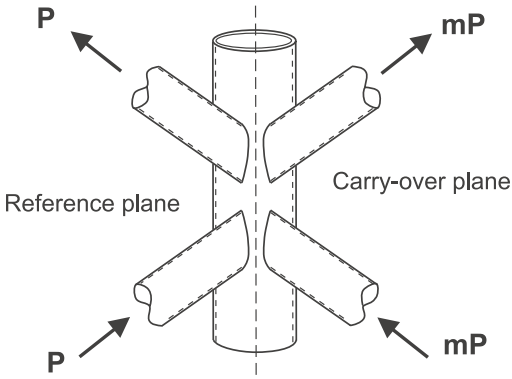

value of m	referred to as
1	symmetrical loading
0	reference-plane loading
–1	anti-symmetrical loading

Figure 4.12 – Axial balanced loading condition in multiplanar CHS KK-joints

The SCFs for multiplanar CHS KK-joints can be determined using the SCFs for uniplanar CHS K-joints (SCF_K) with two correction factors (f_{geom} and f_{load}) accounting for the effects of geometry and loading (Dijkstra et al. [1996] and Karamanos et al. [1997]). The general format is

$$SCF_{KK} = f_{geom}\, f_{load}\, SCF_K$$

The product of the two factors (f_{geom} and f_{load}) varies from 1.0 to 1.25 depending on the geometric parameters and the load conditions. A single factor called the Multiplanar Correction Factor (MCF) is adopted for simplicity (van Wingerde et al. [1998b]). The general format is

$$SCF_{KK} = MCF \cdot SCF_K$$

The values of MCF for $\phi = 180°$ are 1.0 for all m values. The values of MCF for $\phi \leq 90°$ are given in Table 4.2. Interpolation is allowed for m between 0 and –1, and for ϕ between 90° and 180°.

Table 4.2 – Multiplanar correction factors (MCFs) on SCFs for CHS KK-joints with gap ($\phi \leq$ 90°)

Load Case	chord			brace		
	m = +1	m = 0	m = –1	m = +1	m = 0	m = –1
axial balanced brace loading	1.0	1.0	1.25	1.0	1.0	1.25
chord loading	1.0	1.0	1.0	1.0	1.0	1.0

Insight into parameters
Similar conclusions can be made as for uniplanar CHS K-joints.

For axial balanced brace loading, the multiplanar effects are only considered for the anti-symmetrical load case (m = -1). For chord loading, no multiplanar correction is needed.

Detailed formulae and graphs
The detailed SCF formulae and graphs for uniplanar CHS K-joints are summarised in Appendix D.3. The Multiplanar Correction Factors (MCFs) are listed in Table 4.2. It must be noted that the actual SCF value (even if it is less than 2.0) for uniplanar CHS K-joints should be used. The minimum SCF value of 2.0 for multiplanar CHS KK-joints should be considered after multiplying the MCF factor. The ranges of validity in calculating SCFs for multiplanar CHS KK-joints are listed below.

No eccentricity
Equal braces
$0.3 \leq \beta \leq \cos(\theta)$
$24 \leq 2\gamma \leq 48$
$0.25 \leq \tau \leq 1.0$
$30° \leq \theta \leq 60°$
$60° \leq \phi \leq 180°$

5 SCF Calculations for RHS Joints

The SCF calculations for RHS joints are described in this chapter. A summary is given in Table 5.1 where relevant tables and Figures can be found. A minimum SCF = 2.0 is recommended as explained in Appendix C.1 unless otherwise specified such as “negligible” or “no minimum SCF values required“. The SCFs given in this section are valid for square hollow section braces and rectangular hollow section chords with h_o/b_o between 0.75 and 1.5.

Table 5.1 – Summary of SCF calculations for RHS joints

Type of joints	Tables and Figures for SCF calculations
uniplanar RHS T and X-joints	Table E.1, Figures 5.2 to 5.4
uniplanar RHS K-joints with gap	Table E.2, Figures E.1 to E.8
uniplanar RHS K-joints with overlap	Table E.3, Figures E.9 to E.17
multiplanar RHS KK-joints	Table E.2 and Table 5.2

5.1 Uniplanar T and X-Joints

Definition of the joint
A uniplanar RHS T-joint is shown in Figure 5.1 where the geometric parameters and locations of interest (lines of measurement A to E) are defined.

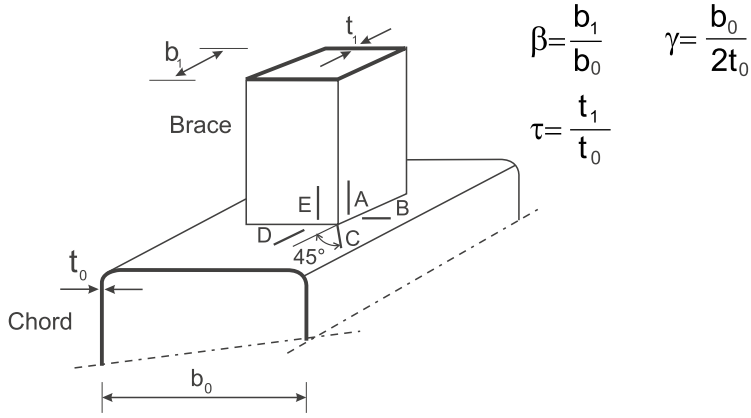

Figure 5.1 – A uniplanar RHS T or X-joint

Typical SCF formulae
The SCF calculations for this type of joint are based on the work by van Wingerde (1992). The general format of the SCF formulae is

$$SCF = (a + b\,\beta + c\,\beta^2 + d\,2\gamma)\,(2\gamma)^{(e+f\beta+g\beta^2)}\;\tau^h$$

where the constants a, b, c, d, e, f, g and h change for each location of interest (lines A to E) and applied loading (in-plane bending on brace, axial loading on brace or chord load). When the load is applied on the chord, the SCF formula is simplified to

$$SCF = a\,(2\gamma)^{e\beta}\;\tau^h$$

Insight into parameters
As an indication, the stress concentration factors are given in Figures 5.2 to 5.4 for some joint configurations. The following observations can be made:

- The highest SCFs generally occur in the chord (for $\tau = 1$) at locations B and C.
- The highest SCFs are found for medium β ratios.
- The lower the 2γ ratio, the lower is the SCF.
- The lower the τ ratio, the lower is the SCF in the chord, whereas it has less influence for the brace.

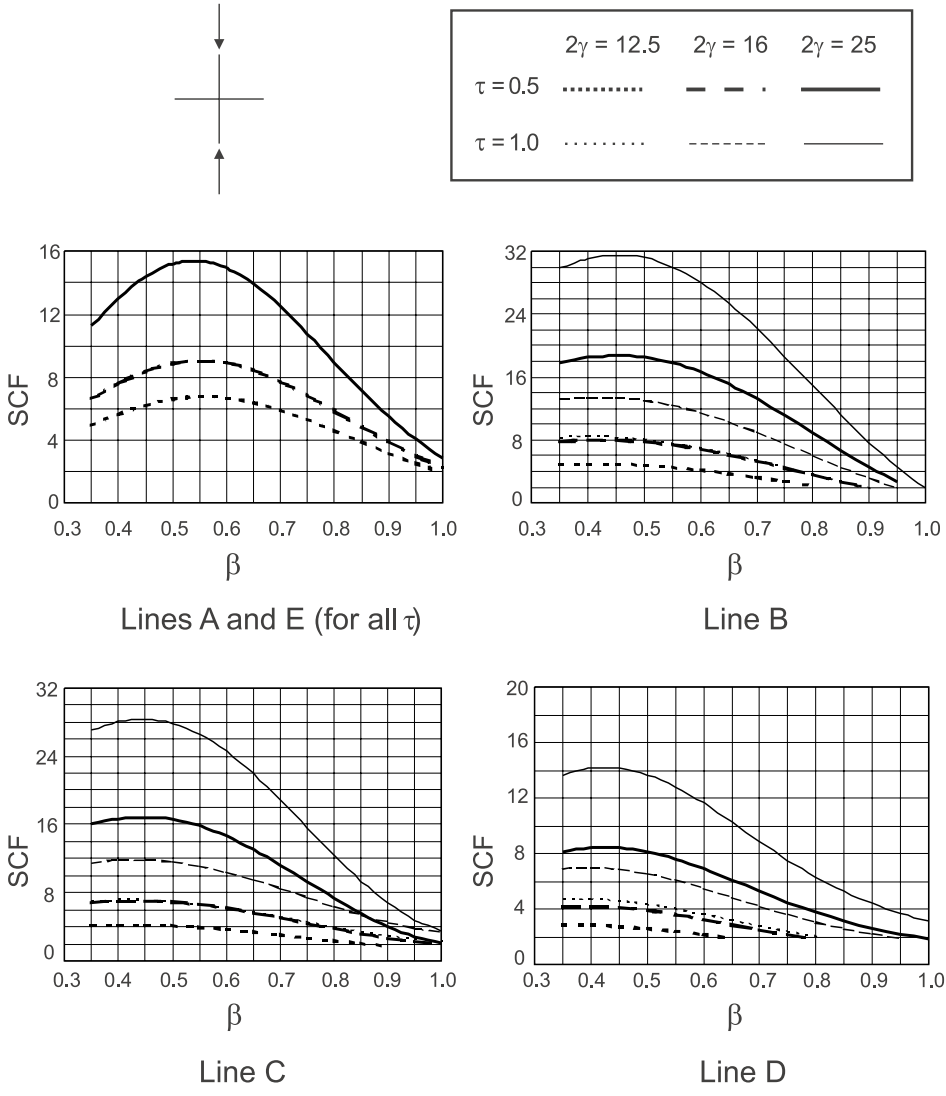

Figure 5.2 – SCFs for T and X-joints of square hollow sections loaded by an axial force on the brace

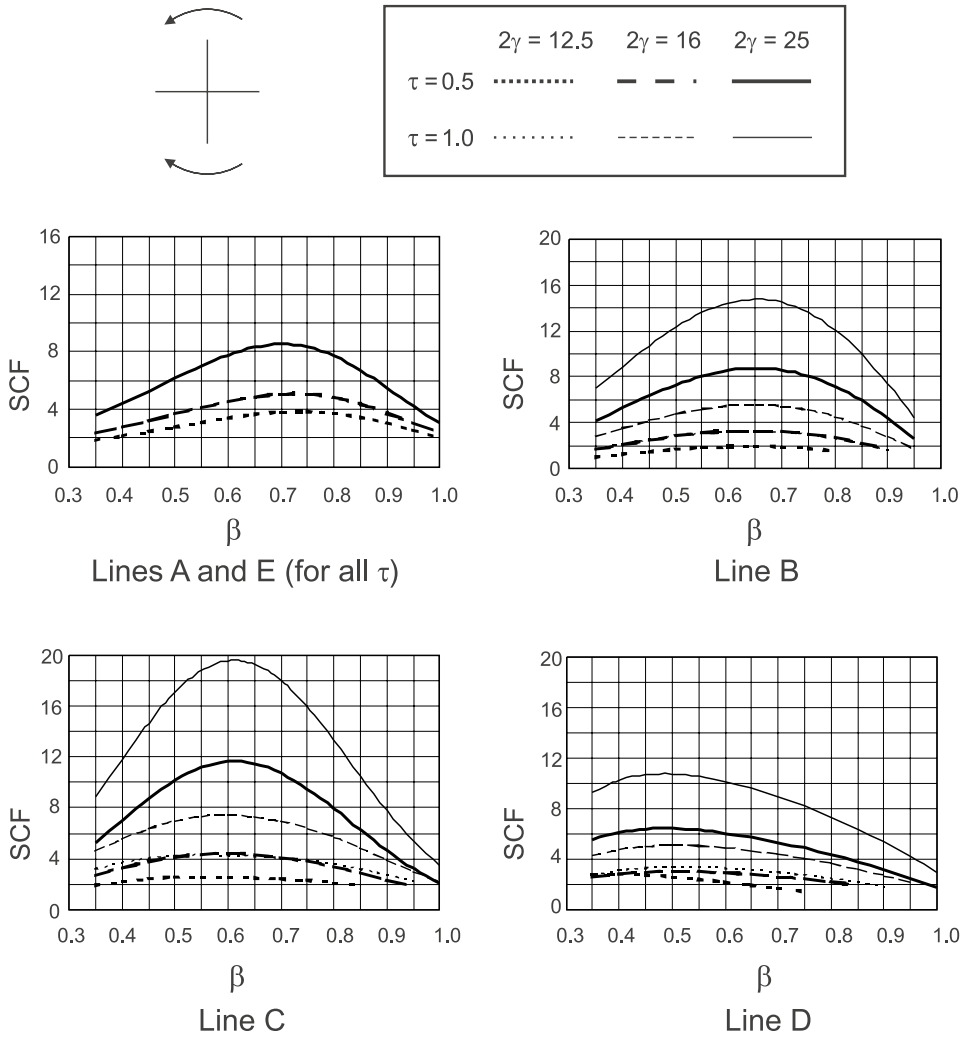

Figure 5.3 – SCFs for T and X-joints of square hollow sections loaded by an in-plane bending moment on the brace

Detailed formulae and graphs

Detailed equations are given in Appendix E.1 for lines of measurement A to E and for different loading conditions with the range of validity listed below.

$0.35 \leq \beta \leq 1.0$
$12.5 \leq 2\gamma \leq 25.0$
$0.25 \leq \tau \leq 1.0$

Attention should be paid to the following notes when using the SCF formulae:

- The effect of bending in the chord for a T-joint, due to the axial force on the brace, should be included separately in the analysis.
- For fillet welded connections: multiply SCFs for the brace by 1.4.

- For non-90° RHS X-joints, SCFs can be determined using SCFs for 90° RHS X-joints with some correction factors (Packer and Wardenier [1998]), i.e.:

  For lines B, C and D on the chord, $SCF_\theta = 1.2 \cdot SCF_{\theta=90°} \cdot \sin^2\theta$
  For lines A and E on the brace, $SCF_\theta = 1.2 \cdot SCF_{\theta=90°} \cdot \sin\theta$
  The above two formulae are valid for $40° \le \theta \le 80°$.

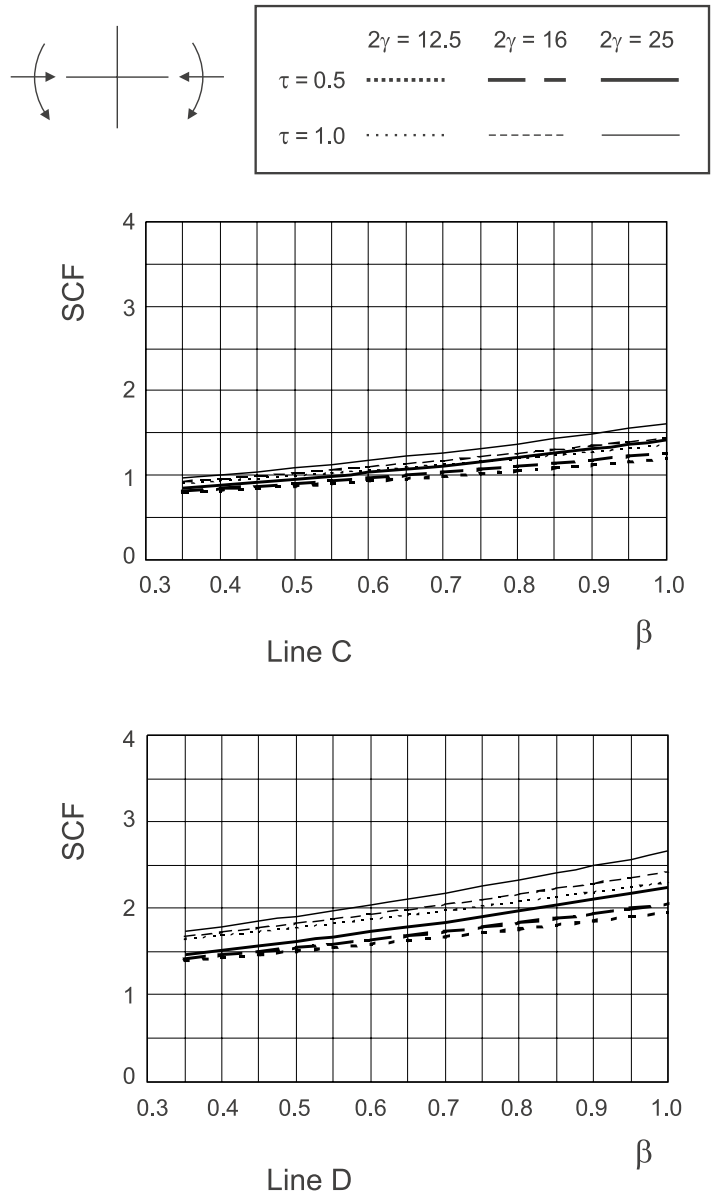

Figure 5.4 – SCFs for T and X-joints of square hollow sections loaded by an axial force or in-plane bending moment on the chord

5.2 Uniplanar K-Joints with Gap

Definition of the joint
A uniplanar RHS K-joint with gap is shown in Figure 5.5 where the locations of interest (lines A to E) are defined.

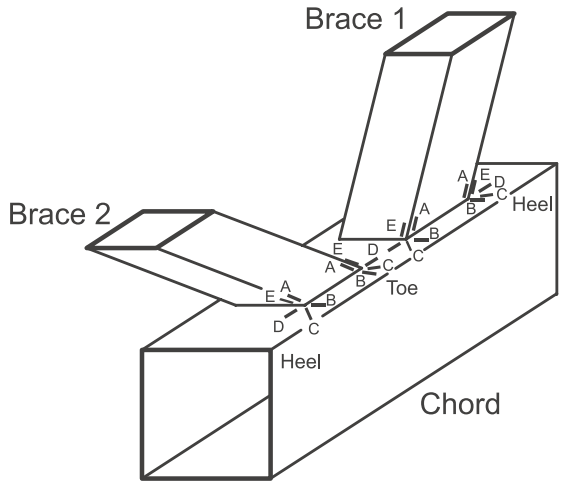

Figure 5.5 – A uniplanar RHS K-joint with gap

Typical SCF formulae
The SCF formulae for this type of joint were derived by van Wingerde et al. (1996), where about 36 formulae were given. These formulae give SCF values for the locations of interest (lines A to E) shown in Figure 5.5. Simplified formulae are given by van Wingerde et al. (1997a, 1997b), where the number of formulae is reduced to three. The simplified formulae correspond to the maximum SCF in chord and brace, and are more conservative (Puthli and Herion [1996], Zhao and Puthli [1998]).

For balanced axial loading, the general format of SCFs can be expressed as (Puthli and Herion [1996]):

$$SCF = f(\beta, 2\gamma, \tau, \theta, g') = SCF_0 \cdot f(2\gamma, \tau)$$

The reference value SCF_0 is the SCF for $2\gamma = 24$ and $\tau = 0.5$. For other values of 2γ and τ a correction factor $f(2\gamma, \tau)$ should be multiplied to SCF_0.

For chord loading, only the SCF in the chord needs to be considered. The formula for the SCF is

$$SCF = (2.45 + 1.23 \cdot \beta) \cdot g'^{-0.27}$$

Insight into parameters
The following conclusions can be made based on the graphs shown in Appendix E.2.

- Highest SCFs occur around medium β ratios
- For chord, SCF decreases as 2γ decreases, and SCF decreases as τ decreases
- For brace, SCF decreases as 2γ decreases, and SCF decreases as τ increases

Detailed formulae and graphs
Detailed expressions of SCF = f(β, 2γ, τ, θ, g´) are given in Appendix E.2 with the range of validity listed below.

$0.35 \le \beta \le 1.0$
$10 \le 2\gamma \le 35$
$0.25 \le \tau \le 1.0$
$30° \le \theta \le 60°$
$2\tau \le g´$
$-0.55 \le e/h_0 \le 0.25$

Graphs for the reference value SCF_0 and the correction factor f(2γ, τ) are also given in Appendix E.2. The SCF_0 of the chord is plotted against β, with different lines for θ = 30°, 45° and 60°, in different graphs for g´ = 1, 2, 4 and 8. For the brace, one graph containing the SCF_0 against β for θ = 30°, 45° and 60° is sufficient, since the gap has only a very small influence on the maximum SCF of the brace. Interpolation is allowed between the lines for other angles and between the graphs for other gaps.

5.3 Uniplanar K-Joints with Overlap

Definition of the joint
A uniplanar RHS K-joint with overlap is shown in Figure 5.6 where the locations of interest (lines A to E) are defined.

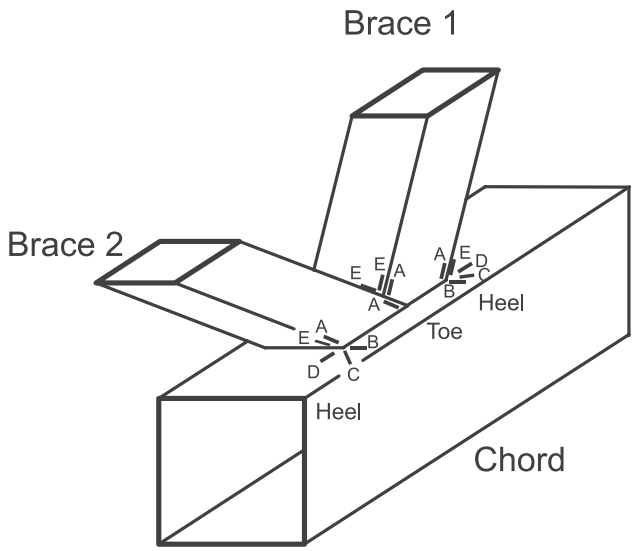

Figure 5.6 – A uniplanar RHS K-joint with overlap

Typical SCF formulae
The SCF formulae for this type of joint were derived by van Wingerde et al. (1996), where about 60 formulae were given. These formulae give SCF values for the locations of interest (lines A to E) shown in Figure 5.6. Simplified formulae are given by van Wingerde et al. (1997a, 1997b), where the number of formulae is reduced to three. The simplified formulae correspond to the maximum SCF in chord and brace, and are more conservative.

For balanced axial loading, the general format of SCFs can be expressed as

$SCF = f(\beta, 2\gamma, \tau, \theta, O_v) = SCF_0 (\beta, \theta, O_v) \cdot f(2\gamma, \tau)$

The reference value SCF_0 is the SCF for $2\gamma = 24$ and $\tau = 0.5$. For other values of 2γ and τ a correction factor $f(2\gamma, \tau)$ should be multiplied to SCF_o.

For chord loading, only the SCF in the chord needs to be considered. The formula for the SCF is

$SCF = 1.2 + 1.46 \cdot \beta - 0.028 \cdot \beta^2$

Insight into parameters
The following conclusions can be made based on the graphs shown in Appendix E.3.

- Highest SCFs occur around medium β ratios for RHS K-joints with 50% overlap
- For chord, SCF decreases as 2γ decreases, and SCF decreases as τ decreases
- For brace, SCF decreases as 2γ decreases, and SCF decreases as τ increases
- SCFs for overlapped K-joints are generally lower than those for gapped K-joints

Detailed formulae and graphs
Detailed expressions of $SCF = f(\beta, 2\gamma, \tau, \theta, O_v)$ are given in Appendix E.3 with the range of validity listed below.

Equal braces
$0.35 \le \beta \le 1.0$
$10 \le 2\gamma \le 35$
$0.25 \le \tau \le 1.0$
$30° \le \theta \le 60°$
$50\% \le O_v \le 100\%$
$-0.55 \le e/h_o \le 0.25$

Graphs for the reference value SCF_0 and the correction factor $f(2\gamma, \tau)$ are also given in Appendix E.3. The graphs for SCF_0 show the SCF against β, with different lines for $\theta = 30°$, 45°, 60°, in graphs for 50%, 75% and 100% overlap. Interpolation is allowed between the lines for other angles and between the graphs for other overlaps.

5.4 Multiplanar KK-Joints with Gap

Definition of the joint
A multiplanar RHS KK-joint is shown in Figure 5.7 where the geometric parameters are defined.

Typical SCF formulae
The SCFs for multiplanar RHS KK-joints can be determined using the SCFs for uniplanar RHS K-joints (SCF_K) with a Multiplanar Correction Factor (MCF) accounting for the effects of geometry and loading (van Wingerde et al. [1998b]), i.e.:

$SCF_{KK} = MCF \cdot SCF_K$

The values of MCF for $\phi \le 90°$ are given in Table 5.2 where the term “m” has the same definition as that used for multiplanar CHS KK-joints shown in Figure 4.12. The values of MCF for $\phi = 180°$ are 1.0 for all m values. Interpolation is allowed for m between 0 and –1, and for ϕ between 90° and 180°.

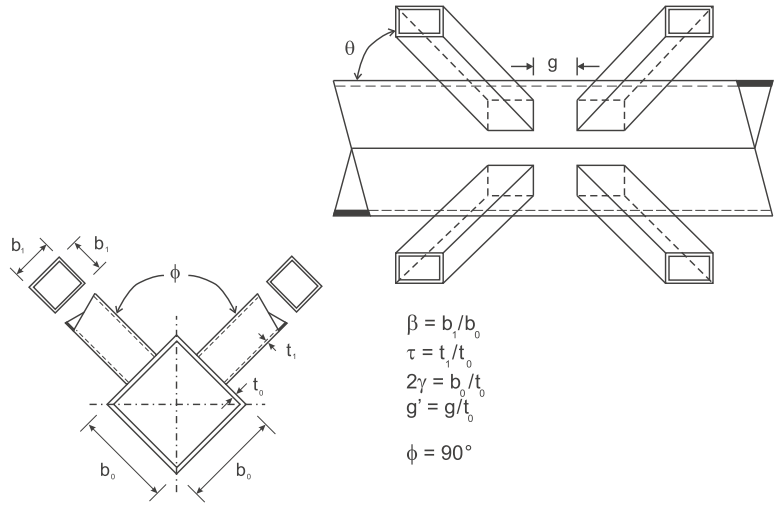

Figure 5.7 – A multiplanar RHS KK-joint with gap

Table 5.2 – Multiplanar correction factors on SCFs for RHS KK-joints with gap ($\phi \leq 90°$)

Load Case	chord			brace		
	m = +1	m = 0	m = –1	m = +1	m = 0	m = –1
axial balanced brace loading	1.0	1.0	1.25	1.0	1.0	1.25
chord loading	1.0	1.0	1.0	1.0	1.0	1.0

Insight into parameters
Similar conclusions can be made as for uniplanar RHS K-joints with gap.

For axial balanced brace loading, the multiplanar effects are only considered for the anti-symmetrical load case (m = –1). For chord loading, no multiplanar correction is needed.

Detailed formulae and graphs
The detailed SCF formulae and graphs for uniplanar RHS K-joints with gap are summarised in Appendix E.2. The Multiplanar Correction Factors (MCFs) are listed in Table 5.2. It must be noted that the actual SCF value (even if it is less than 2.0) for uniplanar RHS K-joints should be used. The minimum SCF value of 2.0 for multiplanar RHS KK-joints should be considered after multiplying the MCF factor. The ranges of validity in calculating SCFs for multiplanar RHS KK-joints are listed below.

Equal braces
$0.25 \leq \beta \leq 0.60$
$12.5 \leq 2\gamma \leq 25$
$0.5 \leq \tau \leq 1.0$
$30° \leq \theta \leq 60°$
$2\tau \leq g'$
$-0.55 \leq e/h_o \leq 0.25$
$60° \leq \phi \leq 180°$

6 Structural Detailing for Fatigue and Reinforcement

6.1 Structural Detailing for Fatigue

6.1.1 Design parameters

The principle that good design and fabrication can considerably reduce the total costs of a structure applies just as well to those structures made from hollow sections as to those made of other sections. This is particularly true for structures subjected to fatigue loading, where both a poor design and poor fabrication and welding can result in significantly more fatigue damage than expected.

Optimal fatigue design is obtained when the SCFs are as low as possible. Considering the influence of all parameters mentioned in Chapters 4 and 5, the following guidelines can be made:

- Avoid medium β ratios; β ratios close to 1.0 give the lowest SCFs
- Make the wall thickness of the bracing as small as possible with respect to that of the chord (i.e. low τ ratio)
- Select relatively thick walled chords (i.e. low 2γ ratio)
- Select overlap K-joints over gap K-joints
- Select butt (groove) welds over fillet welds

Fatigue cracks always occur at a discontinuity or stress raiser. In the case of welded connections this is nearly always associated with a microscopic defect at the weld toe. As a result, fatigue cracks initiate at these locations irrespective of the steel grade. Higher grades of steel can be used, but unless some form of post weld improvement is carried out the fatigue life will not necessarily increase.

6.1.2 Structural details

Welding details, sequences, procedures, etc. will not be provided in this design guide, since they have already been extensively described in two previous CIDECT Design Guides Nos. 6 and 7 (Wardenier et al. [1995], Dutta et al. [1997]). However, for convenience, Figures 6.1 and 6.2 show typical weld details at the main locations of a T-joint constructed with circular and rectangular hollow sections respectively.

Weld start/stop positions for non-continuous welds should not be located at points of high stress concentration, since these can themselves cause stress concentrations. Figure 6.3 shows the recommended locations for these weld start/stop positions (Wardenier et al. [1995]). For RHS braces weld start/stop positions should be sufficiently away from the corners and in CHS braces away from the crown and saddle points.

6.1.3 Weld improvement methods

Various methods of improving the fatigue resistance of welded connections are available (Haagensen [1989, 1997], Bignonnet [1987], Haagensen and Maddox [2000]). They result in a change in the weld geometry to minimise weld defects and stress concentrations, or to reduce the tensile residual stresses in the joint. They can be summarised as two groups.

One is the geometry improvement method which includes the grinding method (Knight [1978]), the remelting method (Haagensen [1978]) and the weld profiling method (AWS [1998], Kobyashi et al. [1977]). The other is the residual stress method which includes the hammer peening and shot peening methods (Knight [1978]).

Section 6.2 describes some methods for the repair of structures already subjected to fatigue cracking.

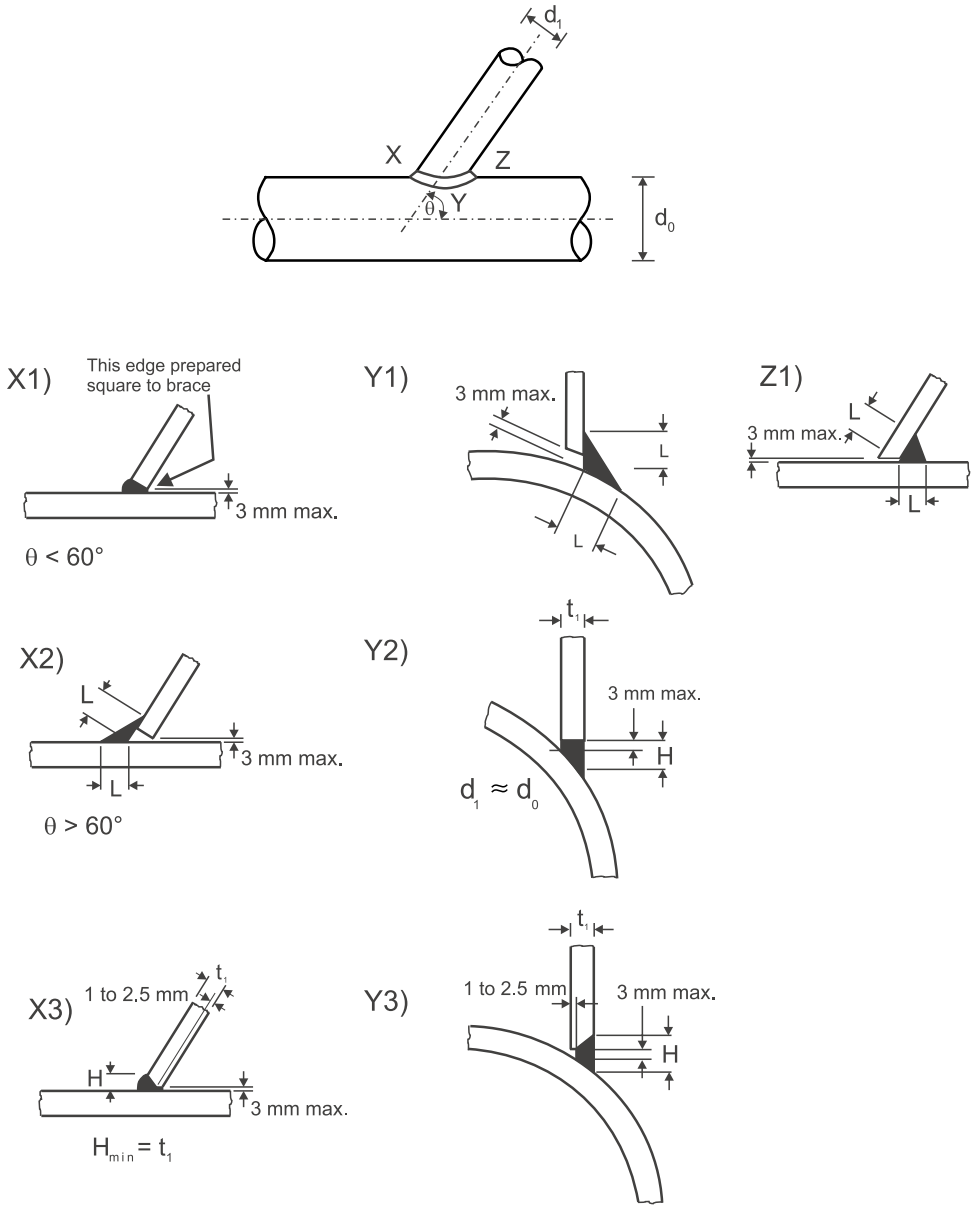

Figure 6.1 – Fillet and butt (groove) welds in lattice joints between circular hollow sections

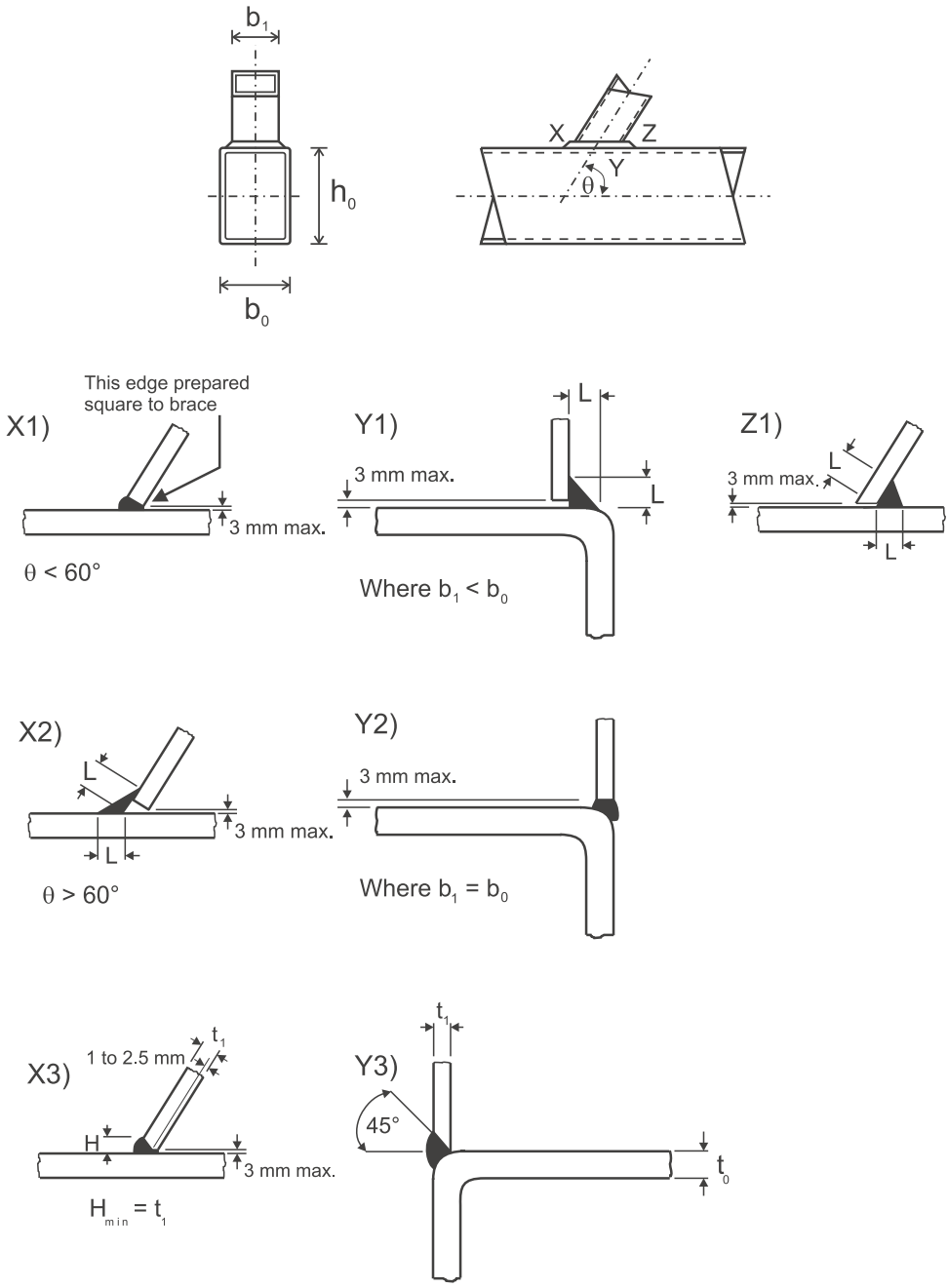

Figure 6.2 – Fillet and butt (groove) welds in lattice joints between rectangular hollow sections

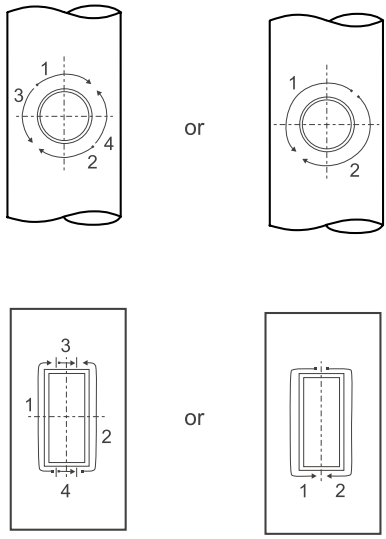

Figure 6.3 – Recommended locations for the weld start/stop positions

6.2 Structural Reinforcement and Repair

6.2.1 General

Steel structures are usually designed for a fatigue life or a fatigue load depending on intended use. Exceeding the calculated lifetime or fatigue loading can result in fatigue damage to the structure. If a further use of the structure is planned, measures of repair will be inevitable. On the other hand it is possible that higher loads have been applied to the structure due to changed demands. In this case methods of structural reinforcement may have to be carried out at the critical joints. Because the methods of repair generally mean some type of reinforcement at the same time, the following sections deal with both methods.

Another possibility is to replace complex welded connections with forgings or casting, as is often done in the nuclear industry. However, the costs involved can be quite high and the delivery times longer than would be in the case with normal welded connections. If this option is used the forging or casting manufacturers should be involved in the project as early as possible.

Fatigue damage of a structure starts with small cracks. The location is usually the toe of a weld in welded joints. Regular inspections of the structure are required in order to detect cracks as early as possible. When a crack is detected in a structural member action should be taken as soon as possible, to prevent it from propagating further. A simple method is to drill a hole into the base metal at each end of the crack at the crack tip, as shown in Figures 6.4 (a) and (b). The diameter of the hole should be approximately equal to the material thickness in order to trap any cracks that run at an angle through the material. At the same time the hole reduces the stress concentration, because the directional change in the flow of stress around the edge of the hole is not as severe as it would have been at the tip of the crack. It should be followed by repair of the member.

Different methods for the repair and/or reinforcement of cracks in hollow section joints are described in the sections 6.2.2 to 6.2.4.

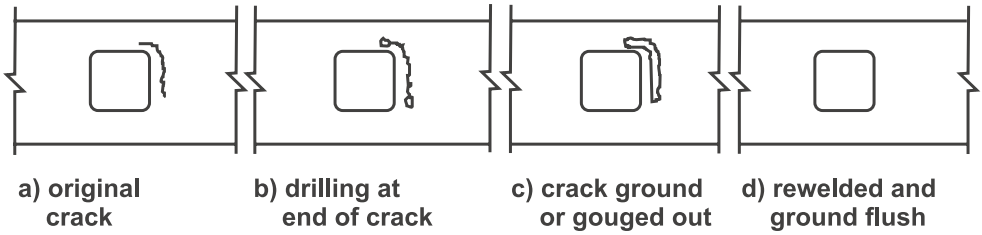

Figure 6.4 – Grinding or gouging out cracks and rewelding

6.2.2 Simple repair

This method of repair without the use of reinforcement is equally applicable to both circular and square hollow sections and is illustrated in Figures 6.4 (a) to (d). It is assumed that the crack has been stopped by drilling as described above. The next stage is to either grind out the whole of the crack with a grind stone, or gouge out using a gouging arc weld electrode, and at the same time to prepare the edges for welding. The repair is completed by welding up the area using normal welding procedures, and then grinding the repair flush, if required.

6.2.3 Reinforcement of CHS T-joints

In the case of fatigue damage to circular hollow section T-joints, where the crack runs from the weld area into the chord, there are three methods of reinforcement.

(a) using internal ring stiffeners

One method is to use internal ring stiffeners, provided access is possible from the inner side, as shown in Figure 6.5 (a). The solution with internal ring stiffeners is frequently found at locations where high localized loadings may occur (such as at supports). A load redistribution to adjacent stiffeners takes place, reducing stress concentrations.

(b) using side plates

The other method is to use side plates as shown in Figure 6.5 (b). Side plates can be welded to the joint before or after fatigue cracking. The ends of the plates should be situated at locations with a relatively homogeneous stress distribution in order to reduce the negative influence of notch stresses.

(c) using castings

Another solution is the replacement of parts of the joint by castings which completely cover the connection area, see Figure 6.5 (c). These are components with a very homogeneous structure offering a long life expectancy. Attention should be paid to the manufacture. Welding details have to be taken into consideration carefully to ensure a good connection between the casting and the original tube. This is time consuming and expensive. For this reason this solution is used only in special cases.

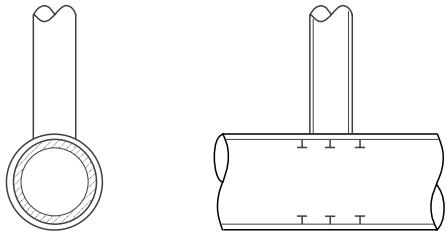

(a) using internal ring stiffeners

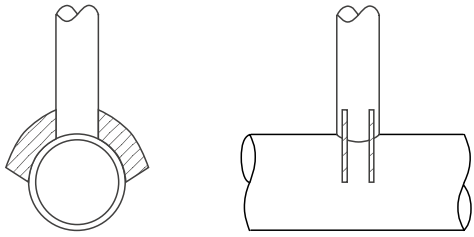

(b) using side plates

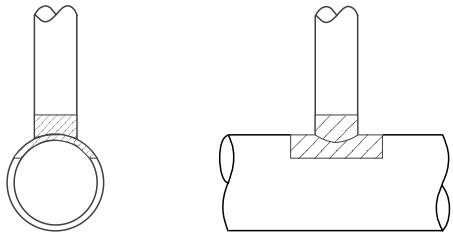

(c) using casting

Figure 6.5 – Reinforcement of CHS T-joints

6.2.4 Reinforcement of RHS T-joints

If at a T-joint a crack has developed in the chord across the main load direction as shown in Figure 6.4, different possibilities for the reinforcement of the joint are presented in Figure 6.6 (a) to Figure 6.6 (c). They are

(a) using chord flange plates
The brace member is separated from the chord and a stiffening plate is welded between the chord and the brace member as shown in Figure 6.6 (a). Because the intermediate plate is loaded in the direction of its thickness, it should have good through thickness properties and be free from laminations.

(b) using lateral gusset plates
Lateral gusset plates are attached in order to reduce the stresses at the connection as shown in Figure 6.6 (b). The length of the recesses should be larger than the outer width

of the brace member. The connection of the brace member and the gusset plates allow the brace loads to be transferred into the chord. This leads to a load redistribution and therefore to reduction of stress concentrations.

(c) using haunch stiffeners
Lateral haunch-like stiffening of hollow sections, arranged lengthwise to the chord, with the same dimensions as the brace member are welded to the joint as shown in Figure 6.6 (c). The recesses are necessary to avoid a superposition of thermal and structural stresses. Moreover the fillet welds can be welded all around. From a structural mechanics point of view this is the best solution, because the connecting surface between chord and brace member increases considerably. However this method can be costly to fabricate.

6.2.5 Reinforcement of K and N-Joints

The fatigue crack in K and N-joints may occur along the weld or in the chord or brace member. Reinforcement can be carried out on both CHS and RHS joints by welding a flange plate as shown in Figure 6.7 (a), a transverse gusset plate as shown in Figure 6.7 (b) or the combination of the above as shown in Figure 6.7 (c). All these repairs are rather difficult to apply. Another possibility for the reinforcement or repair of K-joints is the use of boxed components made from RHS as shown in Figure 6.8 (a) for CHS K-joints and Figure 6.8 (b) for RHS K-joints.

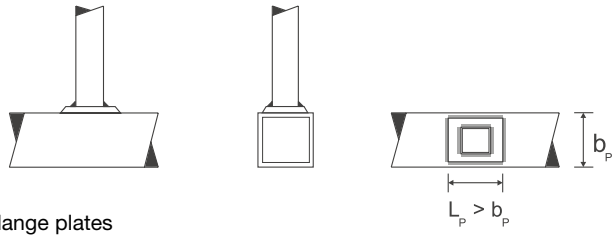

(a) using chord flange plates

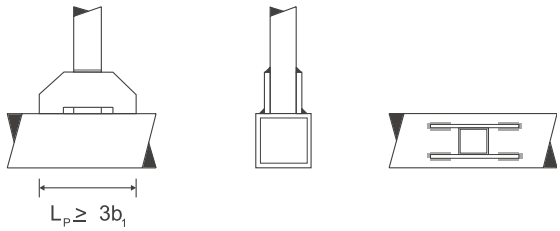

(b) using lateral gusset plates

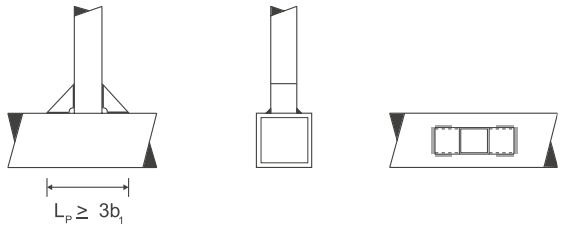

(c) using haunch stiffeners

Figure 6.6 – Reinforcement of RHS T-joints

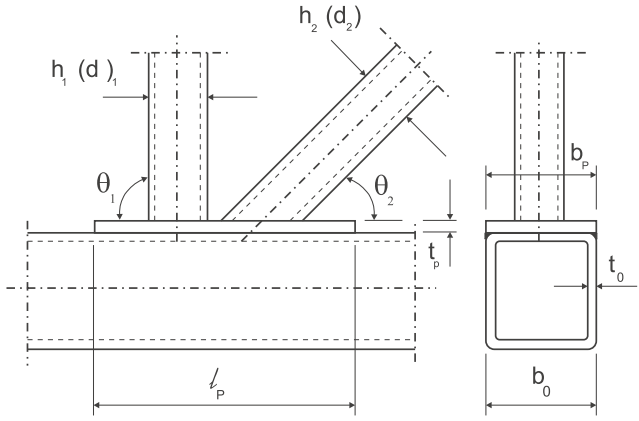

(a) flange plate reinforcement

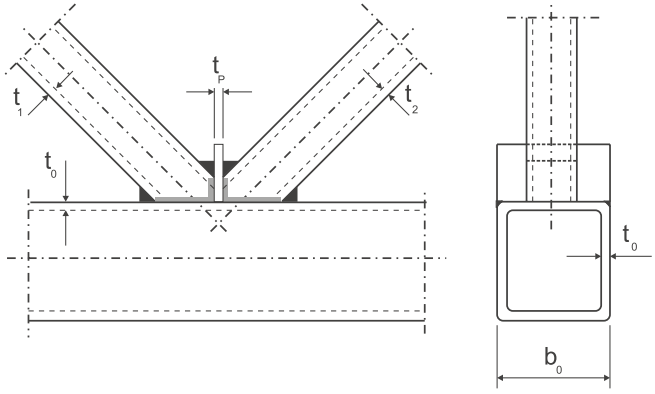

(b) vertical plate reinforcement

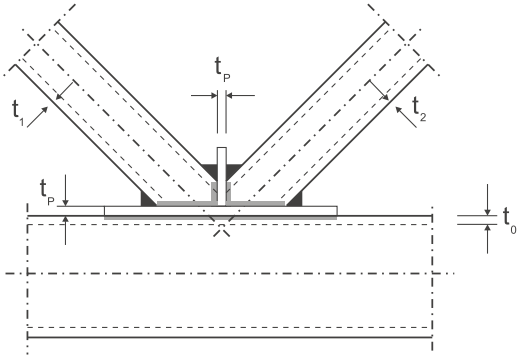

(c) combination of flange and vertical plate reinforcement

Figure 6.7 – Reinforcement of RHS K and N-joints using welded plates

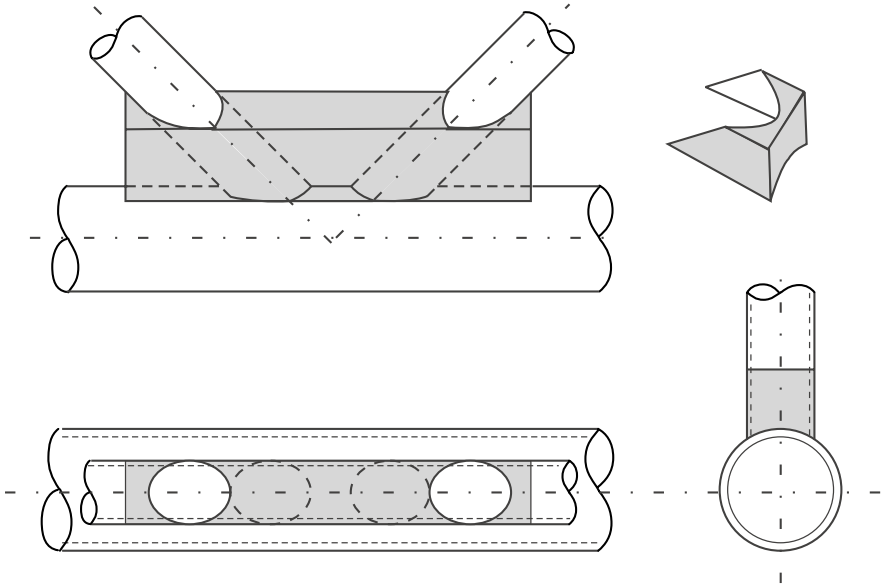

(a) CHS K-joints

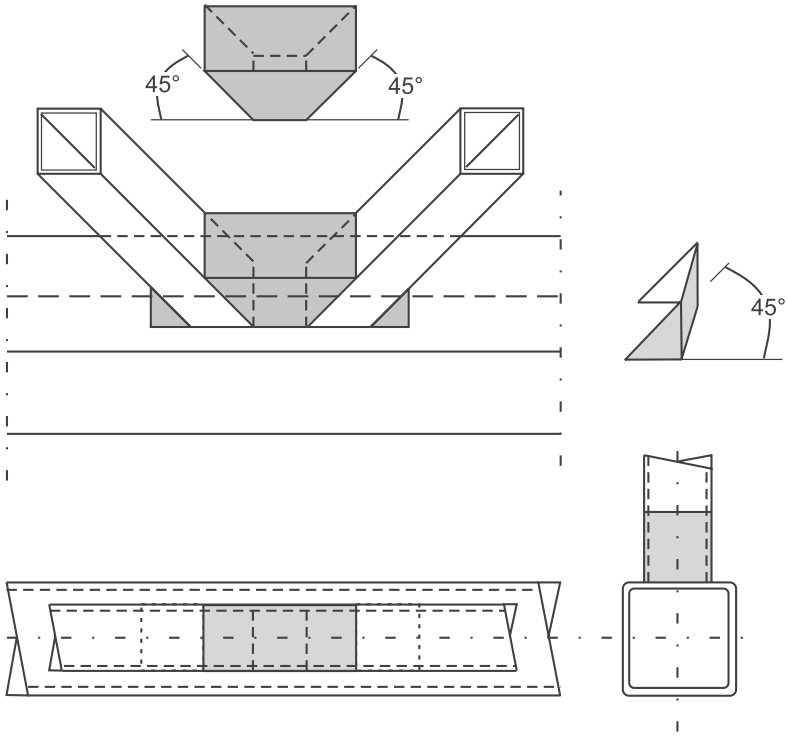

(b) RHS K-joints

Figure 6.8 – Reinforcement of K-joints using corner components

6.2.6 Effect of reinforcement/repair on fatigue life

Indications on improved fatigue strength due to different repair and reinforcement methods are shown in Table 6.1. Detailed experimental results are reported by Puthli et al. (1992) and Mang and Bucak (1996). In Table 6.1, the term N_f is the original life without repair or reinforcement.

Table 6.1 – Extended life according to different repair and reinforement measures

Joint	Repair and reinforcement method	Indications on additional life
CHS K-Joint and RHS K-Joint	Repair with RHS pieces (see Figure 6.8)	$> 200\% \cdot N_f$
	Repair with stiffening plates (see Figure 6.7)	$> 100\% \cdot N_f$
	Repair by gouging out cracks and re-welding (see Figure 6.4)	$> 40\% \cdot N_f$

7 Design Examples for CHS Joints

7.1 Example 1: Uniplanar CHS K-Joints with Gap

Given:
A uniplanar truss is shown in Figure 7.1. The layout of the truss is the same as that shown on page 46 in CIDECT Design Guide for CHS Joints under Predominantly Static Loading (Wardenier et al. [1991]). The joint eccentricity (e) is zero. An applied constant amplitude loading, ranging from zero to the loads shown, is given in Figure 7.1.

The member sizes are:

Top chord:	CHS 219.1 x 7.1,	A_o = 4728 mm^2,	$W_o = 0.243 \times 10^6$ mm^3
Braces:	CHS 88.9 x 4,	$A_{1,2}$ = 1070 mm^2,	$W_{1,2} = 0.0217 \times 10^6$ mm^3
Bottom chord:	CHS 177.8 x 7.1,	A_o = 3807 mm^2,	$W_o = 0.156 \times 10^6$ mm^3

The static strength has been found satisfactory.

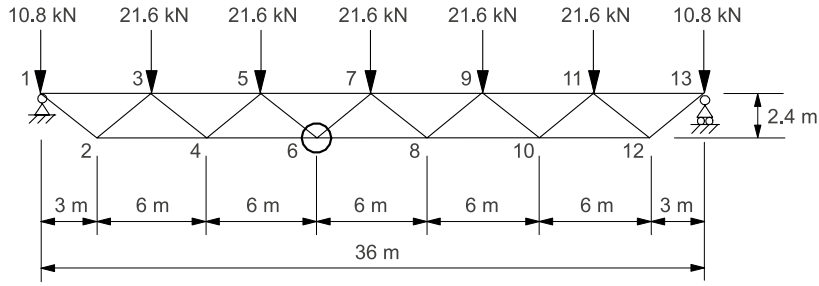

Figure 7.1 – A uniplanar truss subjected to a constant amplitude load range

Problem:
Determine the fatigue life of joint No. 6 indicated in Figure 7.1.

Solution:

Step 1: Parameters

$\beta = d_1/d_o = 88.9/177.8 = 0.5$
$2\gamma = d_o/t_o = 177.8/7.1 = 25$
$\gamma = 12.5$
$\tau = t_1/t_o = 4/7.1 = 0.563$
θ = arc tan (2.4/3.0) = 38.7°

The parameters are within the validity range given in Table D.3.

Step 2: Structural analysis

A structural analysis is carried out assuming a continuous chord and pin-ended braces as described in Section 3.2.2. The axial forces and bending moments found in joint No. 6 are given in Figure 7.2. They can be treated as a combination of two load conditions shown in Figure 7.3, i.e.:

Load condition 1: basic balanced axial loading
Load condition 2: chord loading (axial and bending)

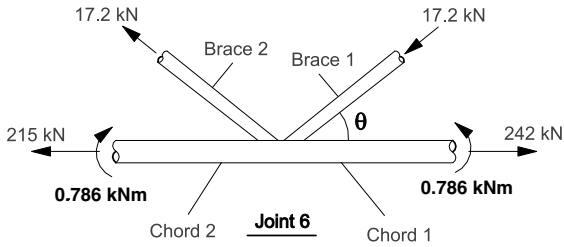

Figure 7.2 – Axial forces and bending moments in joint No. 6

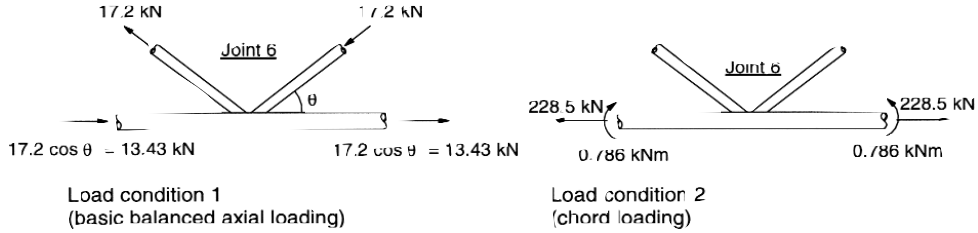

Figure 7.3 – Two load conditions for joint No. 6

Step 3: Nominal stress ranges in critical members

It can be seen from Figure 7.2 that the critical chord loading is in chord 1 due to a larger tension force in it. Brace 2 with a tensile force range will be checked only. Note: In general, it is presumed that only braces which have some parts of their load range in tension will be liable to cause fatigue failure.

For load condition 1 (basic balanced axial loading):

$$\sigma_{brace,ax} = MF \cdot 17.2 \cdot 10^3/1070 = 1.3 \cdot 16 = 21 \text{ N/mm}^2$$

For load condition 2 (chord loading):

$$\sigma_{chord,ch} = \sigma_{chord,ax} + \sigma_{chord,ipb} = MF \cdot 228.5 \cdot 10^3/3807 - 0.786 \cdot 10^6/(0.156 \cdot 10^6)$$
$$= 1.5 \cdot 60 - 5 = 85 \text{ N/mm}^2$$

(Note that the chord bending moment relieves the tensile stress on the connecting face of the chord. The values of MF (magnification factor) are given in Table 2.1).

Step 4: SCF calculation for load condition 1 (basic balanced axial loading)

From Table D.3

Chord

$$SCF_{ch,ax} = \left[\frac{\gamma}{12}\right]^{0.4} \cdot \left[\frac{\tau}{0.5}\right]^{1.1} \cdot SCF_{o,ch,ax} = \left[\frac{12.5}{12}\right]^{0.4} \cdot \left[\frac{0.563}{0.5}\right]^{1.1} \cdot SCF_{o,ch,ax}$$
$$= 1.16 \cdot SCF_{o,ch,ax}$$

where for $\beta = 0.5$ and $\theta = 30°$, $SCF_{o,ch,ax} = 2.6$
for $\beta = 0.5$ and $\theta = 45°$, $SCF_{o,ch,ax} = 2.9$
so that for $\beta = 0.5$ and $\theta = 38.7°$, $SCF_{o,ch,ax} = 2.77$

and $SCF_{ch,ax} = 1.16 \cdot 2.77 = \underline{3.2}$

Brace

$$SCF_{b,ax} = \left[\frac{\gamma}{12}\right]^{0.5} \cdot \left[\frac{\tau}{0.5}\right]^{0.5} \cdot SCF_{o,b,ax} = \left[\frac{12.5}{12}\right]^{0.5} \cdot \left[\frac{0.563}{0.5}\right]^{0.5} \cdot SCF_{o,b,ax}$$
$$= 1.08 \cdot SCF_{o,b,ax}$$

where for $\beta = 0.5$ and $\theta = 30°$, $SCF_{o,b,ax} = 1.3$
for $\beta = 0.5$ and $\theta = 45°$, $SCF_{o,b,ax} = 1.8$
so that for $\beta = 0.5$ and $\theta = 38.7°$, $SCF_{o,b,ax} = 1.59$

and $SCF_{b,ax} = 1.08 \cdot 1.59 = 1.7$

Check minimum SCF value:

for $\theta = 30°$, min $SCF_{b,ax} = 2.64$
for $\theta = 45°$, min $SCF_{b,ax} = 2.30$
so that for $\theta = 38.7°$, min $SCF_{b,ax} = 2.44$

so use minimum SCF value, $SCF_{b,ax} = \underline{2.4}$

Step 5: SCF calculation for load condition 2 (chord loading)

From Table D.3

Chord

$$SCF_{ch,ch} = 1.2 \left[\frac{\tau}{0.5}\right]^{0.3} \cdot (\sin\theta)^{-0.9} = 1.2 \cdot \left[\frac{0.563}{0.5}\right]^{0.3} \cdot (\sin 38.7°)^{-0.9} = 1.9$$

use minimum SCF value, $SCF_{ch,ch} = \underline{2.0}$

Brace

$$SCF_{b,ch} = 0 \text{ (negligible)}$$

Step 6: Hot spot stress ranges

Load condition 1 (basic balanced axial loading):

$$S_{rhs,chord} = SCF_{ch,ax} \cdot \sigma_{brace,ax} = 3.2 \cdot 21 = 67 \text{ N/mm}^2$$
$$S_{rhs,brace} = SCF_{b,ax} \cdot \sigma_{brace,ax} = 2.4 \cdot 21 = 50 \text{ N/mm}^2$$

Load condition 2 (chord loading):

$$S_{rhs,chord} = SCF_{ch,ch} \cdot \sigma_{chord,ch} = 2.0 \cdot 85 = 170 \text{ N/mm}^2$$
$$S_{rhs,brace} = SCF_{b,ch} \cdot \sigma_{chord,ch} = 0 \text{ N/mm}^2$$

Superposition of load conditions 1 and 2:

$$S_{rhs,chord} = 67 + 170 = \underline{237 \text{ N/mm}^2}$$
$$S_{rhs,brace} = 50 + 0 = \underline{50 \text{ N/mm}^2}$$

Step 7: Hot spot stress ranges for design

A partial safety factor on hot spot stress ranges is required for design. For this example the joint is assumed to be non fail-safe and accessible. From Table 1.2, the partial safety factor is 1.25.

$$S_{rhs,chord} = 1.25 \cdot 237 = \underline{296 \text{ N/mm}^2}$$
$$S_{rhs,brace} = 1.25 \cdot 50 = \underline{63 \text{ N/mm}^2}$$

Step 8: Fatigue life of joint No. 6

For Fatigue Cracking in the Chord:

$t = 7.1$ mm and $S_{rhs,chord} = 296$ N/mm^2

Table 3.1 or Figure 3.3 can now be used to determine the fatigue life.

From Table 3.1

$$\log(N_f) = \frac{12.476 - 3 \cdot \log(S_{rhs})}{1 - 0.18 \cdot \log(\frac{16}{t})} = \frac{12.476 - 3 \cdot \log(296)}{1 - 0.18 \cdot \log(\frac{16}{7.1})} = 5.41$$

$$\underline{N_f = 10^{5.41} = 257{,}000 \text{ cycles}}$$

For Fatigue Cracking in the Brace:

$t = 4$ mm and $S_{rhs,brace} = 63$ N/mm^2 . The hot spot stress range of 63 N/mm^2 is lower than the Constant Amplitude Fatigue Limit of 147 N/mm^2 listed in Table 3.2. Therefore no fatigue damage occurs in the brace.

Hence, the fatigue life expectancy of joint No. 6 is 257,000 cycles, with failure in the chord.

7.2 Example 2: Multiplanar CHS KK-Joints with Gap

Given:
It is assumed that a multiplanar CHS KK-joint has the same geometry and internal brace loads in each plane as joint No. 6 in the previous design example for uniplanar CHS K-joints described in Chapter 7.1. It is assumed that the internal brace loads are totally anti-symmetrical, i.e. m = –1. Therefore the loads in the chord member can be considered negligible, see Figure 7.4. The multiplanar parameter (ϕ), i.e. the angle between planes with braces, is 90°.

It should be noted that the external constant amplitude load ranges are different to those given in example 7.1. Therefore it is not the purpose of this example to show the multiplanar effect on fatigue life. The purpose of this example is to demonstrate the design procedures for a multiplanar joint under a given internal load condition.

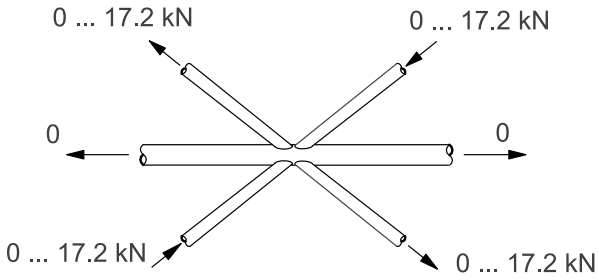

Figure 7.4 – Assumed load range on the multiplanar joint

Problem:
Determine the fatigue life of the multiplanar CHS KK-joint.

Solution:

Step 1: Multiplanar Correction Factors (MCFs) on SCFs

From Table 4.2

For load condition 1 (basic balanced axial loading), m = –1

chord: $MCF_{ch,ax} = 1.25$
brace: $MCF_{b,ax} = 1.25$

For load condition 2 (chord loading), m = –1

chord: $MCF_{ch,ch} = 1.0$
brace: $MCF_{b,ch} = 1.0$

Step 2: Modified SCFs

SCFs for uniplanar joints used in this example have been taken from the example in chapter 7.1.

For load condition 1 (basic balanced axial loading)

chord: $SCF_{ch,ax,mp} = MCF_{ch,ax} \cdot SCF_{ch,ax,up} = 1.25 \cdot 3.2 = \underline{4.0}$
brace: $SCF_{b,ax,mp} = MCF_{b,ax} \cdot SCF_{b,ax,up} = 1.25 \cdot 1.7 = 2.13$
but use minimum SCF value, $SCF_{b,ax,mp} = 2.4$ (see example in 7.1)
where "mp" stands for multiplanar and "up" stands for uniplanar.
Note: $SCF_{b,ax,up}$ of 1.7 is the calculated value, not the required minimum value.

For load condition 2 (chord loading)

chord: $SCF_{ch,ch.mp} = SCF_{ch,ch,up} = 2.0$
brace: $SCF_{b,ch,mp} = SCF_{b,ch,up} = 0$ (negligible)

Step 3: Hot spot stress ranges

For load condition 1 (basic balanced axial loading)

$S_{rhs,chord,mp} = SCF_{ch,ax,mp} \cdot \sigma_{brace,ax} = 4.0 \cdot 21 = 84$ N/mm^2
$S_{rhs,brace,mp} = SCF_{b,ax,mp} \cdot \sigma_{brace,ax} = 2.4 \cdot 21 = 50$ N/mm^2

Load condition 2 (chord loading):

Because the chord stress is zero,
$S_{rhs,chord,mp} = 0$ N/mm^2
$S_{rhs,brace,mp} = 0$ N/mm^2

Superposition of load conditions 1 and 2:

$S_{rhs,chord,mp} = 84 + 0 = \underline{84 \text{ N/mm}^2}$
$S_{rhs,brace,mp} = 50 + 0 = \underline{50 \text{ N/mm}^2}$

Step 4: Hot spot stress ranges for design

A partial safety factor on hot spot stress ranges is required for design. For this example the joint is assumed to be non fail-safe and accessible. From Table 1.2, the partial safety factor is 1.25.

$S_{rhs,chord,mp} = 1.25 \cdot 84 = \underline{105 \text{ N/mm}^2}$
$S_{rhs,brace,mp} = 1.25 \cdot 50 = \underline{63 \text{ N/mm}^2}$

Step 5: Fatigue live of multiplanar joint

For Chord:

t = 7.1 mm and $S_{rhs,chord,mp} = 105$ N/mm^2. The hot spot stress range of 105 N/mm^2 is lower than the Constant Amplitude Fatigue Limit (for t = 7.1 mm) which is between 111 N/mm^2 (for t = 8 mm) and 134 N/mm^2 (for t = 5 mm) listed in Table 3.2. Therefore no fatigue damage occurs in the chord.

For Brace:

t = 4 mm and $S_{rhs,brace,mp} = 63$ N/mm^2. The hot spot stress range of 63 N/mm^2 is lower than the Constant Amplitude Fatigue Limit of 147 N/mm^2 listed in Table 3.2. Therefore no fatigue damage occurs in the brace.

Hence, no fatigue damage would be expected in this multiplanar joint.

8 Design Examples for RHS Joints

8.1 Example 1: Uniplanar RHS T-joints

Given:
A T-joint in square hollow sections is shown in Figure 8.1, where a fillet weld with weld throat thickness of 5 mm is assumed.

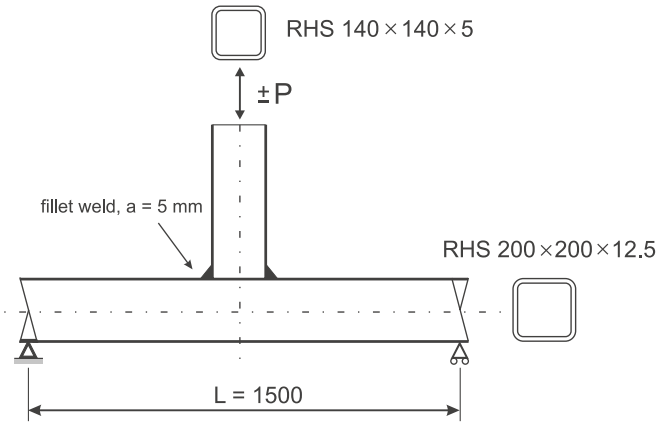

Figure 8.1 – A uniplanar RHS T-joint

The dimensions are:

Chord member:	RHS 200 x 200 x 12.5,	A_o = 8973 mm²,	W_o = 513444 mm³
Brace member:	RHS 140 x 140 x 5,	A_1 = 2661 mm²,	W_1 = 114711 mm³
Chord length:	L = 1500 mm		

The T-joint is assumed to be fail-safe (failure of the joint does not result in failure of the whole structure). The joint is assumed to be poorly accessible and subjected to constant amplitude loading.

Problem:

To determine the nominal range of the brace axial force P for the design of the T-joint at $2 \cdot 10^6$ cycles, for a constant amplitude loading.

Solution:

Step 1: Parameters

$\beta = b_1/b_o = 140/200 = 0.7$
$2\gamma = b_o/t_o = 200/12.5 = 16$
$\gamma = 8$
$\tau = t_1/t_o = 5/12.5 = 0.4$

The parameters are within the validity range given in Table E.1.

Step 2: Nominal stress ranges

The brace nominal axial stress ($S_{n,ax}$) causes a bending stress in the chord ($S_{n,ch}$) of:

$$S_{n,ch} = (1/4) \cdot P \cdot (L–b_1)/W_o = (1/4) \cdot S_{n,ax} \cdot A_1 \cdot (L–b_1)/W_o$$

The general expression for the total hot spot stress becomes

$$S_{rhs} = SCF_{ax} \cdot S_{n,ax} + SCF_{ch} \cdot S_{n,ch} = S_{n,ax} \cdot (SCF_{ax} + SCF_{ch} \cdot (1/4) \cdot A_1 \cdot (L–b_1)/W_o)$$

By substituting the geometric dimensions

$$S_{rhs} = S_{n,ax} \cdot (SCF_{ax} + SCF_{ch} \cdot 1.76)$$

Therefore

$$S_{n,ax} = S_{rhs}/(SCF_{ax} + SCF_{ch} \cdot 1.76)$$

The nominal axial force range can be determined by

$$P_{range} = A_1 \cdot S_{n,ax}$$

Step 3: SCF_{ax} for axial force on the brace

For braces (lines A and E)

From Figure 5.2, a quick estimation of 7.5 is obtained.

From Table E.1

$$\begin{aligned} SCF_{A\&E,ax} &= (0.013 + 0.693 \cdot \beta – 0.278 \cdot \beta^2) \cdot (2\gamma)^{(0.790 + 1.898 \cdot \beta – 2.109 \cdot \beta^2)} \\ &= 0.362 \cdot 16^{1.085} \\ &= 7.33 \end{aligned}$$

In this example, a fillet weld is applied. According to Table E.1, the SCF in the brace (lines A and E) should be multiplied by 1.4 to correct for the weld type. (This correction factor is not applied to the chord side of the fillet weld.)

$$SCF_{A\&E,ax} = 1.4 \cdot 7.33 = 10.3$$

For chord (lines B, C and D)

From Figure 5.2, $SCF_{B,ax}$ is around 5.0.

From Table E.1

$$\begin{aligned} SCF_{B,ax} &= (0.143 – 0.204 \cdot \beta + 0.064 \cdot \beta^2) \cdot (2\gamma)^{(1.377 + 1.715 \cdot \beta – 1.103 \cdot \beta^2)} \cdot \tau^{0,75} \\ &= 0.03156 \cdot 16^{2.037} \cdot 0.4^{0.75} \\ &= 4.5 \end{aligned}$$

Similarly

$$SCF_{C,ax} = 4.27$$
$$SCF_{D,ax} = 2.07$$

Step 4: SCF_{ch} for loads on the chord

From Table E.1

$$SCF_{A\&E,ch} = 0$$

$$SCF_{B,ch} = 0$$

$$SCF_{C,ch} = 0.725 \cdot (2\gamma)^{0.248 \cdot \beta} \cdot \tau^{0.19} = 0.725 \cdot 16^{0.1736} \cdot 0.4^{0.19} = 0.99$$
$$SCF_{C,ch} = 2.0 \text{ (minimum value)}$$

$$SCF_{D,ch} = 1.373 \cdot (2\gamma)^{0.205 \cdot \beta} \cdot \tau^{0.24} = 1.373 \cdot 16^{0.1435} \cdot 0.4^{0.24} = 1.64$$
$$SCF_{D,ch} = 2.0 \text{ (minimum value)}$$

Step 5: SCF_{brace} and SCF_{chord}

As derived before in step 2, the total SCF = $SCF_{ax} + SCF_{ch} \cdot 1.76$

$$SCF_{A\&E} = SCF_{A\&E,ax} = 10.3$$
$$SCF_{B} = SCF_{B,ax} = 4.5$$
$$SCF_{C} = SCF_{C,ax} + SCF_{C,ch} \cdot 1.76 = 4.27 + 2.0 \cdot 1.76 = 7.79$$
$$SCF_{D} = SCF_{D,ax} + SCF_{D,ch} \cdot 1.76 = 2.07 + 2.0 \cdot 1.76 = 5.59$$

Therefore the maximum SCFs in brace and chord are

$$SCF_{brace} = SCF_{A\&E} = \underline{10.3}$$
$$SCF_{chord} = SCF_{C} = \underline{7.8}$$

Step 6: Hot spot stress S_{rhs} at $2 \cdot 10^6$ cycles

From Table 3.1.

For braces (t = 5 mm):

$$\begin{aligned} \log(S_{rhs,brace}) &= (12.476 - \log(N_f))/3 + 0.06 \cdot \log(N_f) \cdot \log(16/t) \\ &= (12.476 - \log(2 \cdot 10^6))/3 + 0.06 \cdot \log(2 \cdot 10^6) \cdot \log(16/5) \\ &= 2.058 + 0.191 = 2.249 \end{aligned}$$

$$S_{rhs,brace} = 10^{2.249} = \underline{177 \text{ N/mm}^2}$$

For chord (t = 12.5 mm):

$$\begin{aligned} \log(S_{rhs,chord}) &= (12.476 - \log(N_f))/3 + 0.06 \cdot \log(N_f) \cdot \log(16/t) \\ &= (12.476 - \log(2 \cdot 10^6))/3 + 0.06 \cdot \log(2 \cdot 10^6) \cdot \log(16/12.5) \\ &= 2.058 + 0.041 = 2.099 \end{aligned}$$

$$S_{rhs,chord} = 10^{2.099} = \underline{126 \text{ N/mm}^2}$$

Step 7: Allowable nominal axial force range

A partial factor of safety should be applied to the hot spot stress range as explained in section 1.6. In this example, a factor of safety of 1.15 should be used based on the conditions given in Table 1.2. The factored hot spot stress ranges become

$$S_{rhs,\ brace} = 177/1.15 = 154\ N/mm^2$$
$$S_{rhs,\ chord} = 126/1.15 = 110\ N/mm^2$$

From Step 2 and Step 5

$$S_{n,ax} = S_{rhs}/SCF = S_{rhs,brace}/SCF_{brace} = 154/10.3 = 15.0\ N/mm^2$$

or

$$S_{n,ax} = S_{rhs}/SCF = S_{rhs,chord}/SCF_{chord} = 110/7.8 = 14.1\ N/mm^2$$

The lower one (14.1 N/mm²) should be used to determine the nominal axial force range.

$P_{range} = A_1 \cdot S_{n,ax} = 2661 \cdot 14.1 = 37520\ N = \underline{37.5\ kN}$

So the nominal axial force range in the brace should not be greater than 37.5 kN.

8.2 Example 2: Uniplanar RHS K-Joints with Gap

Given:
A uniplanar truss is shown in Figure 8.2. The layout of the truss is the same as that shown on page 51 in CIDECT Design Guide for RHS Joints under Predominantly Static Loading (Packer et al. [1992]). The joint eccentricity (e) is zero. An applied constant amplitude loading ranging from zero to the loads shown, is given in Figure 8.2.

The member sizes are:

Top chord:	RHS 180 x 180 x 8,	A_o = 5410 mm²,	W_o =0.282 x 10⁶ mm³
Brace:	RHS 100 x 100 x 4,	$A_{1,2}$ = 1480 mm²,	$W_{1,2}$ =0.0446 x 10⁶ mm³
Bottom chord:	RHS 180 x 180 x 8,	A_o = 5410 mm²,	W_o =0.282 x 10⁶ mm³

The static strength has been found satisfactory.

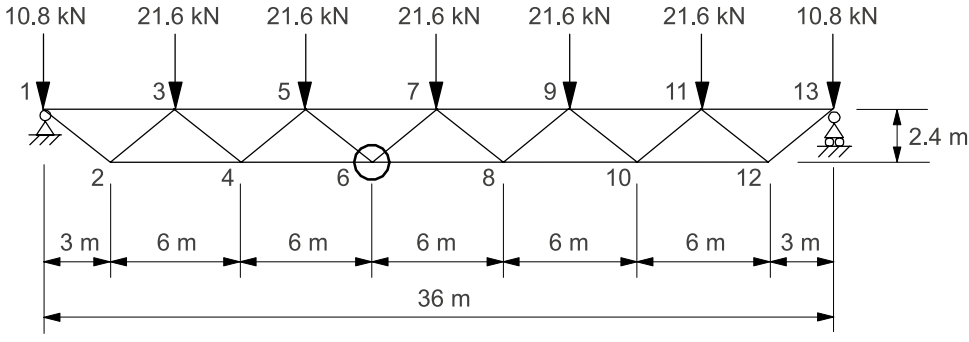

Figure 8.2 – A uniplanar truss subjected to a constant amplitude load range

Problem:

Determine the fatigue life of joint No. 6 indicated in Figure 8.2.

Solution:

Step 1: Parameters

$\beta = b_1/b_o = 100/180 = 0.556$
$2\gamma = b_o/t_o = 180/8 = 22.5$
$\tau = t_1/t_o = 4/8 = 0.5$
θ = arc tan (2.4/3.0) = 38.7°
$g = b_o/\tan(\theta) - b_1/\sin(\theta) = 180/\tan(38.7°) - 100/\sin(38.7°) \approx 64$ mm
$g' = g/t_o = 64/8 = 8$

The parameters are within the validity range given in Table E.2.

Step 2: Structural analysis

A structural analysis is carried out assuming a continuous chord and pin-ended braces as described in Section 3.2.2. The axial forces and bending moments found in joint No. 6 are given in Figure 8.3. They can be treated as a combination of two load conditions shown in Figure 8.4, i.e.:

Load condition 1: basic balanced axial loading
Load condition 2: chord loading (axial and bending)

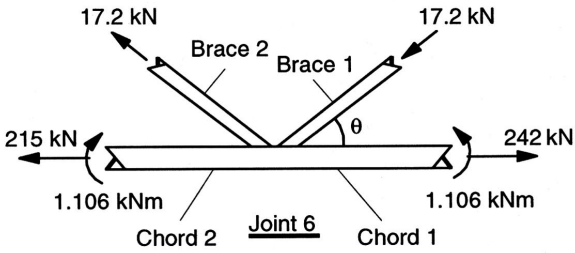

Figure 8.3 – Axial forces and bending moments in joint No. 6

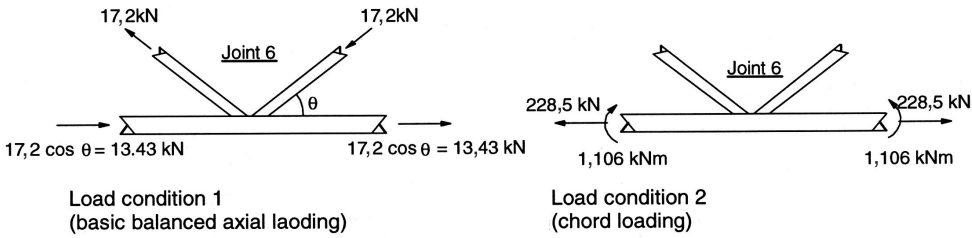

Figure 8.4 – Two load conditions for joint No. 6

Step 3: Nominal stress ranges in critical members

It can be seen from Figure 8.3 that the critical chord loading is in chord 1 due to a larger tension force in it. Brace 2 with a tensile force range will be checked only. Note: In gen-

eral, it is presumed that only braces which have some load range in tension will be liable to cause fatigue failure.

For load condition 1 (basic balanced axial loading):

$$\sigma_{brace,ax} = MF \cdot 17.2 \cdot 10^3/1480 = 1.5 \cdot 12 = 18 \text{ N/mm}^2$$

For load condition 2 (chord loading):

$$\sigma_{chord,ch} = \sigma_{chord,ax} + \sigma_{chord,ipb} = MF \cdot 228.5 \cdot 10^3/5410 - 1.106 \cdot 10^6/(0.282 \cdot 10^6)$$
$$= 1.5 \cdot 42.2 - 3.9 = 59 \text{ N/mm}^2$$

Note that the chord bending moment relieves the tensile stress on the connecting face of the chord. The values of MF (magnification factor) are given in Table 2.2.

Step 4: SCF calculation for load condition 1 (basic balanced axial loading)

Chord

From Figure E.4 (reference value SCF_o)
for $\beta = 0.556$ and $\gamma = 30°$, $SCF_o = 4.7$
for $\beta = 0.556$ and $\gamma = 45°$, $SCF_o = 9.5$
so that for $\beta = 0.556$ and $\gamma = 38.7°$, $SCF_o = 7.5$

From Figure E.5 (correction factor)
for $\tau = 0.5$ and $2\gamma = 20$, Correction Factor = 0.7
for $\tau = 0.5$ and $2\gamma = 25$, Correction Factor = 1.1
so that for $\tau = 0.5$ and $2\gamma = 22.5$, Correction Factor = 0.9

$$SCF_{ch,ax} = 7.5 \cdot 0.9 = \underline{6.8}$$

Brace

From Figure E.6 (reference value SCF_o)
for $\beta = 0.556$ and $\gamma = 30°$, $SCF_o = 6.7$
for $\beta = 0.556$ and $\gamma = 45°$, $SCF_o = 10.5$
so that for $\beta = 0.556$ and $\gamma = 38.7°$, $SCF_o = 8.9$

From Figure E.7 (correction factor)
for $\tau = 0.5$ and $2\gamma = 20$, Correction Factor = 0.8
for $\tau = 0.5$ and $2\gamma = 25$, Correction Factor = 1.06
so that for $\tau = 0.5$ and $2\gamma = 22.5$, Correction Factor = 0.93

$$SCF_{b,ax} = 8.9 \cdot 0.93 = \underline{8.3}$$

Step 5: SCF calculation for load condition 2 (chord loading)

Chord From Figure E.8, $SCF_{ch,ch} = 1.8$,
but use minimum SCF value, $SCF_{ch,ch} = \underline{2.0}$

Brace From Table E.2, $SCF_{b,ch} = \underline{0}$ (negligible)

Step 6: Hot spot stress ranges

Load condition 1 (basic balanced axial load):

$$S_{rhs,chord} = SCF_{ch,ax} \cdot \sigma_{brace,ax} = 6.8 \cdot 18 = 122 \text{ N/mm}^2$$
$$S_{rhs,brace} = SCF_{b,ax} \cdot \sigma_{brace,ax} = 8.3 \cdot 18 = 149 \text{ N/mm}^2$$

Load condition 2 (chord loading):

$$S_{rhs,chord} = SCF_{ch,ch} \cdot \sigma_{chord,ch} = 2.0 \cdot 59 = 118 \text{ N/mm}^2$$
$$S_{rhs,brace} = SCF_{b,ch} \cdot \sigma_{chord,ch} = 0 \text{ N/mm}^2$$

Superposition of load conditions 1 and 2:

$$S_{rhs,chord} = 122 + 118 = \underline{240 \text{ N/mm}^2}$$
$$S_{rhs,brace} = 149 + 0 = \underline{149 \text{ N/mm}^2}$$

Step 7: Hot spot stress ranges for design

A partial safety factor on hot spot stress ranges is required for design. For this example the joint is assumed to be non fail-safe and accessible. From Table 1.2, the partial safety factor is 1.25.

$$S_{rhs,chord} = 1.25 \cdot 240 = 300 \text{ N/mm}^2$$
$$S_{rhs,brace} = 1.25 \cdot 149 = 186 \text{ N/mm}^2$$

Step 8: Fatigue life of joint No. 6

For Fatigue Cracking in the Chord:

$t = 8$ mm and $S_{rhs,chord} = 300$ N/mm^2

Table 3.1 or Figure 3.3 can now be used to determine the fatigue life.

From Table 3.1

$$\log(N_f) = \frac{12.476 - 3 \cdot \log(S_{rhs})}{1 - 0.18 \cdot \log(\frac{16}{t})} = \frac{12.476 - 3 \cdot \log(300)}{1 - 0.18 \cdot \log(\frac{16}{8})} = 5.33$$

$$\underline{N_f = 10^{5.33} = 214{,}000 \text{ cycles}}$$

For Fatigue Cracking in the Brace:

$t = 4$ mm and $S_{rhs,brace} = 186$ N/mm^2

From Table 3.1

$$\log(N_f) = \frac{12.476 - 3 \cdot \log(S_{rhs})}{1 - 0.18 \cdot \log(\frac{16}{t})} = \frac{12.476 - 3 \cdot \log(186)}{1 - 0.18 \cdot \log(\frac{16}{4})} = 6.36$$

$$\underline{N_f = 10^{6.36} = 2{,}270{,}000 \text{ cycles}}$$

Hence, the fatigue life expectancy of joint No. 6 is 214,000 cycles, with failure in the chord.

8.3 Example 3: Multiplanar RHS KK-Joints with Gap

Given:
It is assumed that a multiplanar RHS KK-joint has the same geometry and internal brace loads in each plane as joint No. 6 in the previous design example on uniplanar RHS K-joints described in Chapter 8.2. It is assumed that the internal brace loads are totally anti-symmetrical, i.e. m = –1. Therefore the loads in the chord member can be considered negligible, see Figure 8.5.

It should be noted that the external constant amplitude load ranges are different to those given in example 8.2. Therefore it is not the purpose of this example to show the multiplanar effect on fatigue life. The purpose of this example is to demonstrate the design procedures for a multiplanar joint under a given internal load condition.

The multiplanar parameter (ϕ), i. e. the angle between planes with braces, is 90°.

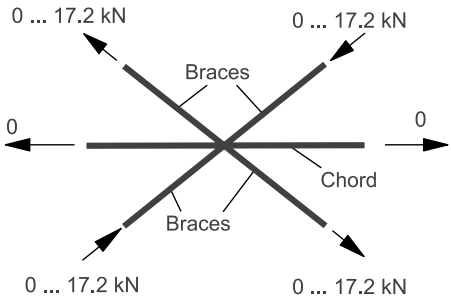

Figure 8.5 – Assumed load range on the multiplanar joint

Problem:
Determine the fatigue life of the multiplanar RHS KK-joint.

Solution:

Step 1: Multiplanar Correction Factors (MCFs) on SCFs

From Table 5.2

For load condition 1 (basic balanced axial loading), m = –1

chord: $MCF_{ch,ax} = 1.25$
brace: $MCF_{b,ax} = 1.25$

For load condition 2 (chord loading), m = –1

chord: $MCF_{ch,ch} = 1.0$
brace: $MCF_{b,ch} = 1.0$

Step 2: Modified SCFs

SCFs for uniplanar joints used in this example have been taken from the example in chapter 8.2.

For load condition 1 (basic balanced axial loading)

chord: $SCF_{ch,ax,mp} = MCF_{ch,ax} \cdot SCF_{ch,ax,up} = 1.25 \cdot 6.8 = \underline{8.5}$
brace: $SCF_{b,ax,mp} = MCF_{b,ax} \cdot SCF_{b,ax,up} = 1.25 \cdot 8.3 = \underline{10.4}$
where “mp” stands for multiplanar and “up” stands for uniplanar.

For load condition 2 (chord loading)

chord: $SCF_{ch,ch.mp} = SCF_{ch,ch,up} = \underline{2.0}$
brace: $SCF_{b,ch,mp} = SCF_{b,ch,up} = \underline{0}$ (negligible)

Step 3: Hot spot stress ranges

For load condition 1 (basic balanced axial loading)

$S_{rhs,chord,mp} = SCF_{ch,ax,mp} \cdot \sigma_{brace,ax} = 8.5 \cdot 18 = 153$ N/mm²
$S_{rhs,brace,mp} = SCF_{b,ax,mp} \cdot \sigma_{brace,ax} = 10.4 \cdot 18 = 187$ N/mm²

Load condition 2 (chord loading):

Because the chord stress is zero,
$S_{rhs,chord,mp} = 0$ N/mm²
$S_{rhs,brace,mp} = 0$ N/mm²

Superposition of load conditions 1 and 2:

$S_{rhs,chord,mp} = 153 + 0 = \underline{153}$ N/mm²
$S_{rhs,brace,mp} = 187 + 0 = \underline{187}$ N/mm²

Step 4: Hot spot stress ranges for design

A partial safety factor on hot spot stress ranges is required for design. For this example the joint is assumed to be non fail-safe and accessible. From Table 1.2, the partial safety factor is 1.25.

$S_{rhs,chord,mp} = 1.25 \cdot 153 = \underline{191\ N/mm^2}$
$S_{rhs,brace,mp} = 1.25 \cdot 187 = \underline{234\ N/mm^2}$

Step 5: Fatigue life of multiplanar joint

For Chord:

$t = 8$ mm and $S_{rhs,chord,mp} = 191\ N/mm^2$

From Table 3.1

$$\log(N_f) = \frac{12.476 - 3 \cdot \log(S_{rhs})}{1 - 0.18 \cdot \log(\frac{16}{t})} = \frac{12.476 - 3 \cdot \log(191)}{1 - 0.18 \cdot \log(\frac{16}{8})} = 5.96$$

$\underline{N_f = 10^{5.96} = 903{,}000\ cycles}$

The fatigue life of the chord in this multiplanar RHS KK-joint is about 903,000 cycles.

For Brace:

$t = 4$ mm and $S_{rhs,brace,mp} = 234$ N/mm2

From Table 3.1

$$\log(N_f) = \frac{12.476 - 3 \cdot \log(S_{rhs})}{1 - 0.18 \cdot \log(\frac{16}{t})} = \frac{12.476 - 3 \cdot \log(234)}{1 - 0.18 \cdot \log(\frac{16}{4})} = 6.02$$

$\underline{N_f = 10^{6.02} = 1{,}050{,}000\ cycles}$

The fatigue life of the brace in this multiplanar RHS KK-joint is about 1,050,000 cycles.

Hence, the fatigue life of the multiplanar joint is 903,000 cycles, with failure in the chord.

9 References

AISC: Load and resistance factor design specification for structural steel buildings, American Institute of Steel Construction, Chicago, USA, 1993.

API: Recommended practice for planning, designing and constructing fixed offshore platforms, API-PR2A, American Petroleum Institute, Dallas, USA, 1991.

AWS: Structural welding code – steel, ANSI/AWS D1.1-98, American Welding Society, Miami, USA, 1998.

Bell, R., Vosikovsky, O. and Bain, S.A.: The significance of weld toe undercut in the fatigue of steel plate T-joints. Int. J. Fatigue, 11(1), 1989, pp 3–11.

Berge, S. and Webster, S.E.: The size effect on the fatigue behaviour of welded joints, Proceedings, Steel in Marine Structures (SIMS'87), 1987, pp 179–203.

Bergmann, R., Mutsui, C., Meinsma, C. and Dutta, D.: Design guide for concrete filled hollow section columns under static and seismic loading. CIDECT-series "Construction with hollow steel sections", Serial no. 5, Verlag TÜV Rheinland, Cologne, Federal Republic of Germany, 1995.

Bignonnet, A.: Improving the fatigue strength of welded steel structures, PS4, International Conference on Steel in Marine Structures, Delft, The Netherlands, June, 1987.

CSA: Limit states design of steel structures, CAN/CSA-S16.1-94, Canadian Standards Association, Toronto, Canada, 1994.

DEn: Offshore installation: guidance on design and construction, Department of Energy, London, UK, 1990.

DEn: Background to new fatigue design guidance for steel joints in offshore structures, Internal Report, Department of Energy, London, UK, 1993.

Dijkstra, O.D., van Foeken, R.J., Romeijn, A., Karamanos, S.A., van Wingerde, A.M., Puthli, R.S., Herion, S. and Wardenier, J.: Fatigue design guide for circular and rectangular hollow section multiplanar joints, Draft Final Report, TNO-Report, 91-CON-R1331, Delft, The Netherlands, 1996.

Dimitrakis, S.D., Lawrence, F.V. and Mohr, W.C.: S-N curves for welded tubular joints, Proceedings, 14th International Offshore Mechanics and Arctic Engineering Symposium (OMAE'95), Volume III, 1995, pp 209–222.

Dutta, D., Wardenier, J., Yeomans, N., Sakae, K., Bucak, Ö. and Packer, J.A.: Design guide for fabrication, assembly and erection of hollow section structures. CIDECT-series "Construction with hollow steel sections", Serial no. 7, Verlag TÜV Rheinland, Cologne, Federal Republic of Germany, 1997.

EC3, ENV 1993-1-1, 1992, Eurocode 3: Design of steel structures – Part 1.1: General rules and rules for buildings. European Committee for Standardisation (CEN), London, UK, 1992.

EC1, Eurocode 1: Basis of Design and Actions on Structures, European Committee for Standardisation (CEN), London, UK, 1994.

ECCS-TC6: Recommendations for the fatigue design of structures. European Convention for Constructional Steelwork, 1985.

Efthymiou, M.: Development of SCF formulae and generalized functions for use in fatigue analyses, OTJ'88, Surrey, UK, 1988.

Efthymiou, M. and Durkin, S.: Stress concentration in T/Y and gap/overlap K-joints, in Behaviour of Offshore Structures, Elsevier Science Publishers B.V., Amsterdam, The Netherlands, 1985, pp 429–440.

Fisher, J., Frank, K.H., Hirt, M.A. and McNamee, B.M.: Effect of weldment on fatigue strength of steel beam, NCHRP Report No. 102, Lehigh University, Bethlehem, Pennsylvania, USA, 1970.

Frater, G.S.: Performance of welded rectangular hollow structural section trusses, PhD thesis, University of Toronto, Canada, 1991.

Gurney, T.R.: Fatigue of welded structures, Cambridge University Press, 2nd edition, Cambridge, UK, 1979.

Haagensen, P.J.: Effect of TIG dressing on fatigue performance and hardness of steel weldment, ASTM STP 648, 1978.

Haagensen, P.J.: Improvement techniques, Proceedings, International Symposium on the Occasion of the Retirement of Prof. J de Back, Delft, The Netherlands, 1989, pp 77–95.

Haagensen, P.J.: IIW's Round Robin and Design Recommendations for Improvement Methods, IIW International Conference on Performance of Dynamically Loaded Welded Structures, July, San Francisco, USA, 1997, pp 305–316.

Haagensen, P. J. and Maddox, S. J.: IIW Recommendations for Weld toe improvement by Burr Grinding, TIG dressing and hammer peening for steel and aluminium Structures, IIW. Doc. XIII-1815-00, June, 2000.

Herion, S.: Multiplanar K-joints made of RHS, PhD thesis, University of Karlsruhe, Germany, 1994.

Herion, S. and Puthli, R.S.: Fatigue design and secondary bending moments in RHS K-joints with gap, The Eighth International Symposium on Tubular Structures, Singapore, August, 1998, pp 315–322.

IIW: Recommended fatigue design procedure for hollow section joints. Part 1 – hot spot stress method for nodal joints. International Institute of Welding Subcommission XV-E, IIW Doc. XV-582-85, IIW Assembly, Strasbourg, France, 1985.

JSSC: Fatigue design recommendations for steel structures, Japanese Society of Steel Construction, English version, December, 1995.

Karamanos, S.A., Romeijn, A. and Wardenier, J.: Stress concentrations and joint flexibility effects in multi-planar welded tubular connections for fatigue design, Stevin Report 6-98-05, CIDECT Report 7R-17/98, Delft University of Technology, Delft, The Netherlands, 1997.

Knight, J.W.: Improving the fatigue strength of fillet welded joints by grinding and peening, Welded Research Int., Vol. 8, No. 6, 1978.

Kobyashi, K. et al.: Improvements in the fatigue strength of fillet welded joint by use of the new welding electrode, IIW Document XIII-828-77, 1977.

Kurobane, Y.: Recent development in the fatigue design rules in Japan. Proceedings, International Symposium on the Occasion of the Retirement of Prof. J. de Back, Delft, The Netherlands, 1989, pp 173–187.

Maddox, S.J.: Fatigue strength of welded structures, Abington Publishing, Cambridge, UK, 1991.

Mang, F. and Bucak, Ö.: Fatigue behaviour of welded joints in trusses of steel hollow sections. IABSE Colloquium on Fatigue of Steel and Concrete Structures, Lausanne, 1982.

Mang, F., Herion, S., Bucak, Ö., Dutta, D.: Fatigue behaviour of K-joints with gap and with overlap made of rectangular hollow sections. The Third International Symposium on Tubular Structures, Lappeenranta, Finland 1989, pp 297–309.

Mang, F. and Bucak, Ö.: Tauglichkeit und Lebensdauer von bestehenden Stahlbauwerken, Stahlbau Handbuch, Band 1 Teil B, Stahlbau, Verlagsgesellschaft mbH, Köln, Germany, 1996.

Marshall, P.W.: Connections for welded tubular structures, IIW International Conference on Welding of Tubular Structures, Boston, USA,1984, pp 1–54.

Marshall, P.W.: Design of welded tubular connections – basis and use of AWS code provisions. Elsevier Science Publishers, Amsterdam, The Netherlands, 1992.

Mashiri, F.R., Zhao, X.-L. and Grundy, P.: Effect of weld profile on the fatigue life of thin-walled cruciform joint, The Eighth International Symposium on Tubular Structures, Singapore, 1998, pp 331–340.

Mori, T., Zhao, X.-L. and Grundy, P.: Fatigue strength of transverse single-sided fillet welded joints, Australian Civil/Structural Engineering Transactions, Vol. CE39, No. 2 and No. 3, 1997, pp 95–105.

Nguyen, T.N. and Wahab, M.A.: A theoretical study of the effect of weld geometry parameters on fatigue crack propagation life, Engineering Fracture Mechanics, 51 (1), 1995, pp 1–18.

Niemi, E.J.: A novel fatigue analysis approach for tubular welded joints. Proceedings, Fatigue Design'95, Helsinki, Finland, 1995, pp 189–201.

Noordhoek, C., Wardenier, J. and Dutta, D.: The fatigue behaviour of welded joints in square hollow sections, Part 2 – Analysis, Stevin Report 6-80-4, TNO-IBBC-Report BI-80-10/0063.4.3821, Delft, The Netherlands, 1980.

Packer, J.A., Wardenier, J., Kurobane, Y., Dutta, D. and Yeomans, N.: Design guide for rectangular hollow section (RHS) joints under predominantly static loading. CIDECT-series "Construction with hollow steel sections", Serial no. 3, Verlag TÜV Rheinland, Cologne, Federal Republic of Germany, 1992.

Packer, J.A. and Wardenier, J.: Stress concentration factors for non-90° X-Connections made of square hollow sections, Can. J. Civ. Eng., 25(2), 1998, pp 370–375.

Puthli, R.S., de Koning, C.H.M., van Wingerde, A.M., Wardenier, J. and Dutta, D.: Fatigue strength of welded unstiffened RHS-joints in latticed structures and vierendeel girders, Final Report Part III: Evaluation for Design Rules, TNO-IBBC Report No. BI-89-097/63.5.3820, Stevin Report No. 25-6-89-36/A1, June, Delft, The Netherlands, 1989.

Puthli, R.S., Wardenier, J., Mang, F. and Dutta, D.: Fatigue behaviour of multiplanar welded hollow section joints and reinforcement measures for repair, Final report Part V – Evaluation and design recommendation, TNO-Bouw Report No. BI-92-0079/21.4.6394, Stevin Report No. 6.92.17/A1/12.06, Sept., Delft, The Netherlands, 1992.

Puthli, R. and Herion, S. (1996): Stress concentration and secondary moment distribution in RHS joints for fatigue design. Background document for fatigue design guide on RHS, University of Karlsruhe, Germany, 1996.

Romeijn, A., Puthli, R.S., de Koning, C.H.M. and Wardenier, J.: Stress and strain concentration factors of multiplanar joints made of circular hollow sections, The Second International Offshore and Polar Engineering Conference, San Francisco, USA, Vol. IV, 1992, pp 384–393.

Romeijn, A., Wardenier, J., de Koning, C.H.M., Puthli, R.S. and Dutta, D.: Fatigue behaviour and influence of repair on multi planar K-joints made of circular hollow sections. The Third International Offshore and Polar Engineering Conference, Singapore, Vol. IV, 1993, pp 27–36.

Romeijn, A.: Stress and strain concentration factors of welded multiplanar tubular joints, PhD Thesis, Delft, The Netherlands, 1994.

Romeijn, A., Karamanos, S.A. and Wardenier, J.: Effects of joint flexibility on the fatigue design of welded tubular lattice structures, The Seventh International Offshore and Polar Engineering Conference, Honolulu, USA, Vol. IV, 1997, pp 90–97.

Rondal, J., Würker, K.G., Dutta, D., Wardenier, J. and Yeomans, N.: Structural stability of hollow sections. CIDECT-series “Construction with hollow steel sections”, Serial no. 2, Verlag TÜV Rheinland, Cologne, Federal Republic of Germany, 1991.

SAA: Steel structures, Australian Standard AS4100, Standards Association of Australia, Sydney, Australia, 1990.

Sedlacek, G., Grotmann, D., Gusgen, J., Jo, J.B. and Dutta, D.: The determination of the fatigue resistance of steel structures on the basis of the combined methods, The Second International Offshore and Polar Engineering Conference, San Francisco, USA, Vol. IV, 1992, pp 296–300.

Sedlacek, G., Grotmann, D., Schäfers, M. and Zhao, X.-L.: Fatigue Behaviour of hollow section joints, CIDECT 7N Project Report, RWTH, Aachen, Germany, 1998.

Swanmidas, A.S.J., Cheema, P.S. and Muggeridge, D.B.: Fatigue strength of fillet-welded cruciform joints. Can. J. Civ. Eng., 16(2), 1989, pp 162–171.

Thorpe, T.W. and Sharp, J.V.: The fatigue performance of tubular joints in air and sea water, MaTSU Report, Harwell Laboratory, Oxfordshire, UK, 1989.

Twilt, L., Hass, R., Klingsch, W., Edwards, M. and Dutta, D.: Design guide for structural hollow section columns exposed to fire. CIDECT-series “Construction with hollow steel sections”, Serial no. 4, Verlag TÜV Rheinland, Cologne, Federal Republic of Germany, 1996.

Wardenier, J.: Hollow section joints, Delft University Press, Delft, The Netherlands, 1982.

Wardenier, J., Kurobane, Y., Packer, J.A., Dutta, D. and Yeomans, N.: Design guide for circular hollow section (CHS) joints under predominantly static loading. CIDECT-series "Construction with hollow steel sections", Serial no. 1, Verlag TÜV Rheinland, Cologne, Federal Republic of Germany, 1991.

Wardenier, J., Dutta, D., Yeomans, N., Packer, J.A. and Bucak, Ö.: Design guide for structural hollow sections in mechanical applications. CIDECT-series "Construction with hollow steel sections", Serial no. 6, Verlag TÜV Rheinland, Cologne, Federal Republic of Germany, 1995.

van Delft, D.R.V.: A two dimensional analysis of the stresses at the vicinity of the weld toes of tubular structures, Stevin Report 6-18-8, Delft University of Technology, Delft, The Netherlands, 1981.

van Delft, D.R.V., Noordhoek, C. and de Back, J.: Evaluation of the European fatigue test data on large-sized welded tubular joints for offshore structures, Offshore Technology Conference, Houston, USA, paper OTC 4999,1985.

van Delft, D.R.V., Noordhoek, C. and Da Re, M.L.: The results of the European fatigue tests on welded tubular joints compared with SCF formulas and design lines, Steel in Marine Structures, Elsevier Applied Science Publishers, Ltd., Delft, The Netherlands, 1987, pp 565–577.

van Wingerde, A.M.: The fatigue behaviour of T and X joints made of square hollow sections, Heron, The Netherlands, Vol. 37, No. 2, 1992, pp 1–180.

van Wingerde, A.M., Packer, J.A., Wardenier, J. and Dutta, D.: The fatigue behaviour of K-joints made of square hollow sections, CIDECT Report 7P-19/96, University of Toronto, Canada, 1996.

van Wingerde, A.M., Packer, J.A., Wardenier, J. and Dutta, D.: Simplified design graphs for the fatigue design of multiplanar K-joints with gap. CIDECT Report 7R-01/97, January, University of Toronto, Canada, 1997a.

van Wingerde, A.M., Packer, J.A. and Wardenier, J.: IIW fatigue rules for tubular joints, IIW International Conference on Performance of Dynamically Loaded Welded Structures, July, San Francisco, USA, 1997b, pp 98–107.

van Wingerde, A.M., van Delft, D.R.V., Wardenier, J. and Packer, J.A.: Scale Effects on the Fatigue Behaviour of Tubular Structures, IIW International Conference on Performance of Dynamically Loaded Welded Structures, July, San Francisco, USA, 1997c, pp 123–135.

van Wingerde, A.M., Wardenier, J. and Packer, J.A.: Commentary on the Draft Specification for Fatigue Design of Hollow Section Joints, The Eighth International Symposium on Tubular Structures, Singapore, August, 1998a, pp 117–127.

van Wingerde, A.M., Wardenier, J. and Packer, J.A.: Simplified design graphs for the fatigue design of multiplanar K-joints with gap, Final Report, Stevin Report 6-98-34, Delft, The Netherlands, 1998b.

Zhao, X.-L. and Puthli, R.S.: Comparison of SCF formulae and fatigue strength for uniplanar RHS K-joints with gap, IIW Document XV-E-98-235, 1998.

Appendix A: Fatigue Actions

The fatigue actions can be included in a design by considering only the service or working conditions, e.g. by specifying the particular ways that cranes are loaded and operated or by specifying particular actions of machinery. These indications may be used to determine the relevant fatigue loading specifically for the structure. The fatigue loading can be taken from appropriate recommendations or guidelines, e.g. the ECCS TC6-Recommendations (1985).

The fatigue actions can also be included in a design by referring to a relevant code for the fatigue loading of railway or road bridges and cranes or that for wind loading, e.g. Eurocode 1 (1994). Additional data, such as spectra, damage equivalent loads and safety factors, may be given in the project specifications, and may supplement or replace code provisions.

A simple example is given in Figure A.1 to demonstrate the general procedures of determination of fatigue loading and fatigue damage assessment. The steps are shown below.

(a) Determination of one or more service sequences, typical for the total service life of the structure, e.g. loads P_A and P_B shown in Figure A.1 (a) are typical load cycles.

(b) Determination of the stress history at the relevant structural detail for these service sequences, e.g. stress range (S) history at the detail X-X location shown in Figure A.1 (b).

(c) Breaking the stress range history into a stress spectrum using a cycle counting method if the stress history is of a variable amplitude type. Two commonly used cycle counting methods are the Rainflow method and the Reservoir method. The Rainflow method is more convenient for analyzing long stress histories using a computer. The Reservoir method is easy to use by hand for short stress histories as shown in Figure A.1 (c).

(d) Simplifying the stress spectrum obtained in step (c) into a manageable number of bands as shown in Figure A.1 (d).

(e) Determination of endurance (N_i) for each stress level (S_i) according to an appropriate fatigue strength curve as shown in Figure A.1 (e).

(f) Application of an appropriate damage accumulation rule such as the Palmgren-Miner's Rule shown in Figure A.1 (f). The rule states that the damage done by all bands together must not exceed unity. If failure is to be prevented before the end of the specified design life, compliance with the Palmgren-Miner's Rule is necessary.

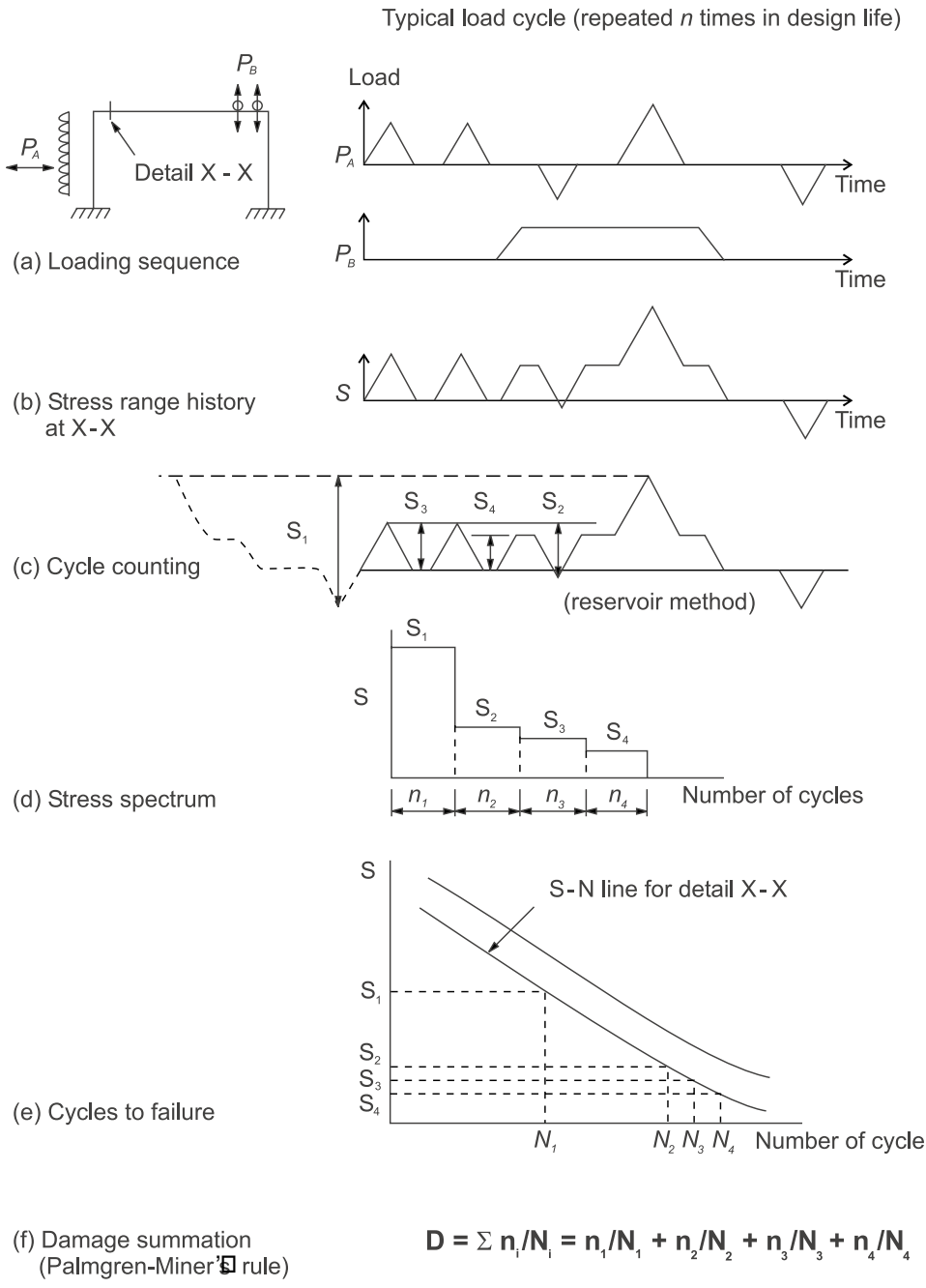

Figure A.1 – A simple example on fatigue assessment procedures

Appendix B: Detailed Categories for Classification Method

The detail categories for the classification method are listed in Table B.1 for simple connections and Table B.2 for lattice girder joints. Note that the values for detail categories shown here are those given in Eurocode 3 [EC3 (1992)]. The values may change slightly in other national codes. The tube thickness in Table B.1 is between 4 mm and 12.5 mm. The tube thickness in Table B.2 is between 4 mm and 8 mm.

Table B.1 – Detail Categories for Hollow Section and Simple Connections

Details loaded by nominal normal stresses		
Detail category m = 3	Constructional detail	Description
160		Rolled and extruded products Non-welded elements. Sharp edges and surface flaws to be improved by grinding.
140		Continuous longitudinal welds Automatic longitudinal welds with no stop-start positions, proven free of detectable discontinuities.
71	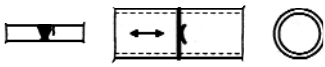	Transverse butt welds Butt welded end-to-end connection of circular hollow sections Requirements: – Height of the weld reinforcement less than 10 % of weld with smooth transitions to the plate surface – Welds made in flat position and proven free of detectable discontinuities – Details with wall thickness greater than 8 mm may be classified two Detail categories higher (⇒ 90).
56	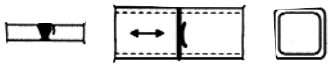	Transverse butt welds Butt welded end-to-end connection of rectangular hollow sections Requirements: – Height of the weld reinforcement less than 10 % of weld with smooth transitions to the plate surface – Welds made in flat position and proven free of detectable discontinuities – Details with wall thickness greater than 8 mm may be classified two Detail categories higher (⇒ 71).
71	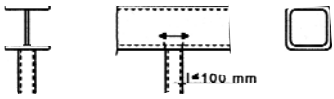	Welded attachments (non-load-carrying welds) Circular or rectangular section, fillet welded to another section. Section width parallel to stress direction ≤ 100 mm.

Table B.1 – Detail Categories for Hollow Section and Simple Connections (continued)

Details loaded by nominal normal stresses			
Detail category m = 3	Constructional detail		Description
50	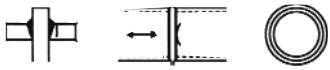		Welded connections (load-carrying welds) Circular hollow sections, end-to-end butt welded with an intermediate plate. Requirements: – Welds proven free of detectable discontinuities – Details with wall thicknesses greater than 8 mm may be classified one Detail category higher (⇒ 56).
45	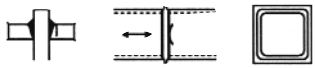		Welded connections (load-carrying welds) Rectangular hollow sections, end-to-end butt welded with an intermediate plate. Requirements: – Welds proven free of detectable discontinuities – Details with wall thicknesses greater than 8 mm may be classified one Detail category higher (⇒ 50).
40	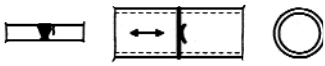		Welded connections (load-carrying welds) Circular hollow sections, end-to-end fillet welded with an intermediate plate. Requirements: – Wall thickness less than 8 mm.
36	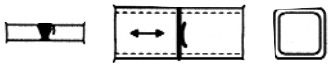		Welded connections (load-carrying welds) Rectangular hollow sections, end-to-end fillet welded with an intermediate plate. Requirements: – Wall thickness less than 8 mm.
80	$\ell \leq$ 50mm		Longitudinal attachments (non-load-carrying welds) The Detail category varies according to the length of the attachment ℓ.
71	50 < ℓ < 80 mm		
63	80 < ℓ < 100 mm		
56	ℓ > 100 mm		
80	t ≤ 12 mm	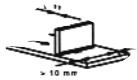	Transverse attachments The end of weld more than 10 mm from the edge of the plate.
71	t > 12 mm		
80	t ≤ 12 mm	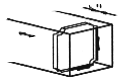	Transverse attachments Diaphragms of rectangular girders welded to the flange or web.
71	t > 12 mm		

Table B.1 – Detail Categories for Hollow Section and Simple Connections (continued)

Details loaded by nominal normal stresses		
Detail category m = 3	Constructional detail	Description
80	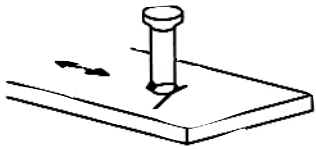	Transverse attachment The effect of welded shear connectors on base material.
71	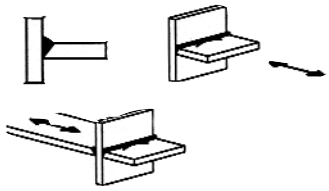	Cruciform joints (load-carrying welds) Full penetration weld. Inspected free of detectable discontinuities. Requirements: – The maximum misalignment of the load-carrying plates should be less than 15 % of the thickness of the intermediate plate.
36	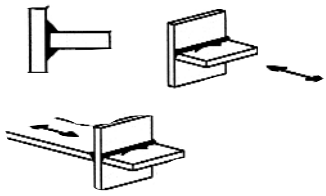	Cruciform joints (load-carrying welds) Fillet welded connection. Two fatigue assessments are required. Firstly, root cracking is evaluated by determining the stress range in the weld throat area. Category 36. Secondly, toe cracking is evaluated by determining the stress range in the load-carrying plates. Category 71. Requirements: – The maximum misalignment of the load-carrying plates should be less than 15 % of the thickness of the intermediate plate. – $t \leq 20$ mm
50	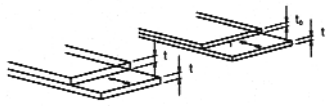	Cover plates (load-carrying welds) End zones of single or multiple welded cover plates, with or without frontal weld. When the reinforcing plate is wider then the flange, a frontal weld, carefully ground to remove undercut, is necessary.

Table B.2 – Detail Categories for Lattice Girder Joints

Details loaded by nominal normal stresses			
Detail category m = 5	Constructional detail		Description
90	$t_0/t_i = 2.0$	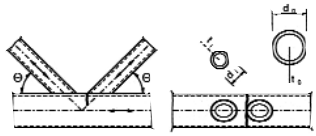	Joints with gap Circular hollow sections, K and N-joints
45	$t_0/t_i = 1.0$		
71	$t_0/t_i \geq 2.0$	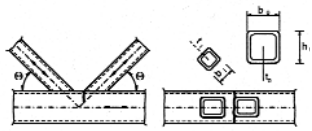	Joints with gap Rectangular hollow sections, K and N-joints Requirements • $0.5\ (b_0 - b_i) \leq g \leq 1.1\ (b_0 - b_i)$ • $g \geq 2\ t_0$
36	$t_0/t_i = 1.0$		
71	$t_0/t_i \geq 1.4$	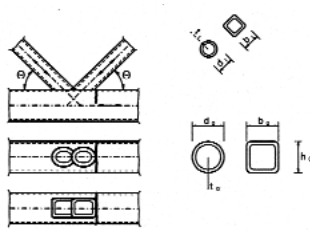	Joints with overlap K-joints Requirements • overlap between 30 and 100 %
56	$t_0/t_i = 1.0$		
71	$t_0/t_i \geq 1.4$	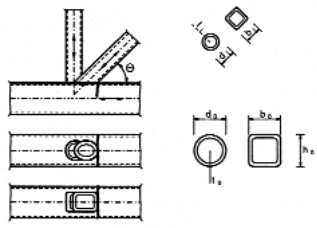	Joints with overlap N-joints Requirements • overlap between 30 and 100 %
50	$t_0/t_i = 1.0$		

General Requirements

$4 \leq t_o \leq 8$ mm*	$4 \leq t_1 \leq 8$ mm*	$35° \leq \theta \leq 50°$	
$b_o \leq 200$ mm	$0.4 \leq b_1/b_o \leq 1.0$	$-0.5\ h_o \leq e \leq 0.25 h_o$	$(b_o/t_o) \cdot (t_o/t_1) \leq 25$*
$d_o \leq 300$ mm	$0.25 \leq d_1/d_o \leq 1.0$	$-0.5\ d_o \leq e \leq 0.25 d_o$	$(d_o/t_o) \cdot (t_o/t_1) \leq 25$*

Out-of-plane eccentricity: $\leq 0.02\ b_0$ or $\leq 0.02\ d_0$
Fillet welds are permitted in braces with wall thicknesses ≤ 8 mm.

– For Intermediate t_0/t_i values, use linear interpolation between nearest Detail Categories
– Note that the braces and chords require separate fatigue assessments
* Based on actual test results. Different from Eurocode 3 where $t_o \leq 12.5$ mm, $t_1 \leq 12.5$ mm, $b_o/t_o \leq 25$ and $d_o/t_o \leq 25$.

Appendix C: The Determination of SCFs by Testing and Finite Element Analysis

C.1 Hot Spot Stress and SCF

The hot spot stress (also called geometric stress) method relates the fatigue life of a joint to the so-called hot spot stress at the joint rather than the nominal stress. It takes the uneven stress distribution around the perimeter of the joint into account directly. The hot spot stress range includes the geometrical influences but excludes the effects related to fabrication such as the configuration of the weld (flat, convex, concave) and the local condition of the weld toe (radius of weld toe, undercut, etc.). The hot spot stress is the maximum geometrical stress occurring in the joint where the cracks are usually initiated. In the case of welded joints, this generally occurs at the toe of the weld.

The stress concentration factor (SCF) is the ratio between the hot spot stress at the joint and the nominal stress in the member due to a basic member load which causes this hot spot stress. The hot spot stress has to be determined at the weld toe position from the stress field outside the region influenced by the local weld toe geometry. The location from which the stresses have to be extrapolated, the so-called "extrapolation region", depends on the dimensions of the joint and on the position around the intersection. The boundaries of the extrapolation region for CHS and RHS joints are defined in Table C.1 and Figure C.1 (Romeijn [1994]).

Table C.1 – Boundaries of extrapolation region for CHS and RHS joints

distances from weld toe		chord		brace	
		saddle	crown	saddle	crown
CHS	$L_{r,min}$ *)	$0.4 \cdot t_0$		$0.4 \cdot t_1$	
	$L_{r,max}$ **)	$0.09\ r_0$	$0.4 \cdot \sqrt[4]{r_0\ t_0\ r_1\ t_1}$	$0.65\ \sqrt{r_1\ t_1}$	
CHS	$L_{r,min}$ *)	$0.4 \cdot t_0$		$0.4 \cdot t_1$	
	$L_{r,max}$	$L_{r,min} + t_0$		$L_{r,max} + t_1$	

*) Minimum value for $L_{r,min}$ is 4 mm.
**) Minimum value for $L_{r,max}$ is $L_{r,\ min} + 0.6 \cdot t_1$

The hot spot stress or the SCF can be determined using strain gauges or by finite element analysis. This appendix will provide advice and suggestions on using these two methods to determine the hot spot stress and SCF.

A minimum SCF = 2.0 is recommended unless it is negligible. The bases for minimum SCF values are:

- The SCFs are determined along limited fixed lines or locations of interest. The hot spot stresses found may underestimate the 'true' hot spot stress if the direction of the principal stresses deviates from these lines, especially if the stress concentration is less pronounced.

- Difficulties in FE modelling, such as the case where $\beta = 1.0$ and the case where weld shapes have a strong influence on SCFs.

- Crack initiation from the root of the weld for low SCF values

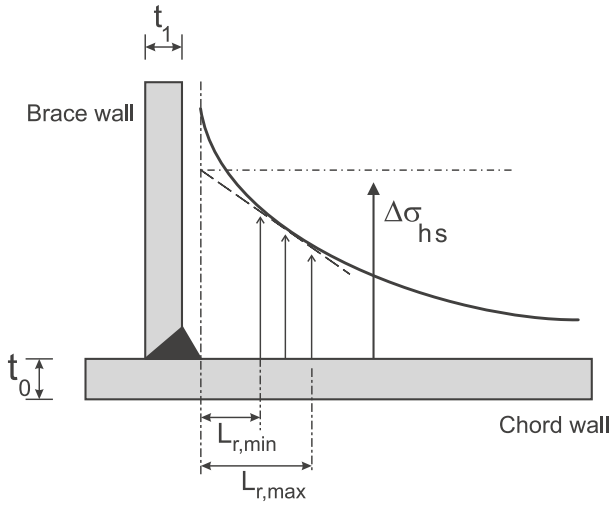

Figure C.1 – Definition of extrapolation region

C.2 Experimental Approach

Advice and suggestions are given for the following aspects:

a) Stress and strain components

Different views exist with regard to which stress (strain) component should be used to determine the SCF: the principal stress (strain) or a stress perpendicular to the weld toe. The principal stress is used in IIW, DEn and EC3, whereas the stress perpendicular to the weld toe is used in AWS and API. The differences between the two stresses become less significant near the weld toe (Marshall [1992], Romeijn et al. [1992]). Strains perpendicular to the weld toe can be measured by simple strain gauges instead of strain gauge rosettes which are required to determine the principal strains. The use of stresses (strains) perpendicular to the weld toe is recommended.

b) Location of strain gauges

Normal strains have to be measured in the extrapolation region perpendicular to the weld toe for the chord and parallel to the brace axis for the brace locations. The extrapolation region is defined in Figure C.1 and Table C.1. Lines of measurement or locations of interest are suggested in Figures 4.1, 4.5, 4.9, 4.10, 4.11, 5.1, 5.5 and 5.6, along which strip strain gauges can be applied to measure the strain distribution.

c) Effect of bending moments

In addition to the applied in-plane bending (IPB) or out-of-plane bending (OPB) moments, secondary bending moments exist in joints, especially those in lattice girders. The secondary bending moment is caused by the inevitable loading eccentricity and the joint flexibility (Wardenier [1982], Romeijn et al. [1997], Herion and Puthli [1998]). It is necessary to measure the strains caused by bending moments and those caused by axial forces in a test. This can be done by applying strain gauges in two or three cross-sections along each brace member. The strains caused by bending and axial force can be separated by a simple superposition technique. The distance between the measuring sections in the brace and the weld toe should be kept to at least $3d_1$ or $3b_1$ where d_1 or b_1 is the diameter or width of the brace member.

d) Extrapolation method

As mentioned before, the hot spot stress range includes the geometrical influences but excludes the effects related to fabrication such as the configuration of the weld (flat, convex, concave) and the local condition of the weld toe (radius of weld toe, undercut, etc.). On the one hand, the extrapolation of strain distribution should be carried out in the “extrapolation region” defined in Table C.1 and Figure C.1. On the other hand, the extrapolation points must be positioned in such a way that the strain gradients due to the global geometry effects are represented. Two extrapolation methods are commonly used, namely linear and quadratic, for the determination of the hot spot stress. They are shown in Figure C.2. For joints in CHS, the linear extrapolation method can be used since the gradient is nearly linear (Romeijn [1994]). For joints in RHS, the quadratic extrapolation method is required because of the strong non-linear strain distribution observed (van Wingerde [1992]).

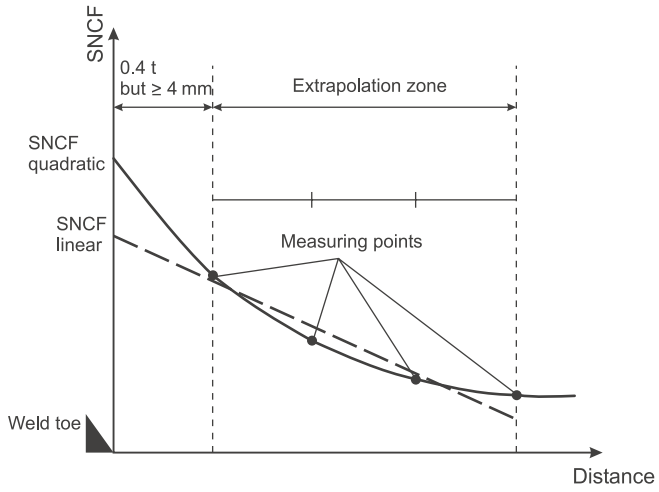

Figure C.2 – Methods of extrapolation

e) Relationship between SNCF and SCF

Because only strains can be directly measured using strain gauges, the strain concentration factor (SNCF) is determined first. Then the SNCF is converted to the stress concentration factor (SCF).

The formulae for SNCF can be expressed as (Herion [1994])

$SNCF_{RHS} = \varepsilon_{max}/(\varepsilon_{ax} + \varepsilon_{IPB} + \varepsilon_{OPB})$ for joints in RHS

$SNCF_{CHS} = \varepsilon_{max}/(\varepsilon_{ax} + \sqrt{(\varepsilon^2_{IPB} + \varepsilon^2_{OPB})})$ for joints in CHS

where ε_{max} is the extrapolated maximum strain, ε_{ax}, ε_{IPB}, and ε_{OPB} are nominal strain components caused by axial force, in-plane bending and out-of-plane bending respectively.

The SNCF can be converted to SCF using (Frater [1991], van Delft et al. [1987])

$SCF_{RHS} = 1.1\ SNCF_{RHS}$ for joints in RHS

$SCF_{CHS} = 1.2\ SNCF_{CHS}$ for joints in CHS

f) Others

The experiments have to be carried out in a well-equipped laboratory by specialists. One should ensure that the boundary conditions and the loading positions are correct.

C.3 Finite Element Analysis

Advice and suggestions are given for the following aspects:

a) Preconsideration about the FE-Model

The FE analysis should be carried out with a validated FE package and by FE analysts experienced in the use of FE programs for determining SCFs. Some of the FE packages used in the past to determine SCFs include ABAQUS, ANSYS, DIANA and MARC. It is also important to ascertain the scope of the problem with regard to the required computer capacities. Geometrical symmetry and the symmetry of applied forces should be utilised to simplify the problem. Attention should be paid to the boundary conditions in the plane of symmetry.

b) Elements

The refinement of the FE mesh of a hollow section joint depends on the type of elements and on the stress/strain gradient over the element. The refinement of the mesh should be such that any further refinement does not result in a substantial change of the stress distribution (outside the notch effect area). Element dimensions of $0.5t_1$ to $0.5t_o$ may be used (Herion [1994]). With the use of solid elements, there should be no problem with this ratio of side length to element thickness. In the case of thin shell elements with this dimension, the reliability of the calculation needs to be checked. The element size in regions of less interest can be increased to save computing time.

c) Modelling of details

Modelling the weld shape greatly improves the accuracy of SCFs. Therefore, using solid elements to model the weld area and the extrapolation region is recommended. Because of the high accuracy requirements, the use of 20-node solid elements with an integration scheme of 2 x 2 x 2 is recommended (Romeijn [1994]).

For rectangular hollow sections, a stress redistribution around the corners can be observed especially for butt (groove) welded joints. Modelling of the corners with several elements is recommended. The minimum number of elements required depends on the thickness of the tube (t), i.e. 2 for $t \leq 8$ mm, 3 for $8 < t < 16$ mm and 4 for $t \geq 16$ mm (Herion [1994]). The radius of corners should also be taken into account. Inside and outside corner radii are different for hot-formed and cold-formed sections. Different values also exist between manufacturers and countries.

d) Judgement of results

The comparison of predicted strain concentration factors (SNCF) with experimental values should be carried out. Before comparing with experimental results, it is recommended to check the following aspects first.

Simple geometry and loading. This can be done by using the check routines of the pre-processor used to generate the model.

Boundary conditions. This can be done by checking the global static equilibrium condition, i.e. comparing the calculated node forces at fixed nodes with applied loads.

Mesh division. This can be done by comparing the stresses in neighbouring elements. If there is a big difference, it is often caused by the big differences in the element dimensions.

e) Others

Stresses and strains have to be determined in the extrapolation region perpendicular to the weld toe or in the direction of the principal strain.

Appendix D: SCF Formulae and Graphs for CHS Joints

A minimum SCF of 2.0 is recommended for all joint types, all locations and all load conditions unless otherwise specified.

D.1 Uniplanar CHS T and Y-Joints

Table D.1 – SCFs for uniplanar CHS T and Y-joints

Locations

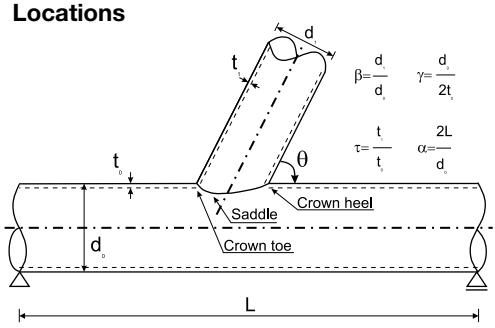

Range of validity

$0.2 \le \beta \le 1.0$
$15 \le 2\gamma \le 64$
$0.2 \le \tau \le 1.0$
$4 \le \alpha \le 40$
$30° \le \theta \le 90°$

Chord-end fixity parameters C

$C_1 = 2\ (C - 0.5)$
$C_2 = C/2$
$C_3 = C/5$
For fixed chord ends, C = 0.5
For pinned chord ends, C = 1.0
Otherwise C = 0.7

Load conditions

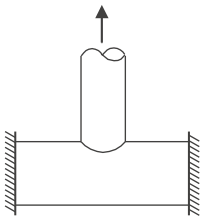

Load condition 1
axial load with chord ends fixed

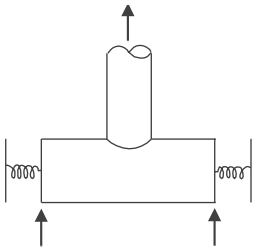

Load condition 2
axial load with general chord fixity

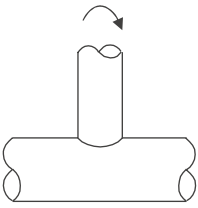

Load condition 3
in-plane bending

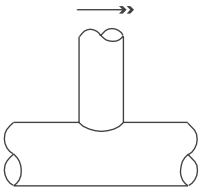

Load condition 4
out-of-plane bending

Table D.1 – SCFs for uniplanar CHS T and Y-joints (continued)

Load condition 1	**axial load with chord ends fixed** (uniplanar CHS T and Y-joints)
chord (saddle and crown)	**brace (saddle and crown)**
$SCF_{ch\_saddle,ax} = T_1 \cdot F_1$ $SCF_{ch\_crown,ax} = T_2$	$SCF_{b\_saddle,ax} = T_3 \cdot F_1$ $SCF_{b\_crown,ax} = T_4$
$T_1 = \gamma \cdot \tau^{1.1}[1.11–3 \cdot (\beta–0.52)^2] \cdot \sin^{1.6}\theta$ $T_2 = \gamma^{0.2} \cdot \tau[2.65+5 \cdot (\beta–0.65)^2] + \tau \cdot \beta(0.25 \cdot \alpha–3) \cdot \sin\theta$ $T_3 = 1.3+\gamma \cdot \tau^{0.52} \cdot \alpha^{0.1}[0.187–1.25 \cdot \beta^{1.1}(\beta–0.96)] \cdot \sin^{(2.7–0.01\alpha)}\theta$ $T_4 = 3+\gamma^{1.2} \cdot [0.12 \cdot \exp(–4\beta)+0.011 \cdot \beta^2–0.045]+\beta \cdot \tau \cdot (0.1\alpha–1.2)$ if $\alpha \geq 12$: $F_1 = 1.0$ if $\alpha < 12$: $F_1 = 1–(0.83 \cdot \beta–0.56 \cdot \beta^2–0.02) \cdot \gamma^{0.23} \cdot \exp[–0.21 \cdot \gamma^{–1.16} \cdot \alpha^{2.5}]$ where $\exp[x] = e^x$	
Load condition 2	**axial load with general chord fixity conditions** (uniplanar CHS T and Y-joints)
chord (saddle and crown)	**brace (saddle and crown)**
$SCF_{ch\_saddle,ax} = T_5 \cdot F_2$ $SCF_{ch\_crown,ax} = T_6$	$SCF_{b\_saddle,ax} = T_3 \cdot F_2$ $SCF_{b\_crown,ax} = T_7$
$T_5 = \gamma \cdot \tau^{1.1}[1.11–3 \cdot (\beta–0.52)^2] \cdot \sin^{1.6}\theta + C_1 \cdot (0.8\alpha–6) \cdot \tau \cdot \beta^2(1–\beta^2)^{0.5} \cdot \sin^2 2\theta$ $T_6 = \gamma^{0.2} \cdot \tau[2.65+5 \cdot (\beta–0.65)^2]+ \tau \cdot \beta \cdot (C_2 \cdot \alpha–3) \cdot \sin\theta$ $T_7 = 3+\gamma^{1.2} \cdot [0.12 \cdot \exp(–4 \cdot \beta)+0.011 \cdot \beta^2–0.045]+\beta \cdot \tau \cdot (C_3 \cdot \alpha–1.2)$ if $\alpha \geq 12$: $F_2 = 1.0$ if $\alpha < 12$: $F_2 = 1–(1.43 \cdot \beta–0.97 \cdot \beta^2–0.03) \cdot \gamma^{0.04} \cdot \exp[–0.71 \cdot \gamma^{–1.38} \cdot \alpha^{2.5}]$ where $\exp[x] = e^x$	

Table D.1 – SCFs for uniplanar CHS T and Y-joints (continued)

Load condition 3	**in-plane bending** (uniplanar CHS T and Y-joints)
chord (saddle and crown)	**brace (saddle and crown)**
$SCF_{ch\_saddle,ipb} = 0$ (negligible) $SCF_{ch\_crown,ipb} = T_8$	$SCF_{b\_saddle,ipb} = 0$ (negligible) $SCF_{b\_crown,ipb} = T_9$
$T_8 = 1.45 \cdot \beta \cdot \tau^{0.85} \cdot \gamma^{(1-0.68\beta)} \cdot \sin^{0.7}\theta$ $T_9 = 1 + 0.65 \cdot \beta \cdot \tau^{0.4} \cdot \gamma^{(1.09-0.77\beta)} \cdot \sin^{(0.06\gamma-1.16)}\theta$	
Load contition 4	**out-of-plane bending** (uniplanar CHS T and Y-joints)
chord (saddle and crown)	**brace (saddle and crown)**
$SCF_{ch\_saddle,opb} = T_{10} \cdot F_3$ $SCF_{ch\_crown,opb} = 0$ (negligible)	$SCF_{b\_saddle,opb} = T_{11} \cdot F_3$ $SCF_{b\_crown,opb} = 0$ (negligible)
$T_{10} = \gamma \cdot \tau \cdot \beta(1.7-1.05\beta^3) \cdot \sin^{1.6}\theta$ $T_{11} = \gamma^{0.95} \cdot \tau^{0.46} \cdot \beta \cdot (1.7-1.05\beta^3) \cdot (0.99-0.47\beta+0.08\beta^4) \cdot \sin^{1.6}\theta$ if $\alpha \geq 12$: $F_3 = 1.0$ if $\alpha < 12$: $F_3 = 1-0.55 \cdot \beta^{1.8} \cdot \gamma^{0.16} \cdot \exp[-0.49 \cdot \gamma^{-0.89} \cdot \alpha^{1.8}]$ where $\exp[x] = e^x$	

D.2 Uniplanar CHS X-Joints

Table D.2 – SCFs for uniplanar CHS X-joints

Locations

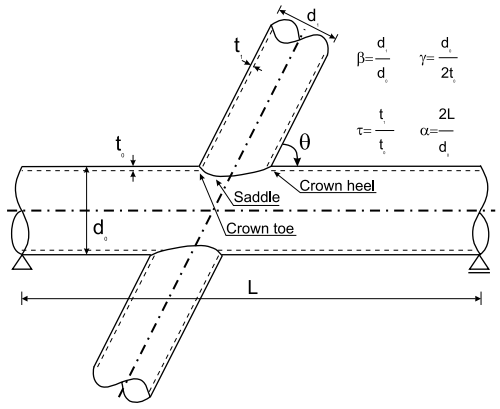

Range of validity

$0.2 \le \beta \le 1.0$
$15 \le 2\gamma \le 64$
$0.2 \le \tau \le 1.0$
$4 \le \alpha \le 40$
$30° \le \theta \le 90°$

Load conditions

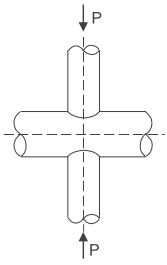

Load condition 1
balanced axial load with chord ends pinned

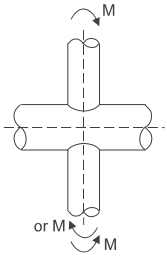

Load condition 2
in-plane bending

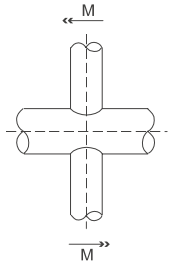

Load condition 3
out-of-plane bending

Table D.2 – SCFs for uniplanar CHS X-joints (continued)

Load condition 1	**balanced axial load with chord ends pinned** (uniplanar CHS X-joints)
chord (saddle and crown)	**brace (saddle and crown)**
$SCF_{ch\_saddle,ax} = X_1 \cdot F_2$ $SCF_{ch\_crown,ax} = X_2$	$SCF_{b\_saddle,ax} = X_3 \cdot F_2$ $SCF_{b\_crown,ax} = X_4$
$X_1 = 3.87 \cdot \gamma \cdot \tau \cdot \beta[1.10-\beta^{1.8}] \cdot (\sin\theta)^{1.7}$ $X_2 = \gamma^{0.2} \cdot \tau[2.65+5 \cdot (\beta-0.65)^2] - 3 \cdot \tau \cdot \beta \cdot \sin\theta$ $X_3 = 1 + 1.9 \cdot \gamma \cdot \tau^{0.5} \cdot \beta^{0.9} \cdot (1.09-\beta^{1.7}) \cdot \sin^{2.5}\theta$ $X_4 = 3 + \gamma^{1.2} \cdot [0.12 \cdot \exp(-4 \cdot \beta)+0.011 \cdot \beta^2-0.045]$ if $\alpha \geq 12$: $F_2 = 1.0$ if $\alpha < 12$: $F_2 = 1-(1.43 \cdot \beta-0.97 \cdot \beta^2-0.03) \cdot \gamma^{0.04} \cdot \exp[-0.71 \cdot \gamma^{-1.38} \cdot \alpha^{2.5}]$ where $\exp[x] = e^x$	
Load condition 2	**in-plane bending** (uniplanar CHS X-joints)
SCFs are the same as those for uniplanar T-joints subjected to in-plane bending, as given in Table D.1.	
Load condition 3	**out-of-plane bending** (uniplanar CHS X-joints)
chord (saddle and crown)	**brace (saddle and crown)**
$SCF_{ch\_saddle,opb} = X_5 \cdot F_3$ $SCF_{ch\_crown,opb} = 0$ (negligible)	$SCF_{b\_saddle,opb} = X_6 \cdot F_3$ $SCF_{b\_crown,opb} = 0$ (negligible)
$X_5 = \gamma \cdot \tau \cdot \beta \cdot (1.56-1.34 \cdot \beta^4) \cdot (\sin\theta)^{1.6}$ $X^6 = \gamma^{0.95} \cdot \tau^{0.46} \cdot \beta \cdot (1.56-1.34 \cdot \beta^4) \cdot (0.99-0.47 \cdot \beta+0.08 \cdot \beta^4) \cdot (\sin\theta)^{1.6}$ if $\alpha \geq 12$: $F_3 = 1.0$ if $\alpha < 12$: $F_3 = 1-0.55 \cdot \beta^{1.8} \cdot \gamma^{0.16} \cdot \exp[-0.49 \cdot \gamma^{-0.89} \cdot \alpha^{1.8}]$ where $\exp[x] = e^x$	

D.3 Uniplanar CHS K-Joints with Gap

Table D.3 – SCFs for uniplanar CHS K-joints with gap

Locations

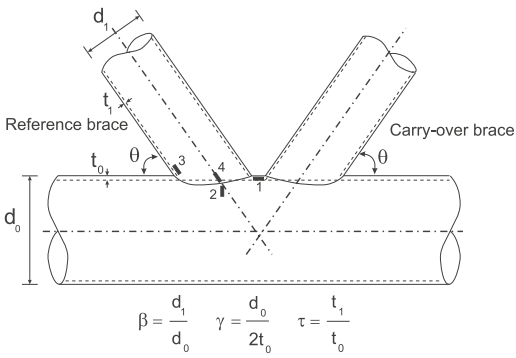

Geometrical conditions:

no eccentricity
equal braces

Range of validity

$0.30 \leq \beta \leq 0.60$
$24 \leq 2\gamma \leq 60.0$
$0.25 \leq \tau \leq 1.00$
$30° \leq \theta \leq 60°$

Load conditions

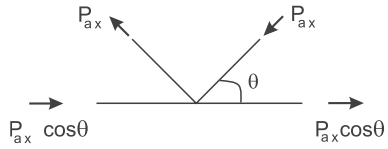

Load condition 1
basic balanced axial loading

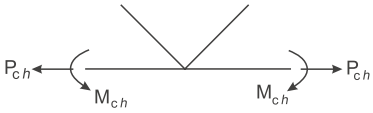

Load condition 2
chord loading (axial and bending)

Table D.3 – SCFs for uniplanar CHS K-joints with gap (continued)

Load condition 1	**basic balanced axial loading** (uniplanar CHS K-joints with gap)

chord

$$SCF_{ch,ax} = \left[\frac{\gamma}{12}\right]^{0.4}\left[\frac{\tau}{0.5}\right]^{1.1} \quad SCF_{o,ch,ax} = \text{correction factor} \cdot SCF_{o,ch,ax}$$

$SCF_{o,ch,ax}$ of chord, balanced axial loading

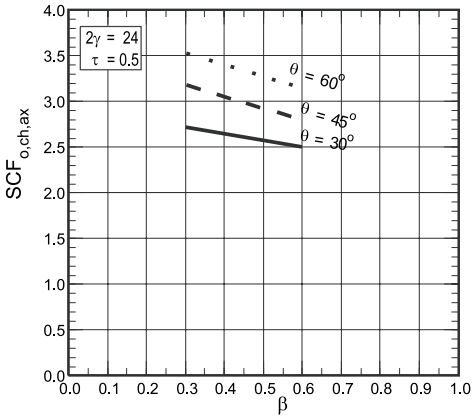

Correction factor for other values of 2γ and τ

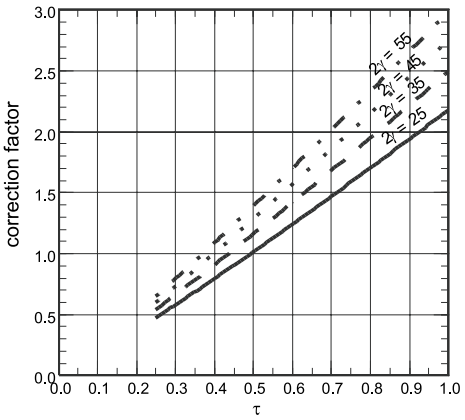

brace

$$SCF_{b,ax} = \left[\frac{\gamma}{12}\right]^{0.5}\left[\frac{\tau}{0.5}\right]^{0.5} \quad SCF_{o,b,ax} = \text{correction factor} \cdot SCF_{o,b,ax}$$

Minimum values of $SCF_{b,ax}$ are 2.64, 2.30 and 2.12 for θ = 30°, 45°, and 60° respectively.

$SCF_{o,b,ax}$ of braces, balanced axial loading

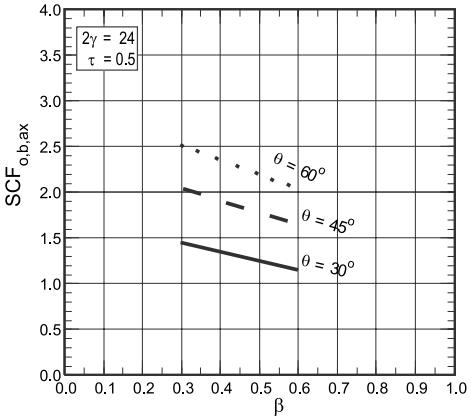

Correction factor for other values of 2γ and τ

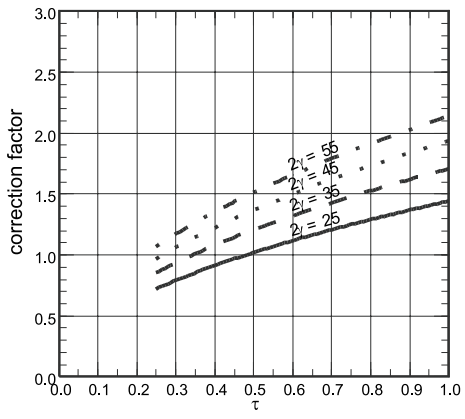

Table D.3 – SCFs for uniplanar CHS K-joints with gap (continued)

Load condition 2	**chord loading (axial and bending)** (uniplanar CHS K-joints with gap)

chord

$$SCF_{ch,ch} = 1.2 \cdot \left[\frac{\tau}{0.5}\right]^{0.3} \cdot (\sin\theta)^{-0.9}$$

$SCF_{ch,ch}$ is also given in the graph below where a minimum SCF of 2.0 is adopted.

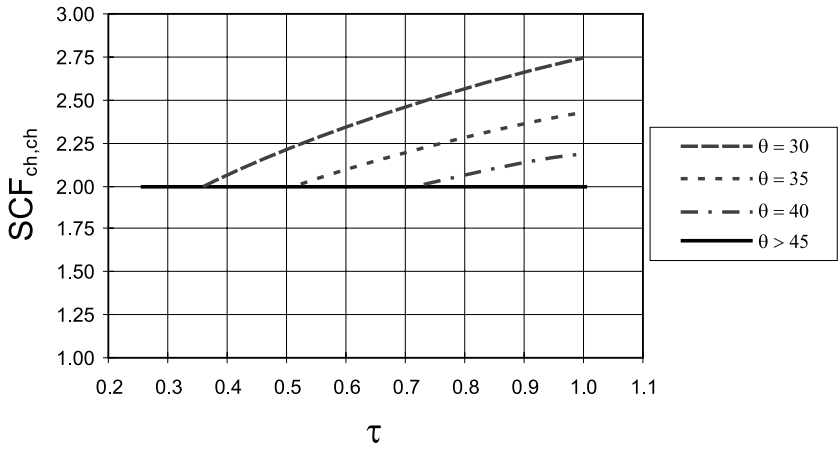

brace

$SCF_{b,ch}$ = 0 (negligible)

D.4 Multiplanar CHS XX-Joints

Table D.4 – SCFs for multiplanar CHS XX-joints

Locations

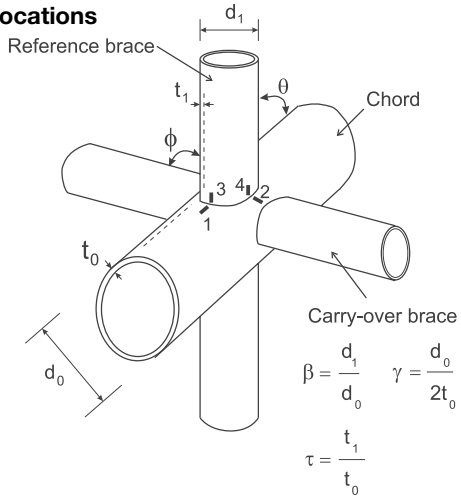

Geometrical conditions:

no eccentricity
equal braces

Range of validity

$0.3 \le \beta \le 0.6$
$15 \le 2\gamma \le 64$
$0.25 \le \tau \le 1.0$
$\theta = 90°$
$\phi = 90°$
$\psi = \phi - 2 \cdot \arcsin(\beta) \ge 16.2°$

Load conditions

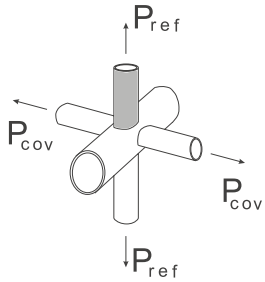

Load condition 1
axial balanced brace loading

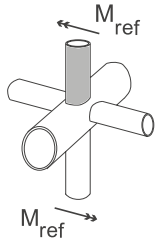

Load condition 2
balanced in-plane bending on braces

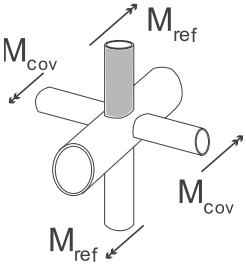

Load condition 3
balanced out-of-plane bending on braces

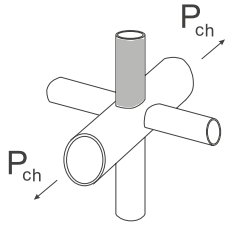

Load condition 4
axial balanced chord loading

Table D.4 – SCFs for multiplanar CHS XX-joints (continued)

Load condition 1	**axial balanced brace loading** (multiplanar CHS XX-joints)

Axial Load in Reference Braces (P_{ref})

axial load in reference braces P_{ref}

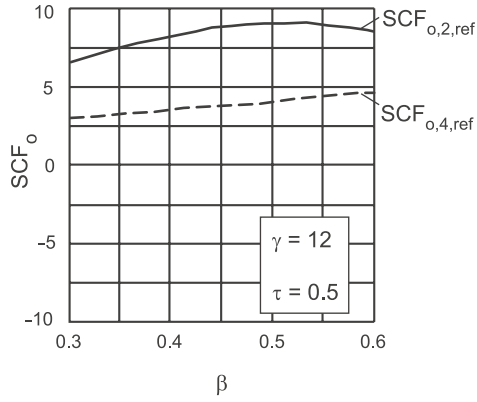

chord (locations 1 and 2)

$$SCF_{1,ref,ax} = 5 \cdot \left[\frac{\gamma}{12}\right]^{0.9} \cdot (1 - \beta)$$

$$SCF_{2,ref,ax} = \left[\frac{\gamma}{12}\right]^{1.1} \cdot \left[\frac{\tau}{0.5}\right]^{1.15} \cdot SCF_{o,2,ref}$$

brace (locations 3 and 4)

$$SCF_{3,ref,ax} = 2.0$$

$$SCF_{4,ref,ax} = \left[\frac{\gamma}{12}\right]^{0.5} \cdot \left[\frac{\tau}{0.5}\right]^{0.75} \cdot SCF_{o,4,ref}$$

Axial Load in Carry-Over Braces (P_{cov})

axial load in carry-over braces P_{cov}

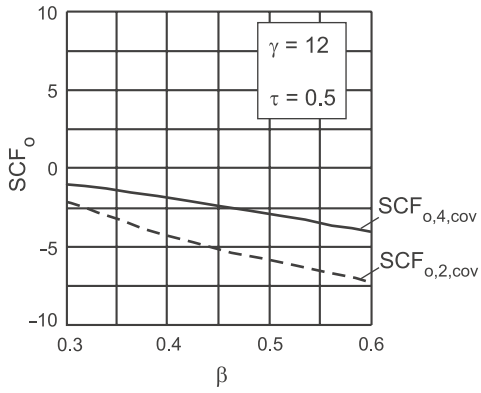

chord (locations 1 and 2)

$SCF_{1,cov,ax} = 0$ (negligible)

$$SCF_{2,cov,ax} = \left[\frac{\gamma}{12}\right]^{1.1} \cdot \left[\frac{\tau}{0.5}\right]^{1.15} \cdot SCF_{o,2,cov}$$

No minimum value for $SCF_{2,cov,ax}$ is required.

brace (locations 3 and 4)

$SCF_{3,cov,ax} = 0$ (negligible)

$$SCF_{4,cov,ax} = \left[\frac{\gamma}{12}\right]^{0.5} \cdot \left[\frac{\tau}{0.5}\right]^{0.75} \cdot SCF_{o,4,cov}$$

No minimum value for $SCF_{4,cov,ax}$ is required.

Table D.4 – SCFs for multiplanar CHS XX-joints (continued)

Load condition 2	**balanced in-plane bending on braces** (multiplanar CHS XX-joints)

In-Plane Bending in Reference Braces (M_{ref})

chord (locations 1 and 2)

$$SCF_{1,ref,ipb} = \left[\frac{\gamma}{12}\right]^{0.6} \cdot \left[\frac{\tau}{0.5}\right]^{0.8} \cdot SCF_{o,1,ref}$$

where $SCF_{o,1,ref} = 1.45 \cdot \beta \cdot \tau^{0.85} \cdot \gamma^{(1-0.68\beta)} \cdot \sin^{0.7}\theta$

$SCF_{2,ref,ipb} = 0$ (negligible)

brace (locations 3 and 4)

$SCF_{3,ref,ipb} = 2.0$

$SCF_{4,ref,ipb} = 0$ (negligible)

In-Plane Bending in Carry-Over Braces (M_{cov})

chord (locations 1 and 2)

$SCF_{1,cov,ipb} = SCF_{2,cov,ipb} = 0$ (negligible)

brace (locations 3 and 4)

$SCF_{3,cov,ipb} = SCF_{4,cov,ipb} = 0$ (negligible)

Load condition 3	**balanced out-of-plane bending on braces** (multiplanar CHS XX-joints)

Out-of-Plane Bending in Reference Braces (M_{ref})

chord (locations 1 and 2)

$SCF_{1,ref,opb} = 0$ (negligible)

$$SCF_{2,ref,opb} = \left[\frac{\gamma}{12}\right]^{1.25} \cdot \left[\frac{\tau}{0.5}\right]^{1.05} \cdot SCF_{o,2,ref}$$

brace (locations 3 and 4)

$SCF_{3,ref,opb} = 2.0$

$$SCF_{4,ref,opb} = \left[\frac{\gamma}{12}\right]^{0.65} \cdot \left[\frac{\tau}{0.5}\right]^{0.65} \cdot SCF_{o,4,ref}$$

out-of-plane bending in reference braces

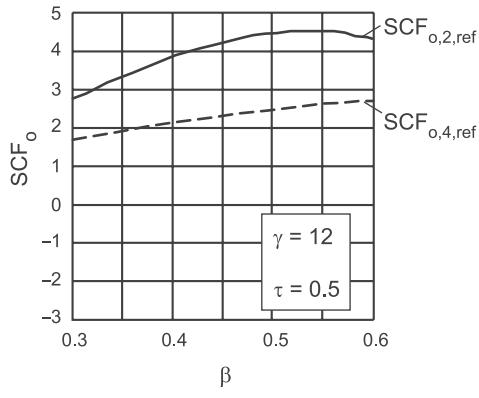

Table D.4 – SCFs for multiplanar CHS XX-joints (continued)

Load condition 3	**balanced out-of-plane bending on braces** (multiplanar CHS XX-joints)

Out-of-Plane Bending in Carry-Over Braces (M_{cov})

out-of-plane bending in carry-over braces

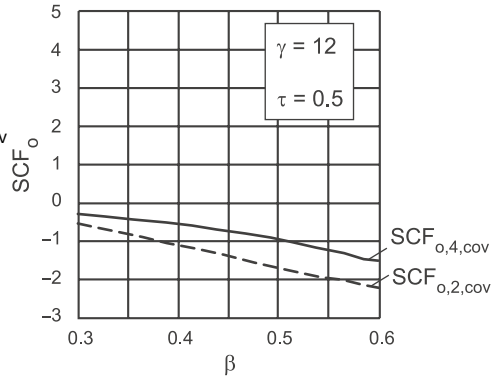

chord (locations 1 and 2)

$SCF_{1,cov,opb} = 0$ (negligible)

$$SCF_{2,cov,opb} = \left[\frac{\gamma}{12}\right]^{1.25} \cdot \left[\frac{\tau}{0.5}\right]^{1.05} \cdot SCF_{o,2,cov}$$

No minimum value for $SCF_{2,cov,opb}$ is required.

brace (locations 3 and 4)

$SCF_{3,cov,opb} = 0$ (negligible)

$$SCF_{4,cov,opb} = \left[\frac{\gamma}{12}\right]^{0.65} \cdot \left[\frac{\tau}{0.5}\right]^{0.65} \cdot SCF_{o,4,cov}$$

No minimum value for $SCF_{4,cov,opb}$ is required.

Load condition 4	**axial balanced chord loading** (multiplanar CHS XX-joints)

chord (locations 1 and 2)

$SCF_{1,ch} = 2.0$

$SCF_{2,ch} = 0$ (negligible)

brace (locations 3 and 4)

$SCF_{3,ch} = 0$ (negligible)

$SCF_{4,ch} = 0$ (negligible)

Appendix E: SCF Formulae and Graphs for RHS Joints

A minimum SCF of 2.0 is recommended for all joint types, all locations and all load conditions unless otherwise specified.

E.1 Uniplanar RHS T and X-Joints

Table E.1 – SCFs for uniplanar RHS T and X-joints

Locations

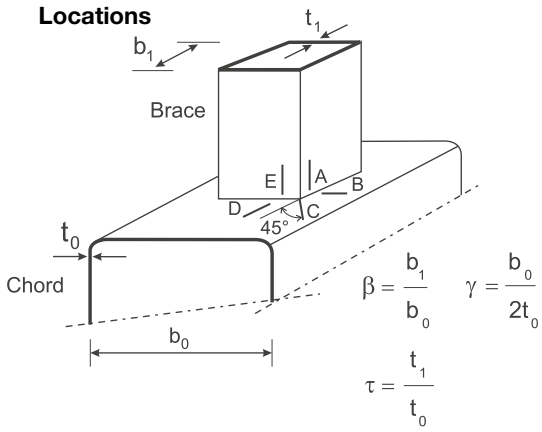

Range of validity

$0.35 \le \beta \le 1.0$
$12.5 \le 2\gamma \le 25.0$
$0.25 \le \tau \le 1.0$

Fabrication

For joints with fillet welds:
Multiply brace SCF's by 1.40.

Load conditions

1. axial force on the brace
2. in-plane bending on the brace
3. chord loading (axial and bending)

Load condition 1 — **axial force on the brace**
(uniplanar RHS T and X-joints)

chord (lines B, C and D)

$$SCF_{B,ax} = (0.143 - 0.204 \cdot \beta + 0.064 \cdot \beta^2) \cdot (2\gamma)^{(1.377 + 1.715 \cdot \beta - 1.103 \cdot \beta^2)} \cdot \tau^{0.75}$$

$$SCF_{c,ax} = (0.077 - 0.129 \cdot \beta + 0.061 \cdot \beta^2 - 0.0003 \cdot 2\gamma) \cdot (2\gamma)^{(1.565 + 1.874 \cdot \beta - 1.028 \cdot \beta^2)} \cdot \tau^{0.75}$$

$$SCF_{D,ax} = (0.208 - 0.387 \cdot \beta + 0.209 \cdot \beta^2) \cdot (2\gamma)^{(0.925 + 2.389 \cdot \beta - 1.881 \cdot \beta^2)} \cdot \tau^{0.75}$$

for X-joints with $\beta = 1.0$:
$SCF_{C,ax}$ is multiplied by a factor of 0.65
$SCF_{D,ax}$ is multiplied by a factor of 0.50

brace (lines A and E)

$$SCF_{A,ax} = SCF_{E,ax} = (0.013 + 0.693 \cdot \beta - 0.278 \cdot \beta^2) \cdot (2\gamma)^{(0.790 + 1.898 \cdot \beta - 2.109 \cdot \beta^2)}$$

For joints with fillet welds:
Multiply brace SCF's ($SCF_{A,ax}$, $SCF_{E,ax}$) by 1.40 for brace side of weld.

Table E.1 – SCFs for uniplanar RHS T and X-joints (continued)

Load condition 2	**in-plane bending on the brace** (uniplanar RHS T and X-joints)
chord (lines B, C and D)	
$SCF_{B,ipb} = (-0.011 + 0.085 \cdot \beta - 0.073 \cdot \beta^2) \cdot (2\gamma)^{(1.722 + 1.151 \cdot \beta - 0.697 \cdot \beta^2)} \cdot \tau^{0.75}$	
$SCF_{C,ipb} = (0.952 - 3.062 \cdot \beta + 2.382 \cdot \beta^2 + 0.0228 \cdot 2\gamma) \cdot (2\gamma)^{(-0.690 + 5.817 \cdot \beta - 4.685 \cdot \beta^2)} \cdot \tau^{0.75}$	
$SCF_{D,ipb} = (-0.054 + 0.332 \cdot \beta - 0.258 \cdot \beta^2) \cdot (2\gamma)^{(2.084 - 1.062 \cdot \beta + 0.527 \cdot \beta^2)} \cdot \tau^{0.75}$	
brace (lines A and E)	
$SCF_{A,ipb} = SCF_{E,ipb} = (0.390 - 1.054 \cdot \beta + 1.115 \cdot \beta^2) \cdot (2\gamma)^{(-0.154 + 4.555 \cdot \beta - 3.809 \cdot \beta^2)}$	
For joints with fillet welds: Multiply brace SCF's ($SCF_{A,ipb}$ and $SCF_{E,ipb}$) by 1.40 for brace side of weld.	
Load condition 3	**chord loading (axial and bending)** (uniplanar RHS T and X-joints)
chord (lines B, C and D)	
$SCF_{B,ch} = 0$ (negligible)	
$SCF_{C,ch} = 0.725 \cdot (2\gamma)^{0.248 \cdot \beta} \tau^{0.19}$	
$SCF_{D,ch} = 1.373 \cdot (2\gamma)^{0.205 \cdot \beta} \tau^{0.24}$	
brace (lines A and E)	
$SCF_{A,ch} = SCF_{E,ch} = 0$ (negligible)	

E.2 Uniplanar RHS K-Joints with Gap

Table E.2 – SCFs for uniplanar RHS K-joints with gap

Locations

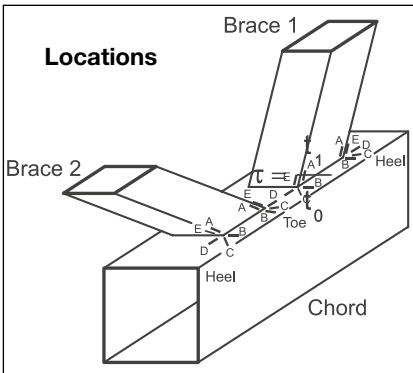

$$\beta = \frac{b_1}{b_0} \qquad \gamma = \frac{b_0}{2t_0} \qquad \tau = \frac{t_1}{t_0} \qquad g' = \frac{g}{t_0}$$

Only the maximum SCFs for the braces (among lines A and E) and chord (among lines B, C and D) are given.

Geometrical conditions:

equal braces

Range of validity

$0.35 \leq \beta \leq 1.0$
$10 \leq 2\gamma \leq 35$
$0.25 \leq \tau \leq 1.0$
$30° \leq \theta \leq 60°$
$2\tau \leq g'$
$-0.55 \leq e/h_0 \leq 0.25$

Load conditions

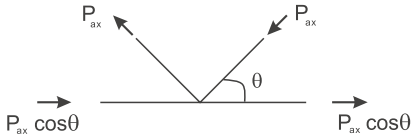

Load condition 1
basic balanced axial loading

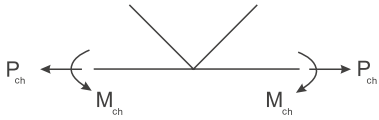

Load condition 2
chord loading (axial and bending)

Load condition 1 — **basic balanced axial loading**
(uniplanar RHS K-joints with gap)

chord (maximum SCF)

$$SCF_{ch,ax} = (0.48 \cdot \beta - 0.5 \cdot \beta^2 - 0.012/\beta + 0.012/g') \cdot (2\gamma)^{1.72} \cdot \tau^{0.78} \cdot (g')^{0.2} \cdot (\sin(\theta))^{2.09}$$

brace (maximum SCF)

$$SCF_{b,ax} = (-0.008 + 0.45 \cdot \beta - 0.34 \cdot \beta^2) \cdot (2\gamma)^{1.36} \cdot \tau^{-0.66} \cdot (\sin(\theta))^{1.29}$$

Load condition 2 — **chord loading (axial and bending)**
(uniplanar RHS K-joints with gap)

chord (maximum SCF)

$$SCF_{ch,ch} = (2.45 + 1.23 \cdot \beta) \cdot (g')^{-0.27}$$

brace (maximum SCF)

$SCF_{b,ch} = 0$ (negligible)

Table E.2 – SCFs for uniplanar RHS K-joints with gap (continued)

<table>
<tr><td colspan="2">General format
(for graphical presentation)

SCF = SCF_o · Correction factor
where SCF_o is the SCF for $2\gamma = 24$ and $\tau = 0.5$. The correction factor depends on 2γ and τ.</td></tr>
<tr><td>Load condition 1</td><td>basic balanced axial loading
(uniplanar RHS K-joints with gap)</td></tr>
<tr><td>chord (SCF_o)

use Figure E.1 for g´ = 1.0
use Figure E.2 for g´ = 2.0
use Figure E.3 for g´ = 4.0
use Figure E.4 for g´ = 8.0

chord (correction factor)

use Figure E.5</td><td>brace (SCF_o)

use Figure E.6 for all g´ values

brace (correction factor)

use Figure E.7</td></tr>
<tr><td>Load condition 2</td><td>chord loading (axial and bending)
(uniplanar RHS K-joints with gap)</td></tr>
<tr><td>chord ($SCF_{ch,ch}$)

use Figure E.8</td><td>brace

$SCF_{b,ch}$ = 0 (negligible)</td></tr>
</table>

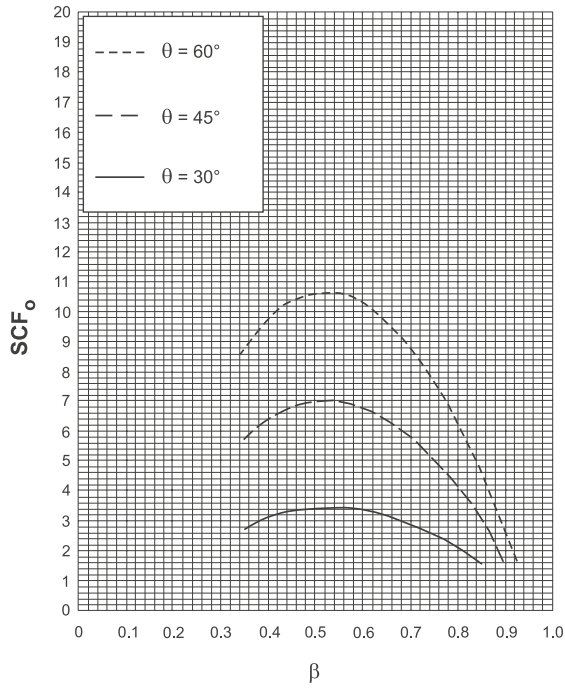

Figure E.1 – The reference value SCF_o for the chord of RHS K-joints with gap – g´ = 1.0 (balanced axial loading)

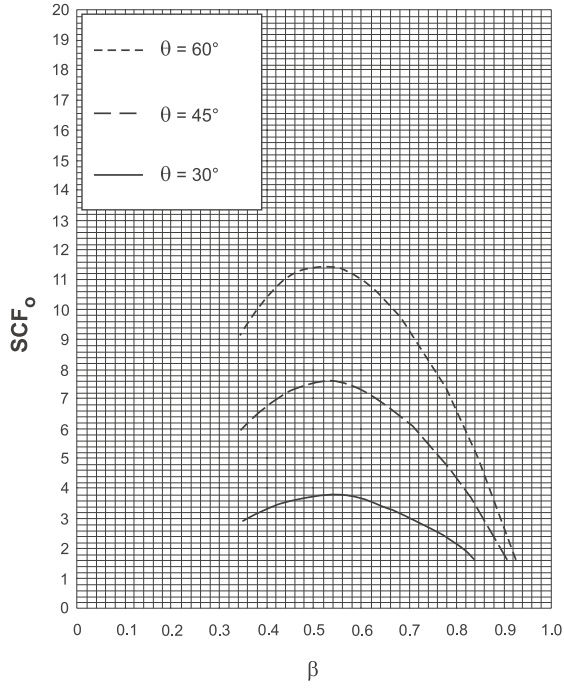

Figure E.2 – The reference value SCF_o for the chord of RHS K-joints with gap – g´ = 2.0 (balanced axial loading)

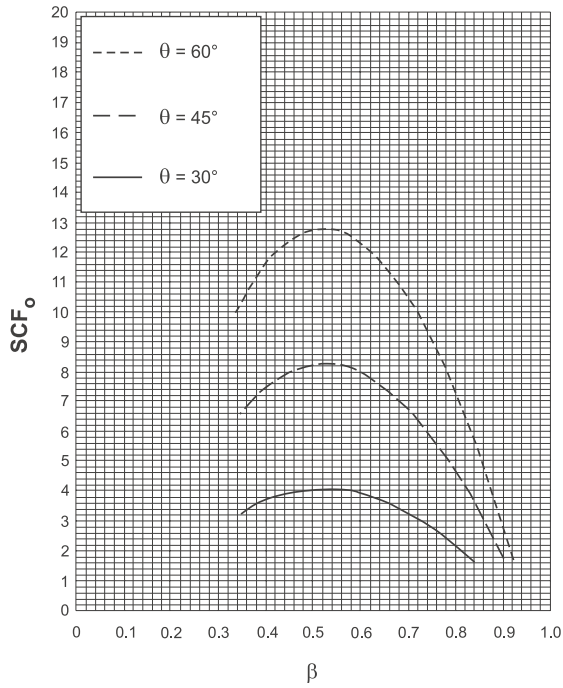

Figure E.3 – The reference value SCF_o for the chord of RHS K-joints with gap – g´ = 4.0 (balanced axial loading)

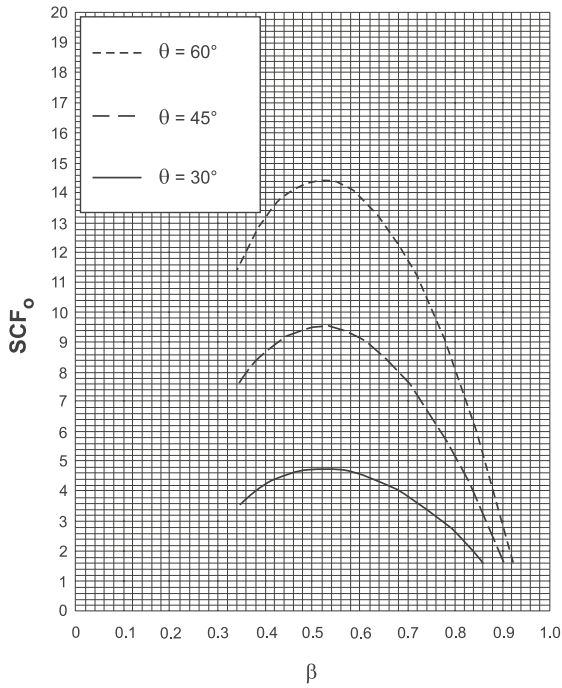

Figure E.4 – The reference value SCF_o for the chord of RHS K-joints with gap – g´ = 8.0 (balanced axial loading)

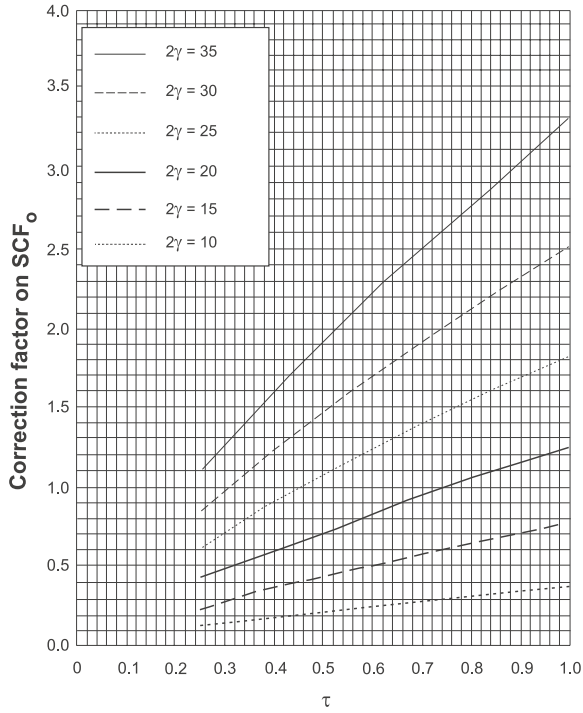

Figure E.5 – The correction factor on SCF_o for the chord of RHS K-joints with gap (balanced axial loading)

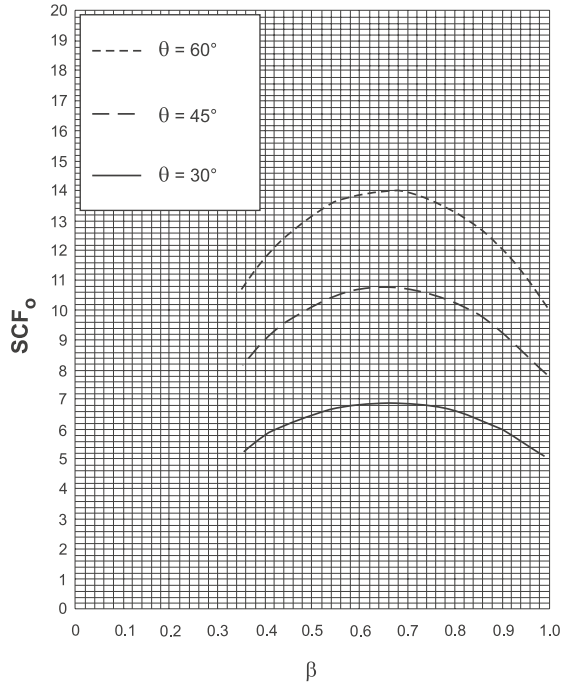

Figure E.6 – The reference value SCF_o for the braces of RHS K-joints with gap – all g´ (balanced axial loading)

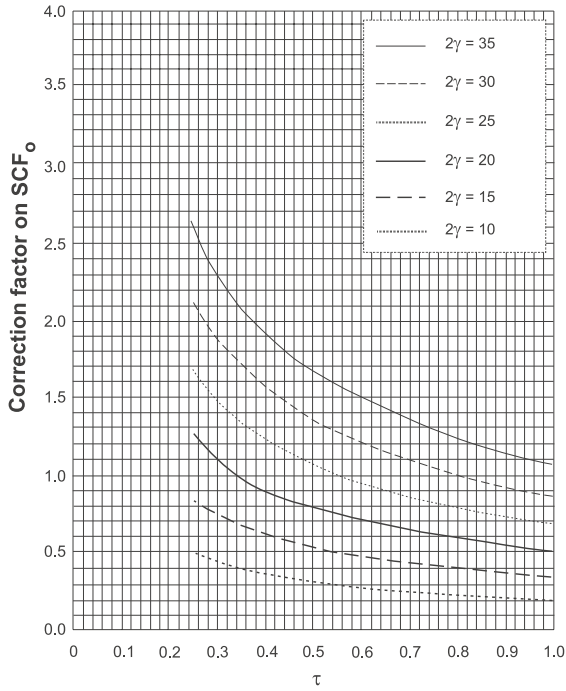

Figure E.7 – The correction factor for SCF for the braces of RHS K-joints with gap (balanced axial loading)

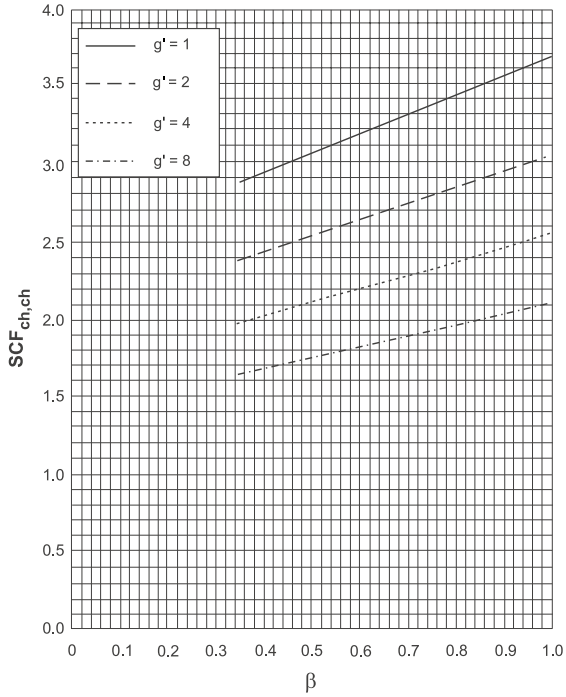

Figure E.8 – The $SCF_{ch,ch}$ for the chord of RHS K-joints with gap (chord loading)

E.3 Uniplanar RHS K-Joints with Overlap

Table E.3 – SCFs for uniplanar RHS K-joints with overlap

Locations

$$\beta = \frac{b_1}{b_0}$$

$$\gamma = \frac{b_0}{2t_0}$$

$$\tau = \frac{t_1}{t_0}$$

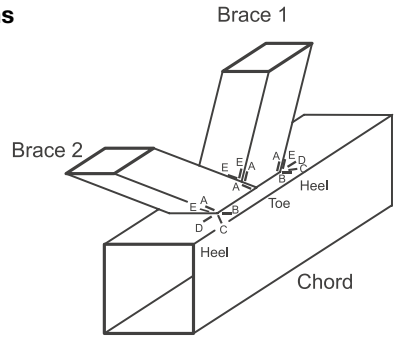

Only the maximum SCFs for the braces (among lines A and E) and chord (among lines B, C and D) are given.

Geometrical conditions:

equal braces

Range of validity

$0.35 \le \beta \le 1.0$
$10 \le 2\gamma \le 35$
$0.25 \le \tau \le 1.0$
$30° \le \theta \le 60°$
$50\ \% \le O_V \le 100\ \%$
$-0.55 \le e/h_O \le 0.25$

Load conditions

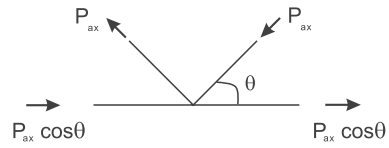

Load condition 1
basic balanced axial loading

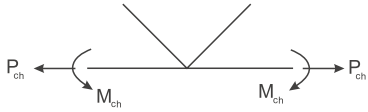

Load condition 2
chord loading (axial and bending)

Table E.3 – SCFs for uniplanar RHS K-joints with overlap (continued – using equations)

Load condition 1	**basic balanced axial loading** (uniplanar RHS K-joints with overlap)
chord (maximum SCF)	
$SCF_{ch,ax} = (0.5 + 2.38 \cdot \beta - 2.87 \cdot \beta^2 + 2.18 \cdot \beta \cdot O_V + 0.39 \cdot O_V - 1.43 \cdot \sin(\theta)) \cdot (2\gamma)^{0.29} \cdot \tau^{0.7} \cdot O_V^{0.73 - 5.53 \cdot \sin^2(\theta)} \cdot (\sin(\theta))^{-0.4 - 0.08 \cdot O_V}$	
brace (maximum SCF)	
$SCF_{b,ax} = (0.15 + 1.1 \cdot \beta - 0.48 \cdot \beta^2 - 0.14/O_V) \cdot (2\gamma)^{0.55} \cdot \tau^{-0.3} \cdot O_V^{-2.57 + 1.62 \cdot \beta^2} \cdot (\sin(\theta))^{0.31}$	
Load condition 2	**chord loading (axial and bending)** (uniplanar RHS K-joints with overlap)
chord (maximum SCF)	
$SCF_{ch,ch} = (1.2 + 1.46 \cdot \beta - 0.028 \cdot \beta^2)$	
brace (maximum SCF)	
$SCF_{b,ch} = 0$ (negligible)	

Table E.3 – SCFs for uniplanar RHS K-joints with overlap (continued – using graphs)

<table>
<tr><td colspan="2">General format
(for graphical presentation)

SCF = SCF_o · Correction factor
where SCF_o is the SCF for $2\gamma = 24$ and $\tau = 0.5$. The correction factor depends on 2γ and τ.</td></tr>
<tr><td>Load condition 1</td><td>basic balanced axial loading
(uniplanar RHS K-joints with overlap)</td></tr>
<tr><td>chord (SCF_o)

use Figure E.9 for 50% overlap
use Figure E.10 for 75% overlap
use Figure E.11 for 100% overlap

chord (correction factor)

use Figure E.12</td><td>brace (SCF_o)

use Figure E.13 for 50% overlap
use Figure E.14 for 75% overlap
use Figure E.15 for 100% overlap

brace (correction factor)

use Figure E.16</td></tr>
<tr><td>Load condition</td><td>chord loading (axial and bending)
(uniplanar RHS K-joints with overlap)</td></tr>
<tr><td>chord ($SCF_{ch,ch}$)

use Figure E.17</td><td>brace

$SCF_{b,ch} = 0$ (negligible)</td></tr>
</table>

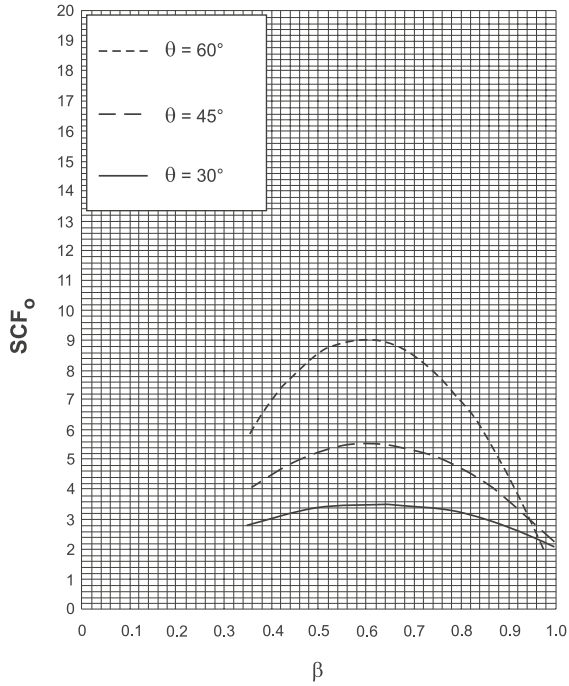

Figure E.9 – The reference value SCF_o for the chord of RHS K-joints with 50% overlap (balanced axial loading)

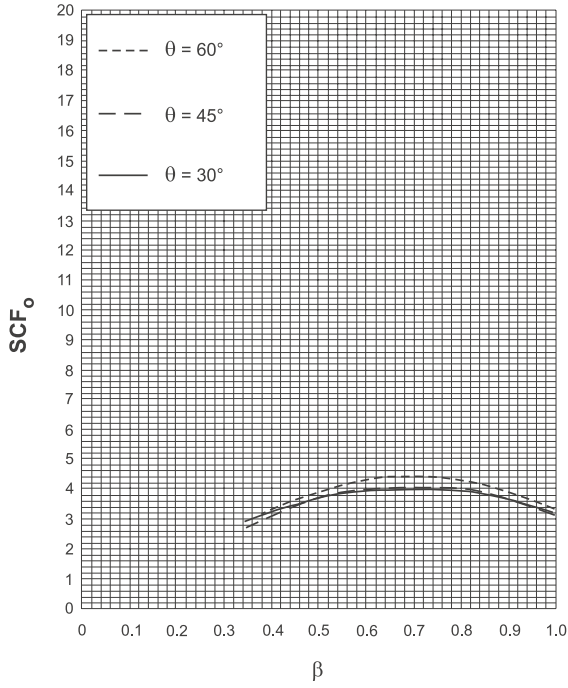

Figure E.10 – The reference value SCF_o for the chord of RHS K-joints with 75% overlap (balanced axial loading)

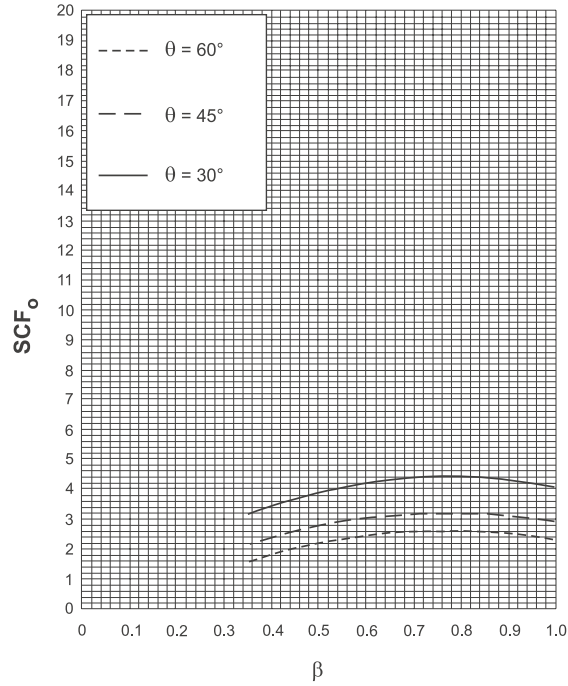

Figure E.11 – The reference value SCF_o for the chord of RHS K-joints with 100% overlap (balanced axial loading)

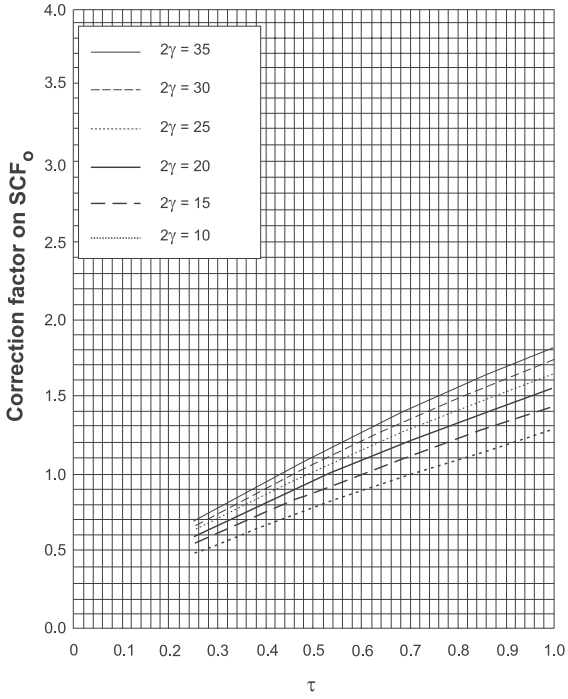

Figure E.12 – The correction factor on SCF_o for the chord of RHS K-joints with overlap (balanced axial loading)

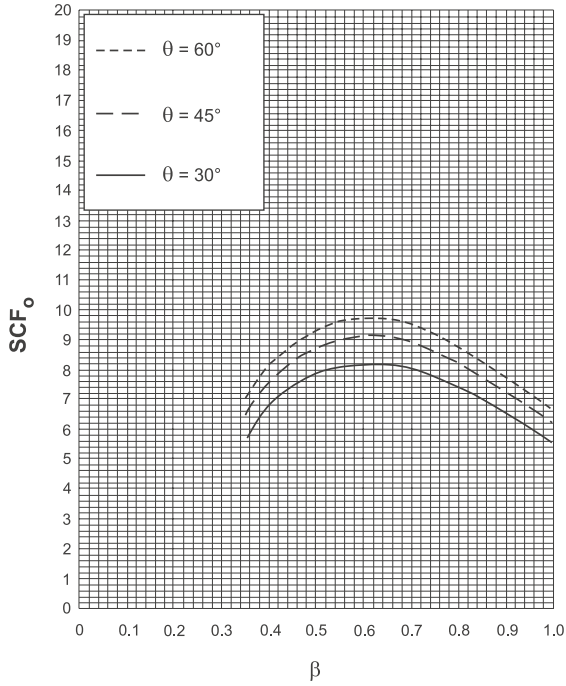

Figure E.13 – The reference value SCF_o for the braces of RHS K-joints with 50% overlap (balanced axial loading)

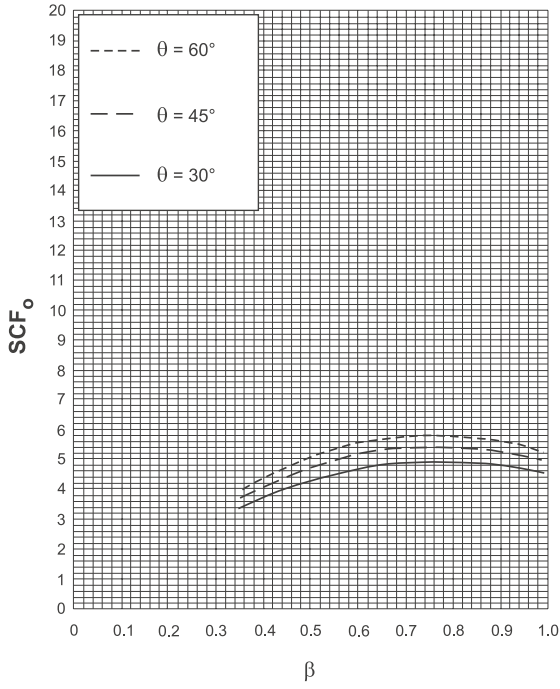

Figure E.14 – The reference value SCF_o for the braces of RHS K-joints with 75% overlap (balanced axial loading)

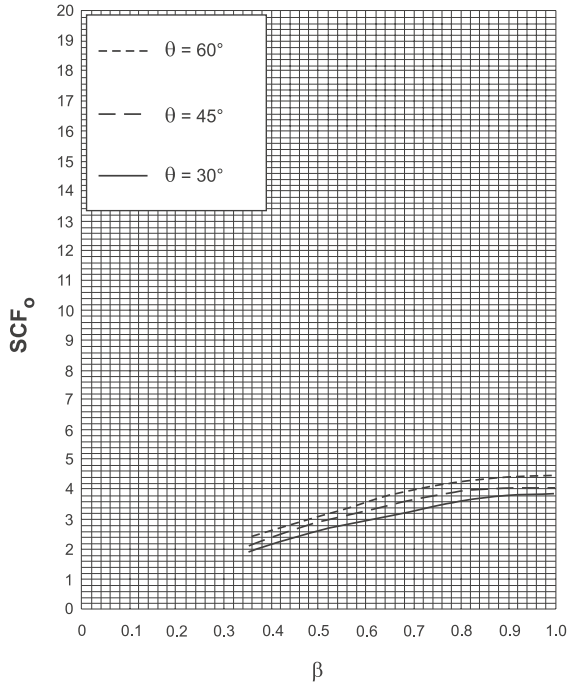

Figure E.15 – The reference value SCF_o for the braces of RHS K-joints with 100% overlap (balanced axial loading)

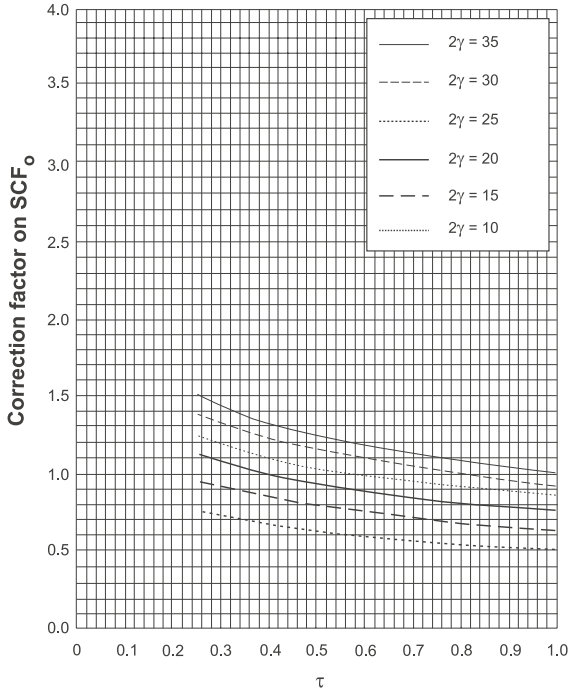

Figure E.16 – The correction factor on SCF_o for the braces of RHS K-joints with overlap (balanced axial loading)

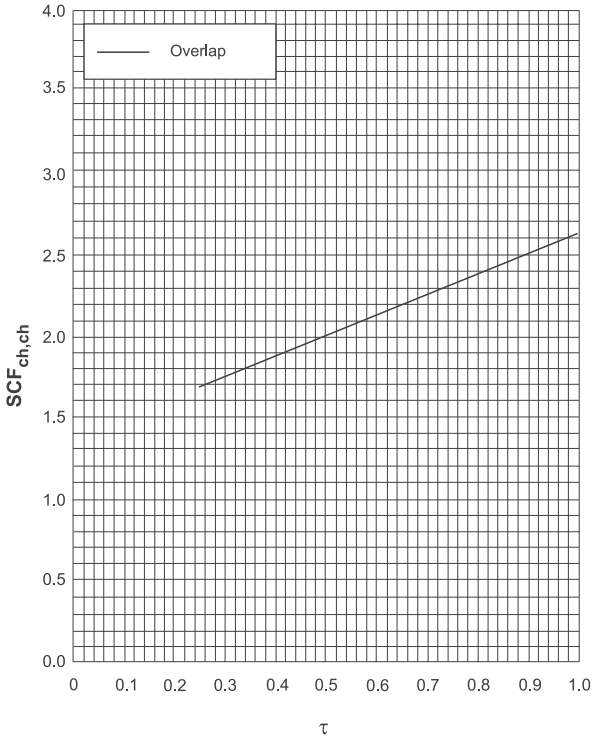

Figure E.17 – The $SCF_{ch,ch}$ for the chord of RHS K-joints with overlap (chord loading)

CIDECT – Comité International pour le Développement et l'Etude de la Construction Tubulaire

International Committee for the Development and Study of Tubular Structures

CIDECT, founded in 1962 as an international association, joins together the research resources of the principal hollow steel section manufacturers to create a major force in the research and application of hollow steel sections worldwide.

The objectives of CIDECT are:

- to increase the knowledge of hollow steel sections and their potential application by initiating and participating in appropriate research and studies

- to establish and maintain contacts and exchanges between the producers of the hollow steel sections and the ever increasing number of architects and engineers using hollow steel sections throughout the world

- to promote hollow steel section usage wherever this makes for good engineering practice and suitable architecture, in general by disseminating information, organizing congresses, etc.

- to co-operate with organizations concerned with practical design recommendations, regulations or standards at national and international level.

Technical activities

The technical activities of CIDECT have centred on the following research aspects of hollow steel section design:

- Buckling behaviour of empty and concrete-filled columns
- Effective buckling lengths of members in trusses
- Fire resistance of concrete-filled columns
- Static strength of welded and bolted joints
- Fatigue resistance of joints
- Aerodynamic properties
- Bending strength of hollow steel section beams
- Corrosion resistance
- Workshop fabrication, including section bending

The results of CIDECT research form the basis of many national and international design requirements for hollow steel sections.

CIDECT Publications

The current situation relating to CIDECT publications reflects the ever increasing emphasis on the dissemination of research results.

The list of CIDECT Design Guides, in the series “Construction with Hollow Steel Sections”, already published, or in preparation, is given below. These design guides are available in English, French, German and Spanish.

1. Design guide for circular hollow section (CHS) joints under predominantly static loading (1991)
2. Structural stability of hollow sections (1992, reprinted 1996)
3. Design guide for rectangular hollow section (RHS) joints under predominantly static loading (1992)
4. Design guide for structural hollow section columns in fire (1995, reprinted 1996)
5. Design guide for concrete filled hollow section columns under static and seismic loading (1995)
6. Design guide for structural hollow sections in mechanical applications (1995)
7. Design guide for fabrication, assembly and erection of hollow section structures (1998)
8. Design guide for circular and rectangular hollow section welded joints under fatigue loading (2000)
9. Design guide for structural hollow section column connections (in preparation)

In addition, taking into account the ever increasing place of steel hollow sections in internationally acclaimed “high tech” structures a new book “Tubular Structures in Architecture” has been published with the sponsorship of the European Community. This is also available in English, French, German and Spanish.

Copies of the design guides, the architectural book and research papers may be obtained from members or from:

The Steel Construction Institute
Silwood Park
Ascot
Berkshire SL5 7QN
England

Tel.: +44 (0) 13 44 62 33 45
Fax: +44 (0) 13 44 62 29 44
E-mail: f.awan@steel-sci.com
URL: http//www.steel-sci.org

CIDECT Organisation (2000)

- President: B. Becher (Germany)
  Vice-President: C. L. Bijl (The Netherlands)

- A General Assembly of all members meeting once a year and appointing an Executive Committee responsible for administration and execution of established policy

- A Technical Commission and Working Groups meeting at least once a year and directly responsible for the research and technical promotion work

Present members of CIDECT are (2000)

- Aceralia Transformados, Spain
- BHP Steel, Australia
- British Steel Tubes and Pipes, United Kingdom
- Hoogovens Buizen, The Netherlands
- IPSCO Inc., Canada
- Mannstaedt Werke GmbH & Co., Germany
- Rautaruukki Oy, Finland
- Tata Iron and Steel Co., India
- Tubeurop, France
- A.G. Tubos Europa, Spain
- Vallourec & Mannesmann Tubes, Germany
- Voest Alpine Krems, Austria

Care has been taken to ensure that all data and information herein is factual and that numerical values are accurate. To the best of our knowledge, all information in this book is accurate at the time of publication.

CIDECT, its members and the authors assume no responsibility for errors or misinterpretation of the information contained in this book or in its use.

Acknowledgements for photographs:

The authors express their appreciation to the following firms for making available the photographs used in this Design Guide:

British Steel Tubes and Pipes
IPSCO Inc. Canada
Tubeurop France
Vallourec & Mannesmann Tubes Germany
Voest Alpine Krems